Disruption of Clever-1 for Novel Anticancer Immunotherapy

Master's Thesis

Miro Viitala, B.Eng.

Master's Degree Programme in Drug Design & Development

Department of Pharmacology, Drug Development & Therapeutics

Faculty of Medicine

University of Turku

Supervisor: Maija Hollmén, Ph.D.

Cell Trafficking Unit

MediCity Research Laboratory

Faculty of Medicine

University of Turku

Contents

Tiivistelmä

Syövän eteneminen riippuu siitä, minkälaisen immuunivasteen kasvain aiheuttaa. Tavallisesti tulehdusta lisäävä eli proinflammatorinen immuunivaste estää ja tulehdusta vähentävä eli anti-inflammatorinen immuunivaste edistää syövän etenemistä. Anti-inflammatoristen valkosolujen, kuten säätelijä-T-solujen ja M2-makrofagien, aiheuttama immuunivasteen vaimennus on yksi onnistuneen syöpähoidon suurimmista esteistä.

Clever-1 on monitoiminen proteiini, jota ilmentää ihmisen monosyyttien ja M2-makrofagien alaluokka. Näissä makrofageissa Clever-1 osallistuu reseptorivälitteiseen endosytoosiin, solunsisäiseen lajitteluun ja transsytoosiin. Clever-1:tä ilmennetään myös imu- ja verisuonten endoteelissä, missä se välittää valkosolujen kulkeutumista imunesteestä ja verestä kudoksiin. Ihmisen syövissä on havaittu Clever-1:tä ilmentäviä imusuonia ja makrofageja, ja esimerkiksi edenneessä peräsuolen syövässä suuri määrä Clever-1-positiivisia makrofageja korreloi heikomman ennusteen kanssa.

Häiritsemällä Clever-1:n toimintaa siihen kohdennetuilla vasta-aineilla ryhmämme on hiljattain osoittanut, että Clever-1-vasta-ainehoito hidastaa syövän etenemistä melanooman ja lymfooman eläinmalleissa. Tulosten perusteella Clever-1:n toiminnan häiritseminen vasta-aineella sekä ennen syöpäsolujen istutusta että sen jälkeen vähentää kasvaimen kasvua ja etäpesäkkeiden muodostumista. Mekanismi, jolla Clever-1 säätelee kasvaimeen liittyvien makrofagien fenotyyppiä ja toimintaa kasvaimen kasvun ja etäpesäkkeiden muodostumisen aikana, on kuitenkin vielä erittäin puutteellisesti tunnettu.

Tässä pro gradu -työssä esitetyt tulokset paljastavat uusia molekulaarisia mekanismeja, joilla Clever-1 säätelee M2-makrofagien toimintaa, ja antavat viitteitä Clever-1-vasta-ainehoidon mahdollisesta immunoterapeuttisesta tehosta myös rintasyövän hoidossa. Saatujen tulosten perusteella Clever-1 lisäsi anti-inflammatorisen mTORC1-kompleksin kautta tapahtuvaa solunsisäistä signaalitransduktiota M2-makrofageissa. Vastaavasti Clever-1:n toiminnan häiritseminen vasta-aineella aiheutti M2-makrofageissa proinflammatorisen vasteen lisäämällä keskeisen tulehduksenvälittäjäaineen tuumorinekroositekijä-α:n tuotantoa ja erittymistä. Lisäksi yhdistelmähoito Clever-1:tä ja PD-1-säätelijäproteiinia estävällä vasta-aineella vähensi kasvaimeen liittyvien anti-inflammatoristen makrofagien suhteellista osuutta ja siten todennäköisesti edisti proinflammatorista tulehdusvastetta kasvaimen sisällä. Sen lisäksi yhdistelmähoito Clever-1- ja PD-1-vasta-aineella näytti estävän kasvaimen kasvua ja etäpesäkkeiden muodostumista triplanegatiivisen rintasyövän hiirimallissa.

Asiasanat: Clever-1, immunoterapia, kasvaimeen liittyvät makrofagit, syöpä

Abstract

The progression of cancer is dependent on the quality of the immune response elicited by the tumour. Typically, proinflammatory immune responses restrain and anti-inflammatory immune responses promote the progression of cancer. The immunosuppression caused by anti-inflammatory leukocytes, such as regulatory T cells and alternatively activated macrophages, is a major obstacle in the successful treatment of cancer.

Clever-1 is a multifunctional protein expressed by a subset of human monocytes and alternatively activated, or M2, macrophages. In these macrophages, Clever-1 is involved in receptor-mediated endocytosis, intracellular sorting, and transcytosis. Clever-1 is also expressed on lymphatic and vascular endothelia, where it mediates the trafficking of leukocytes from the lymph or blood into tissues. Lymphatics and macrophages expressing Clever-1 have been detected in human cancers, and high numbers of Clever-1-positive macrophages correlate with poorer prognoses in advanced colorectal cancer.

By using specific antibodies to interfere with the function Clever-1, we have recently demonstrated that Clever-1 antibody treatment limits the progression of cancer in animal models of melanoma and lymphoma. According to these results, the antibody-mediated interference of Clever-1 both before and after cancer cell implantation limits tumour growth and metastasis. However, the molecular mechanisms by which Clever-1 regulates the phenotype and function of tumour-associated macrophages during this process are very poorly understood.

The data presented in this master's thesis reveal novel molecular mechanisms employed by Clever-1 to regulate the function of M2 macrophages and suggest that Clever-1 antibody treatment may have immunotherapeutic potential in the treatment of breast cancer. According to the obtained results, Clever-1 promoted intracellular signal transduction through the anti-inflammatory mTORC1 complex in M2 macrophages. In accordance, the antibody-mediated interference of Clever-1 induced a proinflammatory response from M2 macrophages by increasing the production and secretion of TNF-α, a major mediator of inflammation. Furthermore, combinatorial antibody-mediated interference of Clever-1 and the immune checkpoint protein PD-1 decreased the relative amount of anti-inflammatory tumour-associated macrophages, thereby likely promoting a more proinflammatory milieu within the tumour microenvironment. Additionally, combinatorial Clever-1 and PD-1 antibody treatment appeared to limit tumour growth and metastasis also in a mouse model of triple-negative breast cancer.

Keywords: cancer, Clever-1, immunotherapy, tumour-associated macrophages

Abbreviations

4E-BP1	eukaryotic translation initiation factor 4E-binding protein 1
AP-1	activator protein 1
APC	antigen-presenting cell
ARG-1	arginase 1
BMDM	bone marrow-derived macrophage
Clever-1	common lymphatic endothelial and vascular endothelial receptor 1
Clever-1$^{-/-}$	homozygous Clever-1 knockout
CSF-1	colony-stimulating factor 1, also known as macrophage colony-stimulating factor
CSF-1R	colony-stimulating factor 1 receptor; also known as CD115
CSF-3R	colony-stimulating factor 3 receptor, also known as granulocyte colony-stimulating factor receptor
CTLA-4	cytotoxic T lymphocyte-associated antigen 4
DAMP	danger-associated molecular pattern
DC	dendritic cell
EMA	European Medicines Agency
IDO	indoleamine 2,3-dioxygenase
IFN-γ	interferon-γ
IL	interleukin
ILC	innate lymphoid cell
LPS	lipopolysaccharide
LDL	low-density lipoprotein
M1 macrophage	classically activated (proinflammatory) macrophage
M2 macrophage	alternatively activated (anti-inflammatory) macrophage
MHC	major histocompatibility complex
MRC1	mannose receptor, C type 1; also known as CD206
mTOR	mechanistic target of rapamycin
mTORC1	mTOR complex 1
NF-κB	nuclear factor κB
NK cell	natural killer cell
NOS2	nitric oxide synthase 2, also known as inducible nitric oxide synthase
PAMP	pathogen-associated molecular pattern
PD-1	programmed death receptor 1
PD-L1	programmed death receptor ligand 1
RPS6	ribosomal protein S6
SI-CLP	Stabilin-1-interacting chitinase-like protein
SPARC	secreted protein, acidic, rich in cysteine; also known as osteonectin
STAT	signal transducer and activator of transcription
TAM	tumour-associated macrophage
T_C cells	cytotoxic T cell
TGFβ	transforming growth factor β
T_H cell	helper T cell
TIL	tumour-infiltrating lymphocyte
TNF-α	tumour necrosis factor α
T_{reg} cell	regulatory T cell
VEGF	vascular endothelial growth factor

Figures

Tables

1 Introduction

The immune system efficiently protects the host from cancer. However, as mutations accumulate over decades, neoplastic cells may gain properties that enable them to turn the host's anticancer immune response to their own advantage. Virtually all tumours elicit an inflammatory response and contain a large proportion of infiltrating immune cells. Accordingly, tumour-promoting inflammation has been recognized as a vital enabling characteristic of carcinogenesis.

Typically, tumour-infiltrating leukocytes consist mostly of macrophages. Macrophages are some of the most diverse cells in the immune system, as they may acquire either pro- or anti-inflammatory properties depending on environmental stimuli. Within tumours, macrophages are the primary cells maintaining the chronic, tumour-promoting inflammation. Classically, macrophages have been categorized into proinflammatory M1 and anti-inflammatory M2 macrophages based on their opposing functions and phenotypes. In the tumour microenvironment, tumour-associated macrophages typically resemble M2 macrophages.

Clever-1 is a large multifunctional protein expressed by monocytes, specialized tissue macrophages, and a subpopulation of M2 macrophages in particular. In these macrophages, Clever-1 regulates receptor-mediated endocytosis, the intracellular sorting of various biomolecules, and transcytosis. Endothelial Clever-1 in blood vessels and lymphatics controls leukocyte trafficking into inflamed tissues. Importantly, lymphatics and macrophages expressing Clever-1 are present in human cancers, and in advanced colorectal cancer, for example, the presence of Clever-1$^+$ macrophages has been correlated with poorer prognoses.

Cancer immunotherapies currently on the market have demonstrated that it is possible to activate the host's anticancer immune response even in advanced cancers. However, none of the immunotherapies currently on the market specifically target the tumour-associated macrophages that sustain tumour-promoting inflammation.

In this master's thesis, I have elucidated some of the molecular mechanisms employed by Clever-1 to regulate the anti-inflammatory phenotype of M2 macrophages and investigated the immunotherapeutic potential of Clever-1 antibody treatment in two mouse models of breast cancer. The results support the hypothetical function of Clever-1 as a novel immune checkpoint protein of the innate immune system. Additionally, Clever-1 antibody treatment may have an immunotherapeutic effect in breast cancer, where it appears to modulate tumour-associated macrophages to activate the anticancer immune response and inhibit metastasis.

2 Review of the Literature

2.1 The Immune System

The immune system consists of an intricate network of molecules, cells, and organs that have evolved to protect the host from harmful agents of both external and internal origin. The immune system of vertebrates is divided into two main classes: the innate and the adaptive immune systems. Briefly, the innate immune system is the host's first line of defence and is constitutively active. The innate immune system includes the mechanical, chemical, and microbiological barriers of the host's epithelia, soluble molecules such as the complement system, and a variety of specialized cells. The adaptive immune system is also made up of specialized cells that become activated if the innate immune system cannot eradicate the harmful agent on its own. Rather than being separate entities, the innate and adaptive immune systems engage one another at multiple levels of cross-talk and require constant input from each other to mount a fully effective immune response.

The major differentiating factor between the cells of the innate and adaptive immune systems is the receptors expressed by them. The cells of the innate immune system express pattern recognition receptors that have developed over evolutionary time and recognize a fixed number of ligands. These are common, conserved structures on pathogens or molecules released or expressed by damaged host cells – called pathogen- and danger-associated molecular patterns, or PAMPs and DAMPs, respectively – neither of which are present on the host's cells under homoeostatic conditions. An obvious pitfall of the innate immune system is the rapid evolution of many pathogens, which may result in antigenic drift. Conversely, the receptors expressed by the cells of the adaptive immune system are created through the random process of gene rearrangement followed by clonal selection and expansion – therefore, each clone expresses a specific receptor that recognizes a specific epitope on an antigen. Consequently, the repertoire of receptors in the adaptive immune system is so massive that it can recognize virtually any infectious agent in existence.

The immune system consists of many distinct types of cells. All cells of the immune system – referred to as leukocytes – arise from a common pluripotent progenitor cell, the haematopoietic stem cell of the bone marrow. Depending on environmental stimuli, the daughter cells of the haematopoietic stem cell become either common myeloid or common lymphoid progenitor cells. Red blood cells and platelets, as well as cells of the innate immune system called granulocytes, mast cells, and monocytes, are the progeny of the common myeloid progenitor cells. The common lymphoid progenitor cells give rise to innate lymphoid cells, which do not express antigen-specific receptors and are therefore classified as cells of the innate immune system, as well as lymphocytes, which are the cells of the adaptive immune system. Additionally, both common myeloid and common lymphoid progenitor cells give rise to the dendritic cells of the innate immune system.

Granulocytes come in three types: neutrophils, eosinophils, and basophils. They are named after their characteristic cytoplasmic granules, which contain many different types of antimicrobial agents. Granulocytes are relatively short-lived and survive only a few days following maturation and departure from the bone marrow. During acute immune responses, the production of granulocytes in the bone marrow is greatly increased. Granulocytes leave the bone marrow in the circulation and rapidly

migrate to sites of infection and inflammation. Of the three types of granulocytes, neutrophils are by far the most abundant. Neutrophils are also the most important type of leukocyte in sites of inflammation during immune responses. They are able to efficiently phagocytose and destroy many different types of pathogens. Neutrophils work as an aggressive strike force meant to eradicate the infecting pathogen as quickly and proficiently as possible, even causing damage to the host's tissues in the process. Eosinophils and basophils are not as well-known as neutrophils but are believed to be involved in immune responses against parasites as well as in generating an allergic response.

Mast cells differentiate in the tissues from currently unidentified precursor cells. Like eosinophils and basophils, mast cells are believed to play a role in the immune response against parasites. They have been studied mostly in the context of allergic responses. Similarly to granulocytes, mast cells contain cytoplasmic granules filled with inflammatory molecules that they release when activated.

During inflammation, monocytes are recruited from the bone marrow, from where they migrate through the circulation into inflamed tissues and differentiate into macrophages. Additionally, many specialized types of tissue macrophages can be found throughout the host – referred to as osteoclasts in bones, microglial cells in the central nervous system, dust cells in the lungs, and Kupffer cells in the liver, to name some – that, for the most part, originate already during embryogenesis. Macrophages are relatively long-lived and, unlike granulocytes, are present in tissues at all times, not only during inflammation. Macrophages perform many important tasks for the host. They are readily phagocytic and clean up dead and dying cells and other unwanted debris from their surroundings. Perhaps one of the most important tasks of macrophages, however, is to patrol the tissues in case of infecting pathogens as a first line of defence. Upon encountering a pathogen, macrophages raise the alarm for other cells of the immune system by secreting signalling molecules called cytokines that promote inflammation and guide other leukocytes – such as circulating neutrophils and, at later stages, activated lymphocytes – to the inflamed tissue. Macrophages are also able to efficiently phagocytose and destroy pathogens themselves. Additionally, macrophages have an important role in the resolution of inflammation, when the immune response needs to be gradually shut down, the debris left behind removed, and the damaged tissue repaired. These opposing properties make macrophages the most plastic and diverse cells in the immune system.

Innate lymphoid cells (ILCs) are classified into groups 1, 2, and 3 according to the profile of cytokines they produce. Group 1 ILCs are the most studied and better known as natural killer (NK) cells. NK cells travel through the circulation, continually inspecting the cell surface molecules presented by other host cells. The composition of these cell surface molecules may be altered by viral infections or genetic mutations. When NK cells come across such an abnormal host cell, the NK cell activates and kills it. By directly removing neoplastic cells, NK cells are an important part of the continuous immune surveillance that protects the host from cancer.

Dendritic cells are divided into conventional and plasmacytoid dendritic cells (DCs). Conventional DCs, like monocytes, leave the bone marrow in the circulation and migrate into tissues. There, they continually sample their surroundings by phagocytosis for the presence of pathogens, similarly to macrophages. However, when a conventional DC encounters a pathogen, it does not remain in the tissue to destroy the infecting pathogens. Instead, it matures and migrates to the lymph nodes, where

it presents the pathogenic antigen in its possession – coupled to the class I or II major histocompati-histocompatibility complex (MHC) – to cells of the adaptive immune system in combination with other stimulatory signals. Conventional DCs are, therefore, the important link between the innate and adaptive immune systems. Macrophages perform similar antigen presentation, which is why macrophages and DCs are collectively referred to as antigen-presenting cells (APCs). Plasmacytoid DCs, on the other hand, continuously migrate though the blood and lymph. They secrete antiviral interferons but also efficiently present antigens when matured.

Lymphocytes – B and T cells – are the cells of the adaptive immune system. B cells develop in the bone marrow, whereas the most significant stages of the development of T cells take place in the thymus. Mature lymphocytes circulate through the blood and lymph and aggregate in lymphoid tissues and organs, such as the lymph nodes. They are referred to as naïve lymphocytes before encountering their specific antigen. After an APC presents a naïve lymphocyte its specific antigen with other stimulatory signals, the naïve lymphocyte activates and differentiates into a fully functional effector lymphocyte. Activated B cells become plasma cells, whose main function is the secretion of antibodies. Effector B cells function also as effective APCs. Effector T cells, on the other hand, have three main functions: Cytotoxic T (T_C) cells kill abnormal host cells – usually those infected by viruses or other intracellular pathogens, but also cells that have acquired genetic mutations – when presented with antigens coupled to the class I MHC. Helper T (T_H) cells orchestrate immune responses by secreting cytokines that activate and direct other cells of the innate and adaptive immune systems and recognize antigens coupled to the class II MHC. Regulatory T (T_{reg}) cells suppress other cells of the immune system when an immune response forms against a self-antigen, allergen, or commensal bacteria, as well as during resolution. During an adaptive immune response, some effector B and T cells differentiate into memory cells that may persist for decades after the original inflammatory agent has been eliminated. When a memory cell encounters its specific antigen a second time, it generates an adaptive immune response so rapid and effective the host rarely has time to even notice the infection. Because of the enormous diversity of antigen-specific receptors, B and T cells may recognize both self- and non-self-antigens. The former may result in autoimmune diseases if the checks and balances that have evolved to actively prevent their pathogenesis fail. However, the latter allows the adaptive immune response to recognize pathogenic antigens that are undetectable to the innate immune system. Importantly, B and T cells can also recognize tumour-associated antigens – antigens that are differentially expressed between neoplastic cells and the host's normal cells – and tumour-specific antigens – antigens that are unique to neoplastic cells – and thus direct anticancer immune responses, as well.

2.2 Classically & Alternatively Activated Macrophages

Traditionally, immune responses have been categorized as type 1 T_H (T_H1) cell and T_H2 cell responses because of the major role that T_H cells have in co-ordinating the immune system (Mosmann & Coffman, 1989). T_H1 cells battle intracellular pathogens and contribute to the pathogeneses of autoimmune diseases, whereas T_H2 cells fight extracellular parasites, induce antibody production, and promote allergic reactions. Although this paradigm is now known to be incomplete due the other subtypes of T_H cells discovered since – particularly T_H17 cells, T_{reg} cells, and follicular T_H cells

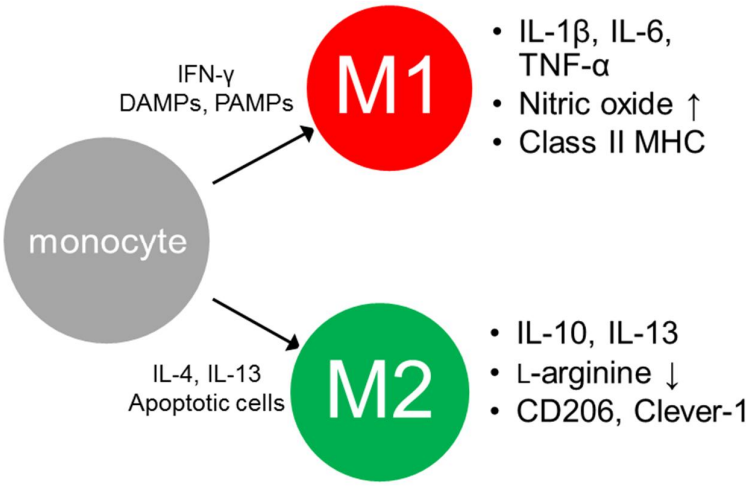

Figure 1. The polarization of monocytes into classically activated M1 and alternatively activated M2 macrophages. Inflammatory stimuli, such as IFN-γ and DAMPs and PAMPs, initiate the polarization of monocytes into M1 macrophages. M1 macrophages secrete proinflammatory cytokines, such as IL-1β, IL-6, and TNF-α, produce cytotoxic nitric oxide, and present antigens coupled to the class II MHC. Anti-inflammatory signals, such as IL-4, IL-13, and apoptotic cells, polarize monocytes into M2 macrophages, which secrete anti-inflammatory and immunosuppressive cytokines, such as IL-10 and IL-13, inhibit cellular proliferation by depleting L-arginine, and express various receptors, such as the mannose receptor CD206 and the scavenger receptor Clever-1. In reality, macrophages exist on a broad spectrum between these two extreme states and retain functional plasticity even after polarization.

(Korn & al., 2007; Tang & Bluestone, 2008; Crotty, 2011) – the opposing functions of macrophages, that is, the initiation of inflammation alongside resolution and tissue remodelling, has led to their similar, simplified classification into the classically activated M1 macrophages and the alternatively activated M2 macrophages (see Figure 1) (Mills & al., 2000; Mantovani & al., 2002). According to present knowledge, macrophages are seen to exist on a spectrum between these two extremes and can rapidly change their phenotype and functionality in response to external stimuli (Stout & al., 2005; Mosser & Edwards, 2008; Biswas & Mantovani, 2010).

Cytokines secreted by T_H1 cells, such as interferon (IFN)-γ, as well as DAMPS and PAMPs initiate the polarization of M1 macrophages. IFN-γ activates the transcription factor signal transducer and activator of transcription (STAT)1, which regulates the expression of genes that induce macrophages to secrete large amounts of proinflammatory cytokines, mainly interleukin (IL)-1β, IL-6, IL-12, and tumour necrosis factor (TNF)-α; to destroy pathogens more efficiently with reactive nitric oxide by upregulating the enzyme inducible nitric oxide synthase (NOS2); and to present antigens to T_H cells more proficiently by expressing higher amounts of the class II MHC than M2 macrophages (Mantovani & al., 2004). Notably, the cytokine TNF-α is an essential autocrine growth factor for macrophages and a major signal for M1 polarization (Witsell & Schook, 1992; Pagliari & al., 2000; Lombardo & al., 2007), although as its name suggests, it is also able to cause necrosis of tumours (Carswell & al., 1975; Wallach, 1984). Upon binding to its receptor, TNF-α activates signalling pathways that both induce and impede apoptosis. The proapoptotic pathway triggers the extrinsic caspase cascade, whereas the antiapoptotic pathways lead to the activation of the transcription factors activator protein (AP)-1 and nuclear factor (NF)-κB, which regulate a host of antiapoptotic, proliferative, and proinflammatory genes (Wajant & al., 2003). A cell's response to TNF-α depends upon which side the balance of pro- and antiapoptotic signalling tips. Unlike many other cells,

macrophages are able to disregard the apoptotic signals initiated by TNF-α by upregulating the ex-expression of antiapoptotic proteins that are induced also by other proinflammatory cytokines, such as IL-6 (Fukada & al., 2006; Takeda & al., 1998; Lin & al., 2001; Lombardo & al., 2007). After binding to its receptor, IL-6 activates STAT3, which regulates genes controlling cellular proliferation, survival, motility, and immunosuppression (Akira & al., 1994; Zhong & al., 1994; Dauer & al., 2005). Proinflammatory cytokines are therefore able to act synergistically to initiate inflammation and the polarization of M1 macrophages. Importantly, during the course of a normal immune response, macrophages gradually lose the proinflammatory M1 phenotype and shift towards the M2 end of the macrophage activation spectrum (Voll & al., 1997; Byrne & Reen, 2002; Antonios & al., 2013).

In contrast, cytokines secreted by T_H2 cells, such as IL-4 and IL-13, as well as lipids, fatty acids, and apoptotic cells polarize M2 macrophages. IL-4 activates STAT6, which regulates genes that induce macrophages to upregulate multiple types of scavenger receptors, such as CD163, and mannose receptor, C type (MRC)1 (also known as CD206), and phagocytose cellular debris more efficiently than M1 macrophages; to dampen inflammation by secreting immunosuppressive cytokines such as IL-10 and IL-13 and the enzyme arginase (ARG)-1; and to promote tissue remodelling and angiogenesis by secreting growth factors, such as vascular endothelial growth factors (VEGFs) and transforming growth factor (TGF)β (Mantovani & al., 2004). IL-10, like IL-6, also activates STAT3, but the effects of IL-6 and IL-10 are largely opposite (Lai & al., 1996; Niemand & al., 2003; Braun & al., 2012). IL-10 suppresses the expression of proinflammatory cytokines, class II MHC, and co-stimulatory molecules required for APCs to activate T_H and T_C cells, but activates T_{reg} cells (Fiorentino & al., 1991; de Waal Malefyt & al., 1991; Ding & Shevach, 1992; Ding & al., 1993; Chaudhry & al., 2011). Additionally, M2 macrophages – as well as activated lymphocytes and dendritic cells – upregulate the expression of inhibitory checkpoint ligands, such as programmed death receptor ligand (PD-L)1 (Liang & al., 2003). The receptor of PD-L1, programmed death receptor (PD)-1, is an immune checkpoint protein expressed by T_C cells (Agata & al., 1996). The binding of PD-L1 to PD-1 directly suppresses T_C cells and maintains the immune response at an appropriate intensity (Freeman & al., 2000). A very important anti-inflammatory cytokine produced by M2 macrophages is TFGβ, which regulates both immunosuppression, tissue remodelling, and angiogenesis (Fadok & al., 1998; Li & al., 2005; Massagué, 2008). By binding to its receptor, TGFβ activates the Smad transcription factors, whose effects on gene expression are highly dependent on the type of cell in question (Feng & Derynck, 2005). In the immunological context, TGFβ maintains immune tolerance by activating T_{reg} cells and inhibiting nearly all other cells of the innate and adaptive immune systems (Li & al., 2006; Massagué, 2008). In general, TGFβ is a growth inhibitor that regulates the production of growth factors by other cells. During wound healing, TGFβ co-ordinates the proliferation, differentiation, and migration of endothelial cells, fibroblasts, and myofibroblasts in angiogenesis and induces the synthesis of extracellular matrix (Massagué, 2008). Additionally, M2 macrophages express the immunosuppressive enzyme indoleamine 2,3-dioxygen-ase (IDO), which catabolizes L-tryptophan into kynurenine. The depletion of tryptophan obstructs the proliferation of all types of cells, but the kynurenine produced by IDO also activates T_{reg} cells directly (Mezrich & al., 2010). M2 macrophages preserve their functional plasticity and strongly respond to inflammatory stimuli, such as proinflammatory cytokines or bacterial lipopolysaccharide (LPS) (Stout & al., 2005; Zheng & al., 2013).

2.3 Clever-1 in Human & Mouse

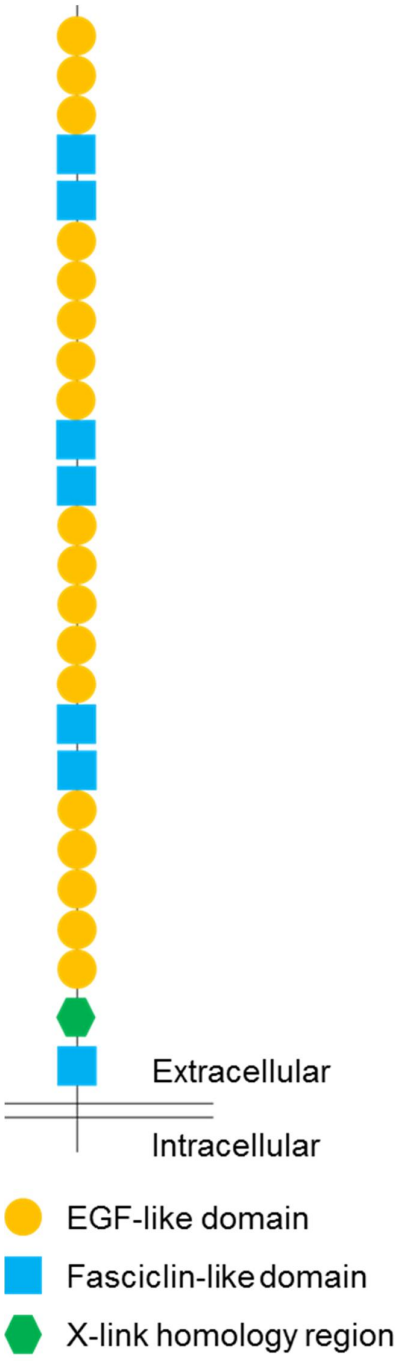

Figure 2. The Clever-1 protein. Clever-1 consists of a large extracellular portion with multiple domains EGF- and fasciclin-like domains, an X-link homology region, and a small cytoplasmic tail, which interacts with protein adaptors. The figure has been adapted from Kzhyshkowska & al. (2006b).

Clever-1 (from common lymphatic endothelial and vascular endothelial receptor 1) – also known as Stabilin-1 and Feel-1 (from fasciclin endothelial growth factor (EGF)-like, laminin-type EGF-like, and link-domain-containing scavenger receptor 1) – is a large, 270–300 kDa type I transmembrane protein coded by the *STAB1* gene in humans and the *Stab1* gene in mice (Adachi & Tsujimoto, 2002; Politz & al., 2002; Tamura & al., 2003). Structurally, the Clever-1 protein consists of a large extracellular portion, which contains seven fasciclin-like domains, several EGF-like domains, and one x-link homology region (see Figure 2) (Politz & al., 2002; Irjala & al., 2003a; Kzhyshkowska, & al., 2006b; Canton & al., 2013). The small intracellular tail of Clever-1 interacts with intracellular protein adaptors that direct its endosomal trafficking upon internalization (Kzhyshkowska & al., 2004; Adachi & Tsujimoto, 2010). Functionally, Clever-1 has been classified as a class H scavenger receptor, a group it shares only with its homologue, Stabilin-2 (Murphy & al., 2005). The Clever-1 and Stabilin-2 proteins are only 55 per cent identical, and while both bind acetylated low-density lipoprotein (LDL), their ligand repertoires, expression patterns, and subcellular localization are mostly divergent (Politz & al., 2002; Falkowski & al., 2003; Harris & al., 2004). For example, Stabilin-2 binds hyaluronic acid, but Clever-1 does not (Politz & al., 2002). Importantly, Stabilin-2 is absent from macrophages (Falkowski & al., 2003). The homology between human and mouse Clever-1 proteins, however, is 86 per cent, which indicates high evolutionary conservation of this protein between the two species (Politz & al., 2002).

Clever-1 is constitutively expressed on the discontinuous sinusoidal endothelia in the adrenal cortex, bone marrow, liver, lymph nodes, and spleen, as well as on post-capillary venous structures called high endothelial venules (Goerdt & al., 1991; Adachi & Tsujimoto, 2002; Irjala & al., 2003a; Prevo & al., 2004; Hansen & al., 2005; Martens & al., 2006; Qian & al., 2009). Inflammatory and proangiogenic stimuli can induce the expression of Clever-1 also on continuous vascular endothelia (Goerdt & al., 1991; Salmi & al., 2001). Additionally, specialized tissue macrophages in the colon, lymph nodes, placenta, skin, and stomach of both humans and mice and a subset of monocytes in the blood of humans – but not mice – have been

reported to express Clever-1 (Goerdt & al., 1991; Walsh & al., 1991; Prevo & al., 2004; Martens & al., 2006; Palani & al., 2011; Palani & al., 2016). The Kupffer cells in the liver make an exception, as they do not express Clever-1 (Martens & al., 2006).

On endothelial cells, Clever-1 functions as a cell adhesion molecule and regulates the trafficking of leukocytes through the lymphatic and vascular systems (Irjala & al., 2003a; Salmi & al., 2004; Karikoski & al., 2009; Shetty & al., 2015). However, neither granulocytes nor lymphocytes express Clever-1 themselves and at present, its counterpart on these leukocytes is unknown. Additionally, Clever-1 functions as a scavenger receptor on sinusoidal endothelial cells and macrophages, both of which are professional scavenger cells and express a wide variety of different types of scavenger receptors with many overlapping ligands and functions. Originally, scavenger receptors were characterized by their ability to bind and internalize oxidized LDL (Brown & Goldstein, 1979; Brown & al., 1979), but later discoveries have broadened the definition to include receptors involved in the binding and clearance of many other self- and non-self-molecules (Canton & al., 2013). In accordance with the classical definition of scavenger receptors, Clever-1 binds and internalizes acetylated and oxidized LDL, but also Gram-negative and -positive bacteria as well as phosphatidylserine, which is localized on the surface of apoptotic host cells (Adachi & Tsujimoto, 2002; Kzhyshkowska & al., 2005; Park & al., 2009). However, some of the identified ligands of Clever-1 exhibit exclusivity, which suggests functional specificity in addition to the functions it shares with other scavenger receptors.

Clever-1 is a widely accepted marker for M2 macrophages both *in vitro* and *in vivo* (Goerdt & al., 1991; Goerdt & al., 1993; Politz & al., 2002; Irjala & al., 2003a; Kzhyshkowska & al., 2004). Although it is expressed by a subset of monocytes in the blood in humans already under homoeostatic conditions (Palani & al., 2016), its expression is greatly increased when cultured *in vitro* in the presence of the glucocorticoid analogue and M2-polarizing factor dexamethasone even without IL-4, whereas M1-polarizing stimuli, such as IFN-γ, decrease its expression (Goerdt & al., 1993; Politz & al., 2002; Kzhyshkowska & al., 2004; Palani & al., 2016). The expression of Clever-1 on monocytes and macrophages has been associated with the anti-inflammatory phenotype of these cells. For example, in the placenta, Clever-1 maintains the immunosuppressive milieu that characterizes normal pregnancies but in pre-eclampsia, its expression is significantly decreased (Palani & al., 2016). Additionally, Clever-1 inhibits the activation of T_H1 cells *in vitro* (Palani & al., 2016). However, the molecular mechanisms by which Clever-1 regulates these anti-inflammatory functions in macrophages are very poorly understood.

Although Clever-1 has clear functions as a cell adhesion molecule and scavenger receptor on the cell surface, its localization is mostly intracellular in both macrophages and endothelial cells (Prevo & al., 2004; Salmi & al., 2004; Shetty & al., 2011). Interestingly, M2-polarizing stimuli appear to induce a change in the localization of Clever-1 from the cell surface to inside the cells, in addition to upregulating its expression (Kzhyshkowska & al., 2004; Palani & al., 2016). Accordingly, as its third major function, Clever-1 participates in the intracellular sorting and transportation of its ligands through distinct endosomal pathways (Kzhyshkowska & al., 2004). Some identified ligands of Clever-1 are SPARC (from secreted protein, acidic and rich in cysteine; also called osteonectin), placental lactogen, and SI-CLP (from Stabilin-1-interacting, chitinase-like protein) (Kzhyshkowska & al.,

2006a; Kzhyshkowska & al., 2006c; Kzhyshkowska & al., 2008). The intracellular trafficking of Clever-1 occurs through a number of pathways. Upon binding to Clever-1, SPARC and placental lactogen are endocytosed and eventually targeted for lysosomal degradation, after which some of the internalized Clever-1 is returned to the cell surface by recycling endosomes (Kzhyshkowska & al., 2006a; Kzhyshkowska & al., 2008). However, a portion of the endocytosed placental lactogen, at least, is redirected to the *trans*-Golgi network, where it dissociates from Clever-1 and accumulates in secretory vesicles (Kzhyshkowska & al., 2008). Additionally, Clever-1 transports SI-CLP from the Golgi apparatus through the *trans*-Golgi network to late endosomes, from where it is transferred to lysosomes and secreted (Kzhyshkowska & al., 2006c). The fact that Clever-1 participates in the transportation of synthesized protein through the Golgi apparatus and into secretory vesicles is particularly interesting in light of data that suggest that Clever-1 may regulate the secretion of specific cytokines from macrophages (Palani & al., 2011; Palani & al., 2016).

Two recent publications on the role of Clever-1 in cancer suggest it supports tumour growth and metastasis as well as the immunosuppressive milieu within the tumour microenvironment, which is discussed in more detail below (Karikoski & al., 2014; Riabov & al., 2016). Using wildtype and homozygous Clever-1 knockout (Clever-1$^{-/-}$) mice, Karikoski & al. (2014) have demonstrated that in the B16 mouse model of melanoma and the EL-4 mouse model of lymphoma, the deletion of Clever-1 inhibits tumour growth and metastasis. Importantly, this finding was replicated by immunotherapeutic Clever-1 antibody treatment. Similarly, Riabov & al. (2016) showed that Clever-1 supports tumour growth in the TS/A mouse model of breast cancer. However, the mechanisms by which Clever-1 regulates tumour growth and metastasis presented in these two publications are quite dissimilar. In Karikoski & al. (2014), Clever-1 aberrantly expressed by the tumour vasculature was found to selectively regulate leukocyte trafficking into the tumour microenvironment. Consequently, the disruption of Clever-1 decreased the numbers of tumour-associated M2 macrophages, defined by the expression of F4/80, a pan-macrophage marker, and CD206, as well as tumour-infiltrating T_{reg} cells, defined by the expression of Foxp3 – but not the numbers of total lymphocytes or T_C cells within the tumour. It was speculated that when the function of Clever-1 is disrupted, the anticancer immune response becomes more active, leading to reduced tumour growth. Additionally, disrupting endothelial Clever-1 inhibited the migration of malignant cells through the lymphatics, leading to reduced metastasis, as proposed by Irjala & al. (2003b). On the other hand, Riabov & al. (2016) present that the deletion of Clever-1 from TAMs leads to the accumulation of SPARC within the tumour microenvironment, which is toxic to the TS/A cancer cell line and therefore inhibits tumour growth. It is possible that the anticancer effect of Clever-1 depletion is mediated by both of these mechanisms, since Karikoski & al. (2014) did not study the clearance of SPARC and Riabov & al. (2016) did not study leukocyte trafficking or the different subpopulations of TAMs in the tumour microenvironment, or by different mechanisms in different types of cancers. Further studies are required in order to determine the immunotherapeutic relevance of these mechanisms, whether Clever-1 might regulate tumour growth and metastasis by other as yet uncovered mechanisms, and whether these effects are replicable in other models of cancer.

2.4 Cancer & the Immune Response

Cancer is a large group of diverse diseases in which normal cellular behaviour has become disrupted during a process called carcinogenesis. Typical cancers develop over decades by the gradual accumulation of genomic mutations that alter the functions of key proto-oncogenes and tumour suppressor genes. These mutations demolish the regulatory mechanisms that have enabled the development of multicellular life, leading to uncontrolled cell proliferation and the formation of a tumour. The final step of carcinogenesis occurs when neoplastic cells undergo malignant transformation and gain the ability to invade their surrounding tissues and migrate throughout the host to form metastases. Hanahan & Weinberg have conceptualized the enabling characteristics of carcinogenesis and the hallmark features shared by nearly all cancers. Both the enabling characteristics and the hallmarks of cancer highlight the significant role of the immune system in the development of cancer. The enabling characteristics – genomic instability and tumour-promoting inflammation – are a requisite for the initiation and progression of carcinogenesis and support the six hallmarks of established cancers, which are autonomous growth signalling, disregard of growth inhibitory signals, evasion of apoptosis, unlimited proliferation, angiogenesis, and invasion and metastasis (Hanahan & Weinberg, 2000; Hanahan & Weinberg, 2011). Two additional, emerging hallmarks of cancer are the reprogramming of cellular energy metabolism and escaping destruction by the immune system (Hanahan & Weinberg, 2011). Notably, cancers cannot achieve these hallmarks without manipulating the untransformed cells of the host – cells of the immune system and the tumour's tissue of origin – into supporting carcinogenesis. The tumour-promoting activity of accessory cells is considered an additional extrinsic hallmark of cancer (Hanahan & Coussens, 2012).

The immune system actively protects the host from cancer by several mechanisms: It prevents and eradicates infection that may in itself be carcinogenic by causing genomic instability, resolves inflammation that can promote the growth of tumours, and sends NK and T_C cells to dispatch neoplastic cells (Dunn & al., 2002; Pagano & al., 2004; Balkwill & al., 2005). Still, the immune system plays a major part in enabling carcinogenesis (Hanahan & Coussens, 2012). These contradictory roles can, in part, be explained by the three-tier process of cancer immunoediting (Dunn & al., 2002; Dunn & al., 2004). As described above, the immune system is able to directly recognize and kill neoplastic host cells during normal immune surveillance. This is called the elimination phase. However, some neoplastic cells can be less immunogenic or more resistant to killing than others, and survive. Thus, the immune system itself participates in the natural selection of neoplastic cells that are able to evade destruction by the immune system (Khong & Restifo, 2002). These neoplastic cells continue growing and accumulating mutations during the equilibrium phase. Eventually, in the escape phase, the neoplastic cells have acquired such mutations that they are no longer targeted for killing by the immune system but rather manipulate it to maintain tumour-promoting inflammation, and the tumour can grow unimpeded. Often, neoplastic cells downregulate immunogenic cell surface molecules, such as class I MHC, stimulatory ligands, and cell adhesion molecules, modulate tumour-specific antigens, and even create physical barriers of extracellular matrix that prevent leukocytes from coming into direct contact with them (Stackpole & al., 1980; Piali & al., 1995; Restifo & al., 1996; Jäger & al., 1998; Raffaghello & al., 2004; Salmon & al., 2012). Other common strategies used by tumours to escape immune surveillance and destruction are repurposed from the immune system's

own toolbox. Many activated oncogenes are normally key mediators of both pro- and anti-inflammatory immune responses. Most tumours secrete a cocktail of both proinflammatory and immunosuppressive cytokines, such IL-6, TNF-α, IL-10, and TGFβ (Naylor & al., 1993; Alleva & al., 1994; Conze & al., 2001; Kulbe & al., 2007; Zins & al., 2007), which maintains tumour-promoting inflammation and suppresses the anticancer immune response but may also directly support the neoplastic cells. As mentioned above, TNF-α activates NF-κB, which has emerged as a central tumour-promoting transcription factor in addition to its immunological functions (Karin, 2006). Some cancers have mutations in pathways up- and downstream of NF-κB that allow them to become resistant to the apoptotic effects of TNF-α and use it as a growth factor instead (Courtois & Gilmore, 2006). The processes mediated by IL-6 and STAT3 are also taken advantage of by many different cancers to proliferate and escape apoptosis as well as to suppress the immune response (Yu & al., 2007; Grivennikov & Karin, 2008). Similarly, some mutations allow cancers to bypass the growth inhibitory signals of TGFβ and appropriate it for immunosuppression, proliferation, and angiogenesis (Massagué, 2008). Most disturbingly, TGFβ is a potent inducer of epithelial-mesenchymal transition in malignantly transformed cells, a major step in invasion and metastasis (Massagué, 2008; Xu & al., 2009). Additionally, many tumours begin to express IDO and inhibitory immune checkpoint ligands, such as PD-L1, that suppress the immune response (Dong & al., 2002; Uyttenhove & al., 2003).

While the tumour shapes the immune response, the immune response shapes the tumour. As noted above, inflammation itself can be a driving force of carcinogenesis and lead to the activation of immunosuppressive mechanisms within the tumour (Balkwill & al., 2005; Mantovani & al., 2008). Additionally, all tumours elicit an inflammatory response themselves and contain varying amounts of infiltrating leukocytes, the most numerous of which are typically tumour-associated macrophages (TAMs) and tumour-infiltrating lymphocytes (TILs) (Ruffell & al., 2012). In many ways, a tumour looks like a wound to the immune system (Dvorak, 1986). The tumour's parenchyma and its surrounding stroma, which together make up the tumour microenvironment, are characteristically acidic and hypoxic and contain an abundance of necrotic cell death because of the unusual metabolic properties of neoplastic cells, the avoidance of apoptosis, and their poorly functioning vasculature (Hanahan & Weinberg, 2011). As a result, the tumour microenvironment contains a multitude of DAMPs as well as tumour-associated and -specific antigens, which are taken up and recognized by macrophages and DCs. Consequently, the immune system initiates an inflammatory response towards the tumour in an attempt to heal it – but which turns into chronic, tumour-promoting inflammation (Dvorak, 1986; Balkwill & al., 2005; Mantovani & al., 2008). Thus, the normal restorative features of M2 macrophages – the principal cells maintaining chronic inflammation – turn against the host and support carcinogenesis instead. However, neither the highly variable phenotypes of TAMs nor their tumour-promoting activity can be explained by a one-way response against the tumour alone. The cocktail of cytokines and other factors secreted by the neoplastic cells directly modulates the tumour's stromal cells, TAMs, and other infiltrating immune cells – whose altered functions, in turn, affect the tumour (Nakamura & al., 1997; Hagemann & al., 2006; Duluc & al., 2007; Bayne & al., 2012; Hollmén & al., 2015a; Kano, 2015). Additionally, tumours may secrete factors that attract and support the uptake and differentiation of only certain types of leukocytes. For example, tumour-derived colony-stimulating factor (CSF)-1 (also known as macrophage colony-

stimulating factor) and IL-34 selectively recruit monocytes into the tumour microenvironment by binding to the CSF-1 receptor (CSF-1R; also known as CD115), which is primarily expressed by monocytes and M2 macrophages (Martinez & al., 2006; Foucher & al., 2013; Stratchan & al., 2013; Ségaliny & al., 2015). Thus, TAMs gain their tumour-promoting properties through a complex back-and-forth between the tumour parenchyma, stroma, and leukocyte infiltrate, where each constituent affects the others (Biswas & Mantovani, 2010; Hanahan & Coussens, 2012; McAllister & Weinberg, 2014; Noy & Pollard, 2014; Ostuni & al., 2015).

Reciprocally, TAMs assist the tumour in acquiring nearly all of the hallmarks of cancer (Biswas & Mantovani, 2010). Usually, TAMs in established tumours exhibit an anti-inflammatory, M2-like phenotype (Biswas & al., 2006). TAMs are efficient at phagocytosis and express many well-established markers of M2 macrophages, such as CD115, CD163, and CD206 – as well as Clever-1 (Lin & al., 2001; Pucci & al., 2009; Movahedi & al., 2010; Pettersen & al., 2011; David & al., 2012). Typically, TAMs have impaired antigen presentation through the downregulation of class II MHC (Wang & al., 2011). The enzyme ARG-1 produced by TAMs depletes the main source of nitric oxide, L-arginine, which is essential for T cells and is instead used to create L-ornithine and polyamines that promote tissue remodelling (Gillette & Mitchell, 1991; Rodriguez & al., 2003; Rodriguez & al., 2004). TAMs also express the enzyme IDO, which activates T_{reg} cells (Zhao & al., 2012). TAMs secrete low levels of proinflammatory cytokines, such as IL-12, but larger amounts of immunosuppressive cytokines and proangiogenic factors, such as IL-10, TGFβ, and VEGFs (Biswas & al., 2006; Lin & al., 2006; Ojalvo & al., 2009; Ruffell & al., 2014), which may also be expressed by the tumour, as described above. These cytokines suppress the functions of NK, T_C, and T_H1 cells but activate T_H2 and T_{reg} cells that further suppress the anticancer immune response and promote the polarization of M2 TAMs by secreting IL-4, IL-10, and IL-13 (DeNardo & al., 2009; Gocheva & al., 2010; Ruffell & al., 2014). Thus, the tumour microenvironment is able to programme TAMs with a tumour-promoting, M2-like phenotype that is strengthened through their interaction with the adaptive immune system. However, it must be noted that TAMs also express many markers that are not typical of M2 macrophages. Although TAMs produce little nitric oxide, they still express NOS2 and use it to suppress the functions of effector T cells in the tumour microenvironment (Hofseth & al., 2003; Nagaraj & al., 2007; Lu & al., 2011; Molon & al., 2011). In addition to immunosuppressive cytokines, TAMs may secrete major proinflammatory cytokines, such as TNF-α and IL-6 (Hagemann & al., 2004; Solinas & al., 2010), which is typically a defining property of M1 macrophages. In the tumour microenvironment, however, these proinflammatory cytokines can promote the growth of the tumour rather than hinder it (Balkwill & al., 2005; Mantovani & al., 2008). Additionally, TNF-α can induce the expression of PD-L1 by macrophages, which suppresses effector T cells directly (Kuang & al, 2009; Kondo & al., 2010). However, the phenotypes of TAMs located in different parts of the tumour are highly heterogeneous, and the same TAMs do not necessarily express the contradictory M1 and M2 markers simultaneously (Movahedi & al., 2010; Pettersen & al., 2011; Wang & al., 2011; Laoui & al., 2014).

2.5 Immunotherapies for Activating the Anticancer Immune Response

The therapeutic potential of activating the host's immune system to treat cancer has been acknowledged decades ago (Mitchison, 1955). Although cancers are able to escape detection and destruction by a variety of different mechanisms, as described above, novel immunotherapeutic treatments have reached the market that prove it possible to activate the anticancer immune response even in patients with advanced cancer. The immunotherapies currently on the market may be classified as therapeutic antibodies that target tumour-associated or -specific antigens; immune checkpoint antagonists that inhibit cancer-derived immunosuppressive signals; and immune system modulators, such as cytokines and CSF-1R antagonists. Other immunotherapies, namely cancer treatment vaccines and immune cell therapy (Kantoff & al., 2010; Maude & al., 2014), may be technically innovative and show high clinical efficiency, but they are not a realistically accessible treatment option for the vast majority of patients with cancer.

Therapeutic antibodies target molecular structures that are expressed primarily by or are specific to neoplastic cells. By binding to their epitope, therapeutic antibodies lead to the destruction of the tumour by apoptosis, antibody-dependent cell-mediated cytotoxicity, or complement-dependent cytotoxicity. A famous example of therapeutic antibodies is trastuzumab, which is used in the treatment of HER2-positive breast cancer. HER2 is an EGF receptor and a proto-oncogene, which is amplified or overexpressed in some types of aggressive breast cancers (Slamon & al., 1987; Reese & Slamon, 1997). Trastuzumab inhibits mitogenic signalling through HER2 and leads to the death of neoplastic cells that overexpress HER2 by antibody-dependent cell-mediated cytotoxicity (Vu & Claret, 2012). Therapeutic antibodies may also be coupled with toxic cargoes such as chemotherapeutic agents, as is the case with trastuzumab emtansine, where the mitotic inhibitor mertansine has been covalently linked to trastuzumab. The antibody-coupled chemotherapeutic agent is efficiently targeted to the tumour, which limits its adverse effects. While therapeutic antibodies have proven efficient in the clinic, they do not directly affect the immune system as such and therefore will not be discussed in further detail here.

An interesting approach to the immunotherapeutic treatment of cancer is the inhibition of immune checkpoints (Pardoll, 2012). The physiological purpose of immune checkpoint proteins, such as cytotoxic T lymphocyte-associated antigen (CTLA)-4 as well as PD-1 and PD-L1, which were discussed above, is to inhibit immune responses from mounting against the host because of their potential to cause injury and autoimmune diseases. The activation of checkpoint proteins leads to immunosuppression, and, therefore, inhibiting the activation of checkpoint proteins in the treatment of cancer promotes the anticancer immune response. Immune checkpoints suppress the effector cells of the immune system at various different stages of the immune response. For example, CTLA-4 moderates the activation of naïve T cells in the lymph nodes by capturing the co-stimulatory ligand B7, which is presented by APCs in conjunction with antigen coupled to the class I MHC. The inhibitory co-receptor CTLA-4 binds to B7 with a much higher affinity than the stimulatory co-receptor CD28, thus decreasing the stimulatory signal received by naïve T cells and inhibiting their excessive activation. On the other hand, PD-1 and PD-L1 suppress the functions of T_C cells in peripheral tissues. After activation, T_C cells begin to express PD-1, whose ligand PD-L1 is expressed

by normal cells of the host that use it as a means of evading immune destruction – a strategy taken advantage of by many cancers as well, as discussed above.

Well-known examples of immune checkpoint antagonists used as cancer immunotherapies are ipilimumab, which targets CTLA-4, and nivolumab and pembrolizumab, which target PD-1. Ipilimumab prevents the inhibitory co-receptor CTLA-4 from binding to the co-stimulatory B7 ligand and frees it to bind CD28, which leads to the increased differentiation of naïve T cells into effector cells and strengthens the anticancer immune response. On the other hand, nivolumab and pembrolizumab prevent PD-1 from binding to its ligands in peripheral tissues and the tumour microenvironment, which inhibits the suppression of effector T_C cells and enhances the anticancer immune response as well. Ipilimumab has been approved for use in the treatment of melanoma, whereas nivolumab is approved for the treatment of non-small-cell lung carcinoma and pembrolizumab for the treatment of melanoma as well as non-small-cell lung carcinoma by the European Medicines Agency (EMA). The search for new indications for the existing immune checkpoint inhibitors as well as for novel immune checkpoint modulators targeting other immune checkpoints at different steps of the immune response are active areas of research in cancer immunology. However, even though ipilimumab, nivolumab, and pembrolizumab have proven effective in the treatment of some cancers, they have not been as successful in the treatment of others (e.g., Royal & al., 2010; Le & al., 2013).

Immunotherapies that directly modulate the immune system may be cytokines, such as interleukins and interferons, or inhibitors of cytokines and their receptors, such as CSF-1R antagonists. The first immunotherapeutic cancer treatment that directly modulated the patient's immune system was a recombinant IL-2 protein. Among its other functions, IL-2 is essential for the expansion of effector T cells, and, therefore, its effects are often suppressed in cancer. Treating patients with recombinant IL-2 results in a powerful adaptive anticancer immune response and tumour regression in advanced melanoma and renal cancer, but does so rarely in other types of cancers (Rosenberg, 2014). Currently, IL-2 is approved for use in the treatment of renal cell carcinoma by EMA. Type I interferons, on the other hand, have a wide range of regulatory functions in the host, and in cancer they mediate antiproliferative effects and the anticancer immune response. Type I interferons have proven efficient in the treatment of some haematological cancers, but in the treatment of solid cancers, their success has been less consistent (Parker & al., 2016). Currently, IFN-α_{2B} is approved for use in the treatment of various types of leukaemia as well as melanoma, carcinoid tumours, and chronic hepatitis B and C by EMA. More specific immune system modulators are required for the efficient immunotherapeutic treatment of other types of cancers for which these treatment options have not been sufficient.

Because of the important tumour-promoting functions of TAMs discussed above, more specific immunotherapeutic approaches aimed at preventing the recruitment and polarization of TAMs have recently been the focus of intensive research (Ruffell & Coussens, 2015). Some current immune system modulators aimed at TAMs are either neutralizing antibodies or small molecules that antagonize CSF-1R by directly blocking the binding of its ligands, CSF-1 and IL-34. CSF-1R antagonists reduce the total amount of infiltrating myeloid cells and increase the proinflammatory

phenotype of TAMs in the tumour microenvironment as well as improve the anticancer immune response. The disruption of signal transduction through CSF-1R has been a successful treatment strategy in a variety of cancer models, including animal models of breast cancer, glioma, pancreatic cancer, and thyroid cancer (Aharinejad & al., 2004; Paulus & al., 2006; Pyonteck & al., 2013; Ryder & al., 2013; Ries & al., 2014; Zhu & al., 2014), as well as in preliminary data from an ongoing phase I clinical trial, where CSF-1R antagonists have been studied both alone and in combination with chemotherapy (Ries & al., 2014). However, in some types of cancers, the wholesale depletion of $CD115^+$ macrophages with CSF-1R antagonists may have detrimental effects, such as the increased incidence of metastasis (Swierczak & al., 2014; Hollmén & al., 2015b).

Even though novel immunotherapies, such as immune checkpoint antagonists and immune system modulators, have proven effective in the treatment of some types of cancer, they are not efficient in the treatment of others. Interestingly, combining CSF-1R antagonism with other immunotherapies or chemotherapy potentiates the effects of both treatments (DeNardo & al., 2011; Mitchem & al., 2013; Mok & al., 2014). Similarly, in an animal model of pancreatic ductal adenocarcinoma, combinatorial immune system modulation with CSF-1R antagonists and immune checkpoint inhibition with CTLA-4 or PD-1 antagonists was more efficient than any of these treatments alone (Zhu & al., 2014). Moreover, the increased incidence of metastasis caused by CSF-1R antagonists could be prevented by the simultaneous antagonism of CSF-3R (also known as granulocyte colony-stimulating factor receptor) (Swierczak & al., 2014). Accordingly, the potential synergistic effects of immunotherapies in combination with each other or with chemotherapy in the treatment of many different types of cancers are an active area of both preclinical and clinical research. Further studies are required to fully understand the most efficient combinations of different immunotherapies. The development of screening strategies is of utmost important in order for clinicians to differentiate the patients who would benefit the most from certain combinations of immunotherapies.

3 Aims of the Thesis

The aims of this master's thesis were to:

- Investigate the molecular mechanisms by which Clever-1 regulates the phenotype and function of M2 macrophages;
- Investigate the immunotherapeutic potential of Clever-1 antibody treatment in two mouse models of breast cancer; and
- Investigate the immunomodulatory effects of Clever-1 antibody treatment on TAMs.

Based on previous publications and our unpublished data, Clever-1 appears to have a role in regulating the anti-inflammatory phenotype of M2 macrophages (Kzhyshkowska & al., 2004; Palani & al., 2011; Palani & al., 2016). However, the molecular mechanisms used by Clever-1 to exert these effects are unknown. The first aim of this thesis was to study how Clever-1 regulates the anti-inflammatory phenotype and functions of M2 macrophages with antibody-mediated interference and Clever-1$^{-/-}$ mice. In particular, the regulation of the anti-inflammatory mTORC1 signalling pathway and the production and secretion of cytokines by M2 macrophages was studied by flow cytometry and enzyme-linked immunosorbent assay (ELISA).

Recent publications by Karikoski & al. (2014) and Riabov & al. (2016) suggest that Clever-1 antibody treatment may have immunotherapeutic potential in the treatment of cancer. Based on the literature reviewed above, the anticancer effects of Clever-1 antibody treatment could be mediated by a variety of mechanisms, including regulation of leukocyte trafficking, regulation of angiogenesis, regulation of metastasis, regulation of tumour-promoting inflammation, and regulation of the composition of the tumour microenvironment. The second aim of this master's thesis was to study whether Clever-1 antibody treatment has an effect on tumour growth and metastasis in two orthotopic mouse models of breast cancer induced with the cancer cell lines E0771 and 4T1. Tumour growth was monitored with digital callipers and metastasis by luminescence photometry with the luciferase-expressing cancer cell line 4T1-luc2.

Because Clever-1 is primarily expressed by M2 macrophages and M2 TAMs, it is hypothesized that the antibody-mediated interference of Clever-1 will disrupt the anti-inflammatory phenotype of M2 TAMs, which, in turn, should activate the anticancer immune response. The third aim of this master's thesis was to study the effects Clever-1 antibody treatment on the phenotype of TAMs. The phenotypic analysis of TAMs was performed by flow cytometry.

4 Materials & Methods

4.1 Experimental Animals

The mice used for experimentation were housed at the Central Animal Laboratory of the University of Turku. The mice were kept in a 12-hour light/dark cycle with controlled humidity and temperature. Food and water were provided *ad libitum*. The wildtype mouse strains used were C57/BL6N and BALB/c. Additionally, the Clever-$1^{-/-}$ mice and their wildtype littermates were from the mixed background C57BL/6N:129/SvJ. All animal experiments were performed in compliance with the 3Rs principles and the Finnish Act on Animal Experimentation (62/2006) and accepted by the local Committee for Animal Experimentation (licence number 5587/04.10.07/2014).

4.2 Primary Cell Culture

Blood was collected from CO_2-asphyxiated mice by cardiac puncture. Red blood cells were removed with BD Pharm Lyse™ lysing buffer (BD Biosciences, catalogue number 555899) and the remaining leukocytes were collected by centrifugation at 400 *g* for 10 min. The peritoneal exudates and bone marrows were collected from CO_2-asphyxiated mice as described by Zhang & al. (2008). For M2 polarization, the cells were cultured in 6-well plates first for four days with 20 ng/mL of CSF-1 (BioLegend®, catalogue number 576406) in IMDM (Gibco™, catalogue number 12440053) supplemented with L-glutamine (GlutaMAX™-I, Gibco™, catalogue number 35050038), 10 % foetal calf serum (FCS) and penicillin and streptomycin (P/S) (complete IMDM) and then an additional three days with 20 ng/mL of CSF-1 and 10 pmol/mL of dexamethasone in complete IMDM. After polarization, the M2 macrophages were used as such or detached with 10 mM EDTA in phosphate-buffered saline (PBS) and transferred to 96-well ultra-low attachment plates for experimental treatments.

All $CD11b^+$ myeloid cells were isolated from digested tumours after surface staining with R-PE-conjugated antibody against CD11b by positive immunomagnetic selection with the mouse PE selection kit (Stemcell™ Technologies, catalogue number 18554) on the EasySep® magnet (Stemcell™ Technologies, catalogue number 18000) according to the manufacturer's instructions. TAMs were left to attach to cell culture dishes overnight in complete IMDM, after which the unattached cells were washed away and the remaining cells visually identified as macrophages. TAMs were then used for experimental treatments.

Primary human monocytes were isolated from the blood of healthy volunteers. First, the peripheral blood mononuclear cells were isolated by Ficoll-Paque® density gradient centrifugation. Then, the isolated cells were left to attach to cell culture dishes overnight in complete IMDM. On the following day, the unattached cells were washed away with PBS and the attached cells were visually identified as monocytes, which were then subjected to experimental treatments.

4.3 Cancer Cell Lines & Cancer Models

The murine cancer cell lines E0771 and 4T1 were maintained in RPMI-1640 (Sigma-Aldrich®, catalogue number R5886) supplemented with L-glutamine (GlutaMAX™-I, Gibco™, catalogue number

35050038), 10 % FCS, and P/S. The E0771 cancer cell line, a kind gift from Professor Burkhard Becher (University of Zurich, Zurich, Switzerland), was originally isolated from a spontaneous mammary gland adenocarcinoma from the C57/BL6 mouse strain (Sugiura & Stock, 1952). The 4T1 cancer cell line is a metastatic variant of the 410.4 cancer cell line that was originally isolated from a spontaneous mammary tumour from the BALB/c mouse strain (Aslakson & Miller, 1992). Both of these cancer cell lines form tumours when injected orthotopically into the mammary fat pads of female mice. Additionally, the tumours formed by these cancer cell lines are metastatic. The 4T1 cancer cell line used in this master's thesis (purchased from Caliper Life Sciences) has been genetically modified to express luciferase, which enables the detection of metastases from different organs.

For the induction of tumours, 1.0×10^6 or 0.1×10^6 E0771 or 4T1 cancer cells in 50 µL of PBS were inoculated orthotopically into the mammary fat pads of syngeneic female mice as detailed for each experiment. Tumour growth was monitored with digital callipers every 2–3 days. The humane endpoint set in the animal licence was the tumour reaching 1 cm in diameter. Mice whose tumours reached the humane endpoint before the end of the experiment were euthanized. The horizontal and vertical diameters were used to calculate tumour areas ($d_{\text{vertical}} \times d_{\text{horizontal}}$). Following experiments, the tumours were resected, minced with scissors, and digested with 10 mg/mL of collagenase IV, 1.0 mg/mL of DNase I, and 2.25 µM of $CaCl_2$ on a shaker at 37 °C for 30 min. The liberated cells were filtered through a 70 µm nylon strainer and aliquoted for further use.

4.4 Antibody Treatments

The antibodies used for both *in vitro* and *in vivo* treatments have been compiled in Table 1.

For *in vitro* treatments, M2 macrophages, primary human monocytes, or TAMs were seeded at approximately 0.5×10^6 cells/mL in IMDM (Gibco™, catalogue number 12440053) without serum into 6-well plates. Indicated antibodies were added at 20 µg/mL. For the analysis of secreted TNF-α, the cells were incubated with antibody at 37 °C for the time periods indicated for each experiment, after which the supernatants were collected and analysed by ELISA. For the analysis of intracellular TNF-α, the cells were seeded into 96-well ultra-low attachment plates and incubated with antibody at 37 °C for 6 h with 10 µg/mL of brefeldin A and with or without 0.1 µg/mL of LPS, after which the cells were collected, stained, and analysed by flow cytometry.

Table 1. Antibodies used for treatments in both *in vitro* and *in vivo* experiments. Antibodies without indicated antigens are isotype controls.

Antigen	Clone	Host	Isotype	Supplier
human Clever-1	Fu HI-3-372/2	mouse	IgG_1	InVivo
murine Clever-1	mStab1-1.26	mouse	IgG_1	InVivo
murine PD-1	RMP1-14	rat	IgG_{2a}	BioXCell
murine PD-L1	10F.9G2	rat	IgG_{2b}	BioXCell
–	2A3	rat	IgG_{2a}	BioXCell
–	AK-1	mouse	IgG_1	InVivo
–	LTF-2	rat	IgG_{2b}	BioXCell
–	MOPC-21	mouse	IgG_1	BioXCell

For *in vivo* treatments, the indicated antibodies were administered by intraperitoneal injection in doses of 100 µg in 150 µL of PBS every 2–3 days starting on day 3 or 4 after cancer cell inoculation. The duration of each experiment, the numbers of administered doses, and the numbers of animal per control and treatment groups are detailed in the results for each experiment.

4.5 Flow Cytometry

The antibodies used for flow cytometric staining have been compiled in Table 2. All centrifugations in these protocols were performed at 300 *g* for 5 min. All flow cytometry samples were run on the BD LSRFortessa™ and analysed with the FlowJo single cell analysis software (v. 10.1).

For surface staining, cells were collected in EPICS I (PBS supplemented with 2.0 % FCS and 0.2 % NaN_3) and divided to 96-well plates. Antibodies were diluted 1:200 with BD Fc Block™ (BD Pharmingen™, catalogue number 553141), added to the cells in 50 µL of EPICS I, and incubated on ice for 30–45 min on ice in dark, after which the cells were washed twice by centrifugation with 200 µL of EPICS I, re-suspended in 200 µL of EPICS II (PBS supplemented with 0.2 % NaN_3), and analysed by flow cytometry or fixed with 4 % formaldehyde for 15 min at room temperature, washed twice with EPICS II, and stored at +4 °C.

For surface staining of unconjugated primary antibodies, conjugated secondary antibodies were diluted 1:500, added to the cells in 50 µL of EPICS I, and incubated on ice in the dark for 30–45 min, after which the cells were washed twice with 200 µL of EPICS I, re-suspended in 200 µL of EPICS II, and analysed by flow cytometry or fixed with 4 % formaldehyde for 15 min at room temperature, washed twice with EPICS II, and stored at +4 °C.

For intracellular staining, cells were first surface stained as described above and then fixed with 4 % formaldehyde at room temperature for 15 min and permeabilized with 0.2 % saponin or fixed and permeabilized with methanol at −20 °C for 30 min and washed twice with EPICS I. Saponin permeabilization was used for the detection of intracellular Clever-1 and TNF-α, whereas methanol permeabilization was used for the detection of phosphoproteins (but also works for the detection of Clever-1). For saponin-permeabilized cells, antibodies were diluted 1:200, added to the cells in 50 µL of 0.2 % saponin, and incubated at room temperature in the dark for 45–60 min, after which the cells were washed once with 0.2 % saponin, once with EPICS I, re-suspended in 200 µL EPICS II, and analysed by flow cytometry. For methanol-permeabilized cells, antibodies were diluted 1:200, added to the cells in 50 µL of EPICS I, and incubated on ice in the dark for 45–60 min, after which the cells were washed twice with EPICS I, re-suspended in 200 µL of EPICS II, and analysed by flow cytometry.

4.6 ELISA

Cellular debris was removed from the supernatants by centrifugation at 10,000 *g* for 10 min. Supernatants were stored at −80 °C until use. ELISA was performed and analysed according to the manufacturer's instructions. Mouse TNF-α was analysed with the mouse TNF-α ELISA kit (Thermo

Scientific™, catalogue number KMC3012) and human TNF-α with the human TNF-α ELISA kit (Thermo Scientific™, catalogue number KHC3011).

4.7 *Ex Vivo* Imaging

Metastasis in the 4T1 cancer models was analysed by *ex vivo* imaging with IVIS® Spectrum (Perkin-Elmer). Mice were administered 150 mg/kg of D-luciferin, sodium salt (SynChem, Inc.) by intraperitoneal injection, ten minutes after which they were CO_2-asphyxiated and the draining inguinal lymph nodes and lungs were dissected and imaged with the following settings: exposure time = 10 s (lungs) or 60 s (lymph nodes and livers), f/top = 1, medium binning, field of view = 3.9 × 3.9 cm². The luminescence signals were quantified with the Living Image software and reported as units of tissue radiance (photons/s/cm²/sr). Signal above background was considered a positive metastasis for assessing the incidence of metastasis on a yes or no basis.

4.8 Statistical Analysis

All data are presented as mean ± standard error of the mean (s.e.m.). Statistical analyses were performed with GraphPad Prism® 4. The boundary of statistical significance was set at $p < 0.05$. For simplicity, in the text, $p < 0.05$, $p < 0.01$, and $p < 0.001$ were used to denote whether the difference between groups was statistically significant, very statistically significant, or highly statistically significant, respectively. In the figures, the levels of significance have been marked with asterisks (*, $p < 0.05$; **, $p < 0.01$; and ***, $p < 0.001$). Statistical significances have been determined by paired or unpaired two-tailed Student's *t*-tests unless otherwise stated. Paired *t*-tests were used when one sample had been divided for different treatments. Unpaired *t*-tests were used when the samples were from different individuals. When the variance between two groups was determined significantly unequal, Welch's correction was applied. For the growth curves, control and treatment groups were compared to each other with two-way ANOVA and individual time points to each other by unpaired two-tailed Student's *t*-test.

Table 2. Antibodies used for flow cytometric staining. For conjugates, refer to separate experiments. All antibodies in this table have been raised against the indicated murine antigen. Antibodies without indicated antigens are isotype controls.

Antigen	Clone	Host	Isotype	Supplier
CD3	17A2	rat	IgG_{2b}, κ	BD Biosciences
CD11b	M1/70	rat	IgG_{2a}, κ	BD Biosciences
CD45	30-F11	rat	IgG_{2b}, κ	eBioscience
CD115	AFS98	rat	IgG_{2a}, κ	eBioscience
CD117	ACK2	rat	IgG_{2b}, κ	BioLegend®
CD135	A2F10.1	rat	IgG_{2a}, κ	BD Biosciences
CD206	unavailable	rat	IgG_2	AbD Serotec
Clever-1	mStab1-1.26	mouse	IgG_1	InVivo
class II MHC	M5/114.15.2	rat	IgG_{2b}, κ	eBioscience
F4/80	BM8	rat	IgG_{2a}, κ	eBioscience
Ly-6C	HK1.4	rat	IgG_{2c}, κ	eBioscience
Ly-6G	1A8	rat	IgG_{2a}, κ	BioLegend®
PD-L1	MIH5	rat	IgG_{2a}, λ	BD Biosciences
p-4E-BP1	V3NTY24	mouse	IgG_{2b}, κ	eBioscience
p-mTOR	MRRBY	mouse	IgG_{2a}, κ	eBioscience
p-RPS6	cupk43k	mouse	IgG_1, κ	eBioscience
TNF-α	MP6-XT22	rat	IgG_1, κ	eBioscience
–	AK-1	mouse	IgG_1	InVivo
–	B39-4	rat	IgG_{2a}, λ	BD Biosciences
–	eBM2a	mouse	IgG_{2a}, κ	eBioscience
–	eBMG2b	mouse	IgG_{2b}, κ	eBioscience
–	eBR2a	rat	IgG_{2a}, κ	eBioscience
–	eBRG1	rat	IgG_1, κ	eBioscience
–	NS-1	mouse	IgG_1	InVivo
–	P3.6.2.8.1	mouse	IgG_1, κ	eBioscience
–	unavailable	rat	IgG_2	AbD Serotec

5 Results

5.1 Clever-1 is expressed by inflammatory Ly-6C^{high} monocytes in the blood and bone marrow of mice under homoeostatic conditions

Recently, our group has reported that Clever-1 is expressed on the surface of a subset of primary monocytes in the blood of humans under homoeostatic conditions (Palani & al., 2016). Therefore, it was investigated whether different monocyte and macrophage populations in mice also express Clever-1 under homoeostatic conditions using either the biotinylated NS-1 isotype control or the antibody against murine Clever-1 (the clone mStab1-1.26, referred to here as mStab1) as the primary antibody and R-PE-conjugated streptavidin as the secondary, fluorescent label in order to increase

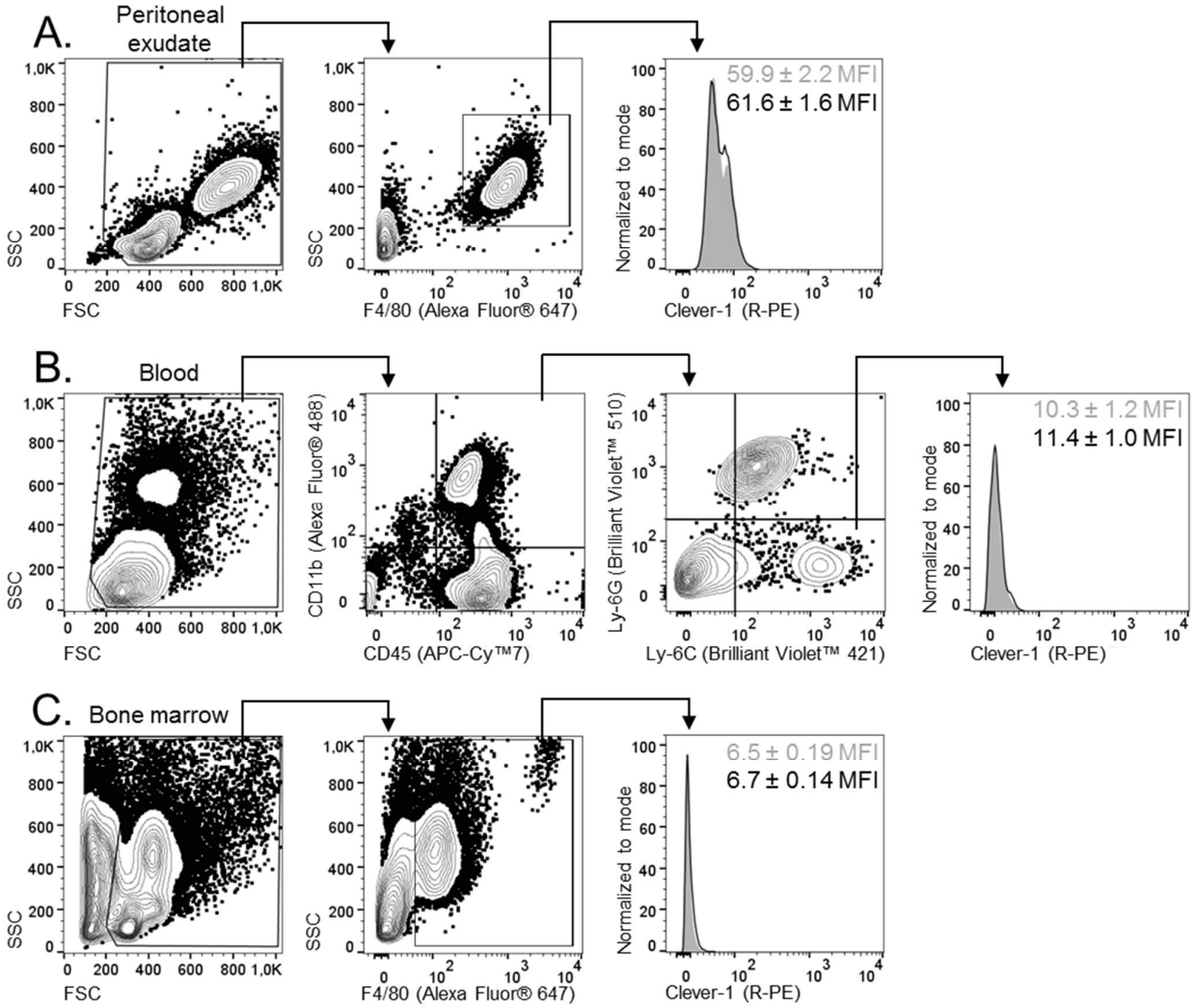

Figure 3. Clever-1 expression on the cell surface of different monocyte and macrophage populations in the mouse under homoeostatic conditions. **A.** The cell surface expression of Clever-1 on peritoneal macrophages. **B.** The cell surface expression of Clever-1 on peripheral monocytes. **C.** The cells surface expression of Clever-1 on monocytes and macrophages in the bone marrow. **A.**, **B.**, & **C.** The used gating strategies and histograms from representative samples (grey fill, the NS-1 isotype control; black line, the mStab1 antibody). Data are presented as mean ± s.e.m., *n* = 3 for all. Antibody conjugates are indicated in the figure.

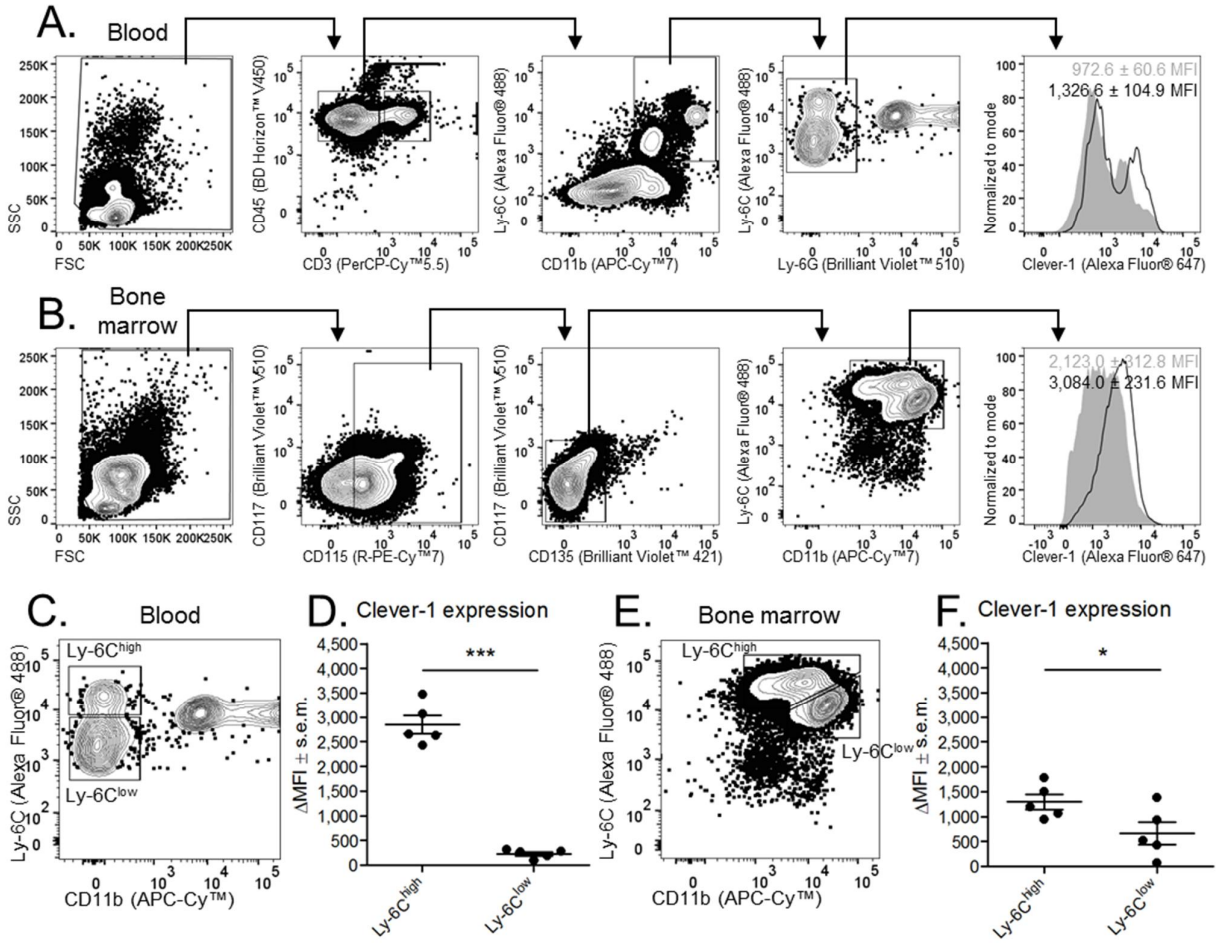

Figure 4. Clever-1 expression in different monocyte populations in the mouse under homoeostatic conditions. **A.** & **B.** The used gating strategies and histograms from representative samples for the blood and bone marrow, respectively (grey fill, the AK-1 isotype control; black line, the mStab1 antibody). **C.** & **E.** The separation of monocytes from **A.** & **B.**, respectively, into the Ly-6C^{high} and Ly-6C^{low} monocyte subpopulations. **D.** & **F.** The differential expression of Clever-1 between the Ly-6C^{high} and Ly-6C^{low} monocyte subpopulations in the blood and bone marrow, respectively, as determined by their ΔMFI values for Clever-1. Data are presented as mean ± s.e.m., $n = 5$ for all. Statistical significance was calculated with paired Student's two-tailed *t*-test (*, $p < 0.05$; ***, $p < 0.001$). Antibody conjugates are indicated in the figure.

sensitivity. 6–12-week-old C57/BL6N mice were CO_2-asphyxiated and the cells from the peritoneal exudate and blood were stained with antibody against the cell surface marker F4/80 and cells from the bone marrow with antibodies against the cell surface markers CD11b, CD45, Ly-6C, and Ly-6G; and either the biotinylated NS-1 isotype control or mStab1 antibody followed by R-PE-labelled streptavidin, after which the cells were analysed by flow cytometry using the BD LSRFortessa™. The F4/80$^+$ cells in the peritoneal exudate and bone marrow and the CD11b$^+$ CD45$^+$ Ly-6C$^+$ Ly-6G$^-$ cells in the blood were considered as monocytes or macrophages.

When compared to the NS-1-stained negative control, neither the mStab1-stained monocytes nor macrophages present in the peritoneal exudate, blood, or bone marrow expressed Clever-1 under homoeostatic conditions, as determined by their median fluorescence intensity (MFI) values (59.9 ± 2.2 vs 61.6 ± 1.6; 10.3 ± 1.2 vs 11.4 ± 1.0; and 6.5 ± 0.19 vs 6.7 ± 0.14 MFI, respectively, $n = 3$ for all)

(see Figure 3, A., B., & C.). None of these differences were statistically significant ($p > 0.05$ for all). Therefore, Clever-1 is not expressed on the cell surface of primary monocytes or macrophages of mice under homoeostatic conditions.

However, since previous publications and unpublished data from immunofluorescence microscopy experiments performed in our group suggest that the localization of Clever-1 is mostly intracellular, I investigated whether Clever-1 could be detected from the primary monocytes and macrophages in the blood and bone marrow of mice by flow cytometry after permeabilization of the cell membrane. The blood and bone marrow from C57/BL6N mice where collected and the stained cells analysed by flow cytometry as described above. Unlike above, the collected cells were pre-incubated for one hour at 37 °C with either the directly-conjugated AK-1 isotype control or mStab1 antibody and then surface stained with antibodies against the cell surface markers CD3, CD11b, CD45, Ly-6C, and Ly-6G for the blood and CD11b, CD115, CD117, CD135, and Ly-6C for the bone marrow. Inclusion of CD3 in the blood panel allowed for the more reliable exclusion of lymphocytes from the monocyte population. The panel for bone marrow was adapted from Hettinger & al. (2013) and allows a more refined identification of monocytes in the bone marrow. The $CD3^-$ $CD11b^+$ $CD45^+$ Ly-$6C^+$ Ly-$6G^-$ cells in the blood and the $CD115^+$ $CD117^-$ $CD135^-$ $CD11b^+$ Ly-$6C^+$ cells in the bone marrow were considered as monocytes (see Figure 4, A. & B.).

When compared to the AK-1-pre-incubated negative control, the mStab1-pre-incubated primary monocytes in both the blood and bone marrow did express Clever-1 under homoeostatic conditions, as determined by their MFI values (972.6 ± 60.6 vs 1,326.6 ± 104.9 and 2,123.0 ± 312.8 vs 3,084.0 ± 231.6, respectively; $n = 5$ for all) (see Figure 4, A. & B.). These differences were also statistically significant ($p < 0.05$ for both). Furthermore, because the cells had been pre-incubated with directly-conjugated antibodies, the signal detected with the mStab1 antibody above that detected with the AK-1 isotype control was presumably from antibody bound and endocytosed in complex with the Clever-1 protein. This suggests that Clever-1 is actively recycled to and from the cell surface under homoeostatic conditions. Interestingly, when the identified monocyte and macrophage populations were subdivided according to their cell surface expression of Ly-6C into inflammatory Ly-$6C^{high}$ and patrolling Ly-$6C^{low}$ monocytes (see Figure 4, C. & E.), Clever-1 was found to be more highly expressed by the Ly-$6C^{high}$ monocytes, which are typically described as proinflammatory and antimicrobial, than in the Ly-$6C^{low}$ monocytes in both the blood and bone marrow, as determined by their ΔMFI values ($MFI_{specific\ antibody} - MFI_{isotype\ control}$) (2,848.8 ± 167.2 vs 229.2 ± 35.2 and 1,296.2 ± 136.5 vs 665.6 ± 202.9; $n = 5$ for both) (see Figure 4, D. & F.). These differences were also highly statistically significant ($p < 0.001$) and statistically significant ($p < 0.05$), respectively. Additionally, based on the ΔMFI values, the expression of Clever-1 was 2.3 ± 0.1 times higher in $Ly6^{high}$ monocytes in the blood than in the bone marrow. This difference was also highly statistically significant ($p < 0.001$).

Taken together, these results demonstrate that Clever-1 is expressed by inflammatory Ly-$6C^{high}$ monocytes in the blood and bone marrow of mice already under homoeostatic conditions and suggest that its expression is mostly intracellular. Moreover, the expression of Clever-1 appears to increase once the Ly-$6C^{high}$ monocytes depart from the bone marrow and enter circulation. These results suggest that in primary monocytes and perhaps in macrophages as well, Clever-1 is actively

recycled to and from the cell membrane, which would increase the proportion of intracellular Clever-1 and explain the negative results obtained with surface staining only.

5.2 The expression of Clever-1 can be induced on the cell surface of monocytes and macrophages isolated from the peritoneal exudate, blood, or bone marrow of mice by *in vitro* culture in M2-polarizing conditions

Clever-1 is a widely accepted marker of M2 macrophages and its expression can be induced on monocytes and macrophages by *in vitro* culture in M2-polarizing conditions. In order to establish a reliable source of macrophages that express Clever-1 for *in vitro* experiments, cells from the peritoneal exudate, blood, and bone marrow of CO_2-asphyxiated 6–12-week-old wildtype C57/BL6N mice were cultured in M2-polarizing conditions for one week, after which the cells were detached and surface stained with antibody against the F4/80 cell surface pan-macrophage marker and either the directly-conjugated AK-1 isotype control or mStab1 antibody, after which the cells were analysed by flow cytometry using the BD LSRFortessa™ (see Figure 5, A., C., & E.). When compared to the AK-1-stained negative control, the mStab1-stained macrophages derived from the peritoneal exudate, blood, and bone marrow all expressed Clever-1, as determined by their MFI values (11.9 ± 1.2 vs 38.3 ± 7.6; 22.0 ± 0.6 vs 78.7 ± 7.7; and 11.3 ± 1.1 vs 83.1 ± 12.6 MFI, respectively, $n = 3$ for all) (see Figure 5, B., D., & F.) as well as the relative amounts of Clever-1$^+$ F4/80$^+$ macrophages (0.89 ± 0.17 vs 49.7 ± 6.0; 0.36 ± 0.23 vs 65.7 ± 5.7; and 0.14 ± 0.052 vs 64.7 ± 7.4 %, respectively, $n = 3$ for all) (see Figure 5, G.). The differences in MFI values between the AK-1- and mStab1-stained samples were statistically significant for the macrophages derived from blood and bone marrows ($p < 0.05$ for both) but not in the macrophages derived from the peritoneal exudate ($p > 0.05$). The differences in relative amounts of Clever-1$^+$ macrophages between the AK-1- and mStab1-stained samples derived from the peritoneal exudate, blood, and bone marrow were all statistically significant ($p < 0.05$ for all). Taken together, the bone marrow-derived M2-polarized macrophages (M2 BMDMs) exhibited the highest expression of Clever-1 in terms of both MFI values and the relative amounts of Clever-1$^+$ cells. Because the bone marrows also yielded the highest numbers of cells when compared to the peritoneal exudate and blood, M2 BMDMs were selected as the source for Clever-1-expressing M2 macrophages for further *in vitro* experiments.

5.3 Clever-1 positively regulates signal transduction through the mTORC1 complex in M2 macrophages

In a high-throughput kinase panel, treating primary monocytes isolated from the blood of healthy human volunteers with a Clever-1 antibody, when compared to samples treated with isotype control antibodies, affected the phosphorylation of signalling proteins in pathways known to be important for the survival, activation, and polarization of monocytes and macrophages, such as mTOR, c-Jun, and STAT6 (data not shown) (Szanto & al., 2010; Byles & al., 2013; Hefetz-Sela & al., 2014).

M2 BMDMs derived from wildtype or Clever-1$^{-/-}$ mice were used to study this effect in the mouse. The bone marrow cells were collected and cultured in M2-polarizing conditions for one week as described above, after which the M2 BMDMs were detached and transferred to 96-well plates and left

to recuperate overnight. On the following day, the M2 BMDMs were fixed with 4 % formaldehyde, surface stained with antibody against F4/80, permeabilized with methanol, and stained intracellularly with either the AK-1 isotype control or the mStab1 antibody.

As expected, when compared to the AK-1-stained negative controls, the mStab1-stained M2 BMDMs originating from wildtype mice highly expressed Clever-1, whereas the macrophages originating

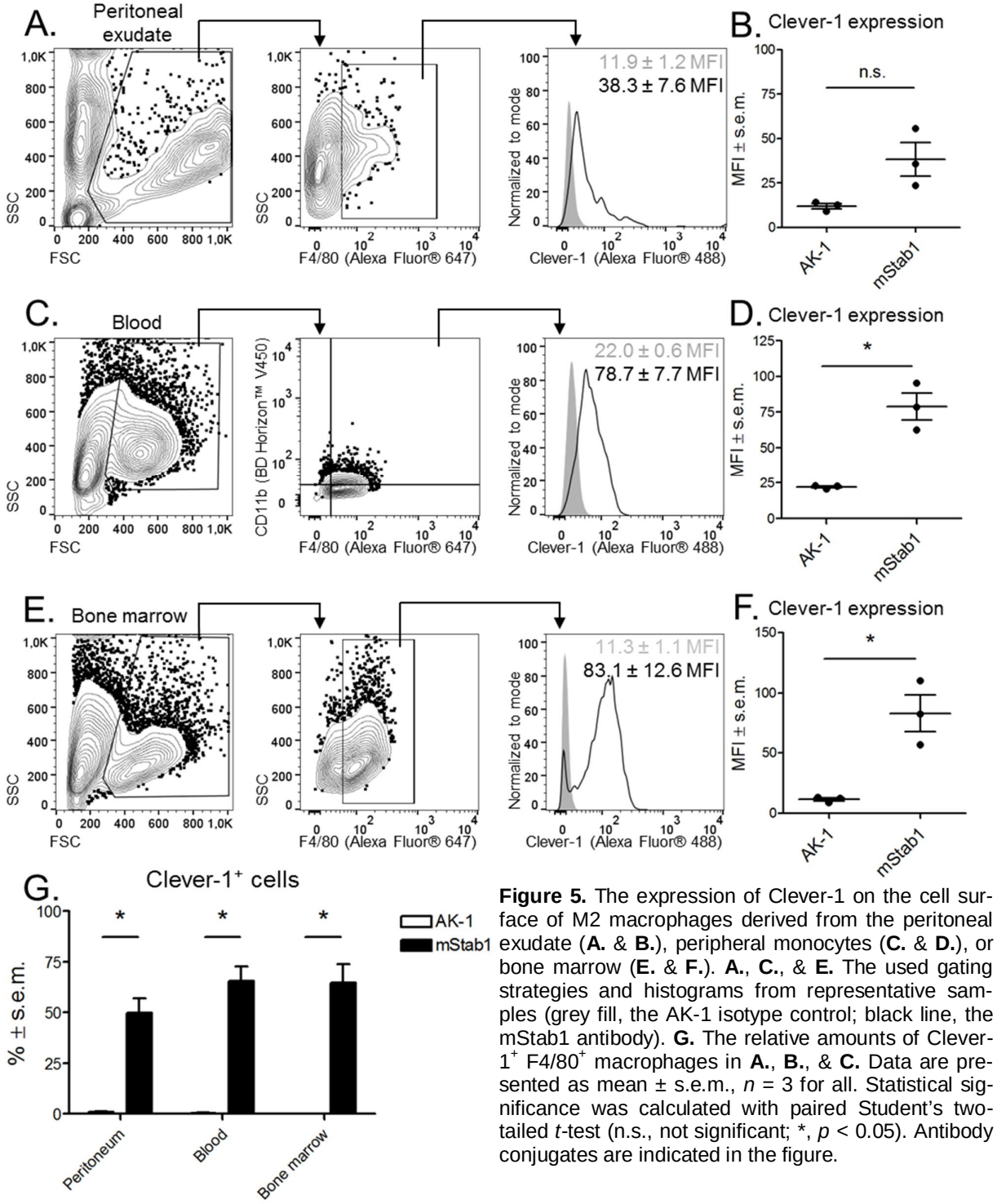

Figure 5. The expression of Clever-1 on the cell surface of M2 macrophages derived from the peritoneal exudate (**A.** & **B.**), peripheral monocytes (**C.** & **D.**), or bone marrow (**E.** & **F.**). **A.**, **C.**, & **E.** The used gating strategies and histograms from representative samples (grey fill, the AK-1 isotype control; black line, the mStab1 antibody). **G.** The relative amounts of Clever-1$^+$ F4/80$^+$ macrophages in **A.**, **B.**, & **C.** Data are presented as mean ± s.e.m., n = 3 for all. Statistical significance was calculated with paired Student's two-tailed t-test (n.s., not significant; *, $p < 0.05$). Antibody conjugates are indicated in the figure.

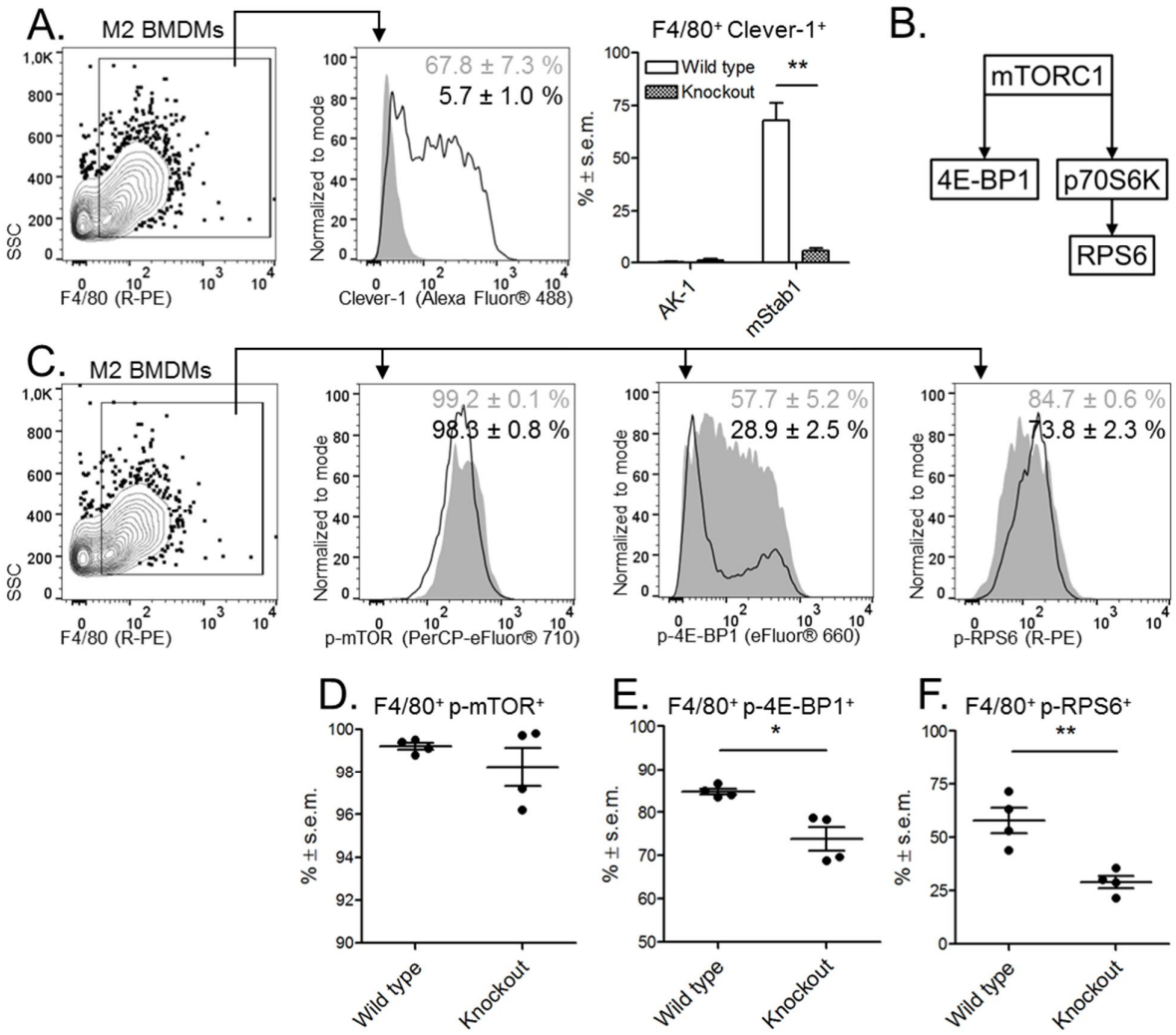

Figure 6. Activity of the mTORC1 signalling pathway in wildtype and Clever-1$^{-/-}$ mice. **A.** The relative amounts of Clever-1^{+} F4/80^{+} M2 BMDMs in samples derived from wildtype or Clever-1$^{-/-}$ knockout mice. The used gating strategy and histogram are shown from a representative sample. **B.** A schematic representation of the mTORC1 pathway. mTOR is a component of the mTORC1 complex. **C.** The used gating strategy and histograms from a representative sample (grey fill, wildtype; black line, Clever-1$^{-/-}$ F4/80^{+} M2 BMDMs). **D.**, **E.**, & **F.** The relative amounts of p-mTOR^{+}, p-4E-BP1^{+}, and RPS6^{+} F4/80^{+} M2 BMDMs, respectively, in wildtype and Clever-1$^{-/-}$ knockout mice. Data are presented as mean ± s.e.m., $n = 4$ for all. Statistical significance was calculated with unpaired Student's two-tailed *t*-test (*, $p < 0.05$; **, $p < 0.01$). Antibody conjugates are indicated in the figure.

from Clever-1$^{-/-}$ mice did not, as determined by the relative amounts of Clever-1^{+} F4/80^{+} M2 BMDMs (0.33 ± 0.19 vs 67.8 ± 7.3 % and 1.0 ± 0.71 vs 5.7 ± 0.97 %, respectively, n = 4 for all) (see Figure 6, A.). The difference in the relative amount of Clever-1^{+} F4/80^{+} M2 BMDMs between the mStab1-stained wildtype and Clever-1$^{-/-}$ mice was very statistically significant ($p < 0.01$). Therefore, the induction of Clever-1 expression was successful and the specificity of the mStab1 antibody was verified.

In order to investigate whether Clever-1 affects signal transduction through the mTORC1 pathway in the mouse (see Figure 6, B.), M2 BMDMs originating from wildtype or Clever-1$^{-/-}$ mice were stained

intracellularly with antibodies against the phosphorylated (p-)mTOR, p-4E-BP1, and p-RPS6 proteins after surface staining with antibody against F4/80 and fixation and permeabilization with methanol. Between the F4/80$^+$ M2 BMDMs from wildtype or Clever-1$^{-/-}$ mice, no statistically significant differences were observed in the relative amounts of F4/80$^+$ M2 BMDMs positive for p-mTOR, a component of the mTORC1 complex (99.2 ± 0.14 vs 98.3 ± 0.78 %, respectively, n = 4 for both) (see Figure 6, C. & D.). However, a significant decrease in the phosphorylation 4E-BP1 and RPS6 was observed when comparing the F4/80$^+$ M2 BMDMs from wildtype or Clever-1$^{-/-}$ mice with each other, as determined by the relative amounts of p-4E-BP1$^+$ and p-RPS6$^+$ F4/80$^+$ M2 BMDMs (57.7 ± 5.2 vs 28.9 ± 2.5 and 84.7 ± 0.6 vs 73.8 ± 2.3 %, respectively, n = 4 for both) (see Figure 6, E. & F.). These differences were also statistically significant (p < 0.05) and very statistically significant (p < 0.01), respectively. Taken together, Clever-1 appears to positively regulate signal transduction either through or downstream of the mTORC1 complex.

5.4 The antibody-mediated interference of Clever-1 in TAMs and M2 macrophages increases the secretion and production of TNF-α

Because the siRNA-mediated knockdown of Clever-1 in the primary monocytes and placental macrophages of humans increases the secretion of TNF-α, it was investigated whether the antibody-mediated interference of Clever-1 would result in the same effect in the macrophages of mice (Palani & al., 2011; Palani & al., 2016). However, in mice, Clever-1 is typically expressed by M2 macrophages, which normally secrete little TNF-α. Because of the observation that TAMs isolated from orthotopic E0771 tumours secrete ample quantities of TNF-α but concurrently express Clever-1 led them to be selected as a platform for testing whether treating Clever-1$^+$ TAMs in a mouse model of mammary carcinoma with the mStab1 antibody has the same effect as silencing Clever-1 in human monocytes and macrophages (Burke & al., 2013). To this end, approximately 0.1 × 10^6 E0771 cells suspended in PBS were injected subcutaneously into the mammary fat pads of 6–12-week-old female C57/BL6N mice. After three weeks, the mice were CO_2-asphyxiated, the tumours resected, and the CD11b$^+$ myeloid cells isolated by positive immunomagnetic selection. The CD11b$^+$ cells were left to attach to cell culture dishes overnight in complete IMDM. On the following day, the unattached cells were washed away with PBS and the attached cells visually identified as macrophages, or TAMs. The TAMs were then incubated in IMDM without serum either without antibody or with 20 µg/mL of either the AK-1 isotype control or the mStab1 antibody for two days, after which the culture media were collected and analysed for the presence of TNF-α by ELISA.

As has been reported previously, the TAMs isolated from orthotopic E0771 tumours had secreted TNF-α into the cell culture medium at a well-detectable level without any antibody treatment (126.6 ± 14.3 pg/mL, n = 4) (similarly observed by Burke & al., 2013) (see Figure 7, A.). Treatment with the AK-1 isotype control antibody did not have a statistically significant effect on the amount TNF-α secreted by TAMs when compared to the no-antibody control (117.9 ± 15.7 pg/mL, n = 4; p > 0.05). However, treating TAMs with the mStab1 antibody resulted in an over twofold increase in the amount of secreted TNF-α when compared to either the no-antibody or the AK-1-treated control samples (288.4 ± 44.7, n = 4). This increase in TNF-α secretion was statistically significant when compared to either the no-antibody or the AK-1 isotype control samples (p < 0.05 for both).

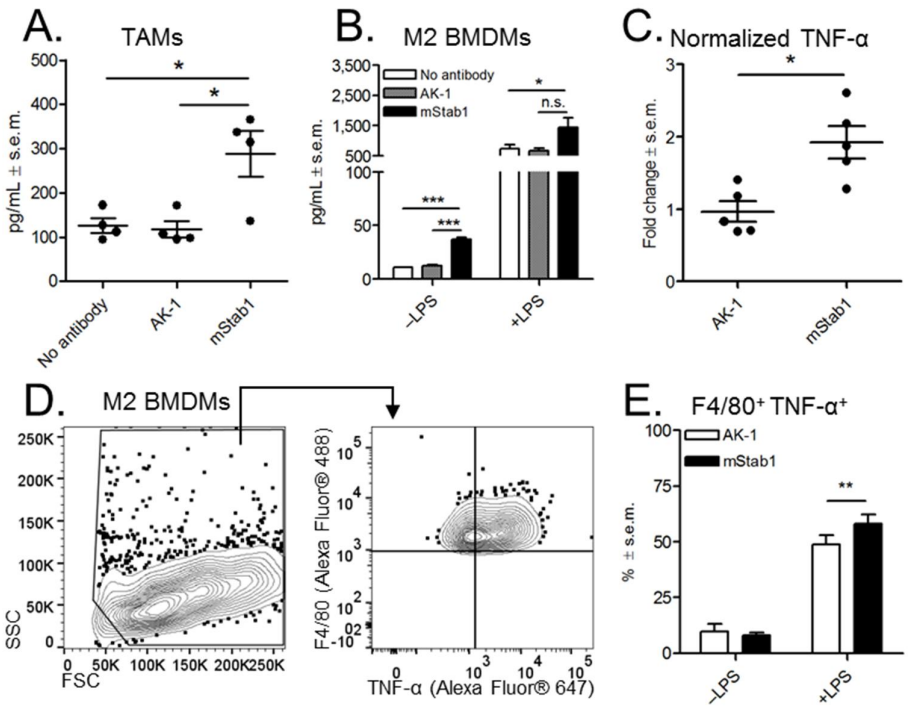

Figure 7. TNF-α secretion by TAMs and M2 BMDMs in response to the antibody-mediated interference of Clever-1. **A.** The amount of TNF-α secreted by TAMs in response to the indicated treatments. **B.** The amount of TNF-α secreted by M2 BMDMs in response to the indicated treatments. **C.** Results from **B.** normalized to the no-antibody control. **D.** The used gating strategy from a representative sample. **E.** The relative amounts of TNF-α^+ F4/80$^+$ M2 BMDMs in response to the indicated antibody treatments without or with LPS activation. Data are presented as mean ± s.e.m., n = 4 (**A.**), 5 (**B.** & **C.**), and 4 (**D.** & **E.**). Statistical significance was calculated with paired Student's two-tailed t-test (n.s., not significant; *, $p < 0.05$; **, $p < 0.01$; *** $p < 0.001$). Antibody conjugates are indicated in the figure.

Therefore, the antibody-mediated interference of Clever-1 increases the secretion of the proinflam-proinflammatory cytokine TNF-α from TAMs.

Because of these positive findings, I investigated the effects of Clever-1 antibody treatment on M2 BMDMs derived from wildtype BALB/c mice. The bone marrows were collected and differentiated into M2 BMDMs as described above. The M2 BMDMs were then incubated in IMDM without serum either without antibody or with 20 µg/mL of either the AK-1 isotype control or the mStab1 antibody for one hour. Following the antibody incubation, the cells were left to incubate either as such or activated with 100 ng/mL of LPS for 24 h. LPS activation was included because M2 macrophages do not normally secrete large quantities of TNF-α, but do so in response to inflammatory stimuli. After 24 h, the culture media were collected and analysed for the presence of TNF-α by ELISA.

Even without LPS activation, the M2 BMDMs had secreted TNF-α at a detectable, albeit low concentration even without antibody or LPS activation (10.7 ± 0.3 pg/mL, n = 5) (see Figure 7, B.). Treatment with the AK-1 isotype control antibody did not have a statistically significant effect on the amount of TNF-α secreted by M2 BMDMs when compared to the no-antibody control (12.5 ± 0.7 pg/mL, n = 5; $p > 0.05$). Remarkably, treating M2 BMDMs with the mStab1 antibody increased the amount of secreted TNF-α by threefold on average when compared to either the no-antibody or

the AK-1-treated control samples (37.2 ± 1.6 pg/mL, $n = 4$). Both of these differences were also highly statistically significant ($p < 0.001$ for both). In response to LPS activation, a major increase in the secretion of TNF-α was observed from the no-antibody, AK-1 isotype control, and mStab1-treated samples, as would be expected (736.8 ± 110.8, 668.4 ± 72.0, and 1,430.7 ± 288.6 pg/mL, respectively, $n = 4$ for all). Even following LPS activation, a statistically significant increase in the secretion of TNF-α in response to treatment with the mStab1 antibody was observed when compared to the no-antibody control group ($p < 0.05$). Although the mean concentration of TNF-α secreted by the AK-1-treated control samples was lower than that of the samples treated with the mStab1 antibody, the difference between these two groups was not statistically significant ($p > 0.05$). However, following normalization to their respective no-antibody controls, it was observed that the mStab1-treated samples had secreted 2.2 ± 0.4 times more TNF-α than the AK-1-treated control samples, and this difference was statistically significant ($p < 0.05$) (See Figure 7, C.). Based on these data, the antibody-mediated interference of Clever-1 increases the secretion of TNF-α from M2 macrophages.

In order to clarify whether the antibody-mediated interference of Clever-1 leads to the release of already synthetized TNF-α or if it increases the production of TNF-α in macrophages, I studied the amount of intracellular TNF-α produced by M2 BMDMs derived from wildtype C57BL/6N mice by flow cytometry. For this, M2 BMDMs were incubated in IMDM without serum with 20 µg/mL of either the AK-1 isotype control or the mStab1 antibody for one hour. Following the antibody incubation, the cells were left to incubate either as such or activated with 0.1 µg/mL of LPS for six hours. To prevent the exocytosis of newly-synthetized TNF-α, brefeldin A was added to all samples to block protein transport from the endoplasmic reticulum to the Golgi apparatus. After six hours, the cells were surface stained with antibody against the cell surface marker F4/80, fixed with 4 % formaldehyde, permeabilized with 0.2 % saponin, intracellularly stained with antibody against TNF-α, and analysed by flow cytometry, as described above.

Without LPS activation, no statistically significant difference in the relative amount of F4/80$^+$ M2 BMDMs positive for intracellular TNF-α was observed between the AK-1- and mStab-1-treated samples (9.9 ± 3.0 vs 7.8 ± 1.2 %, respectively, $n = 4$ for both; $p > 0.05$) (see Figure 7, D. & E.). In response to LPS activation, the relative amount of TNF-α$^+$ F4/80$^+$ M2 BMDMs had increased significantly in both the AK-1 isotype control and the mStab1 antibody treatment groups (48.8 ± 3.7 vs 58.3 ± 3.4 %, respectively, $n = 4$ for both). The increase in the relative amount of TNF-α$^+$ F4/80$^+$ M2 BMDMs in response to mStab1 was also very statistically significant in the LPS-activated samples when compared to the AK-1-treated controls ($p < 0.01$). It is possible that the six-hour incubation period was not long enough to reveal differences in the production of TNF-α in response to different antibody treatments in unstimulated macrophages, since their baseline secretion of TNF-α is comparatively low. In response to activation with LPS, however, the relative amount of TNF-α$^+$ F4/80$^+$ M2 BMDMs in the mStab1-treated samples had significantly increased during six hours of incubation when compared to the AK-1-treated controls. Therefore, the antibody-mediated interference of Clever-1 increases the production of TNF-α in M2 macrophages.

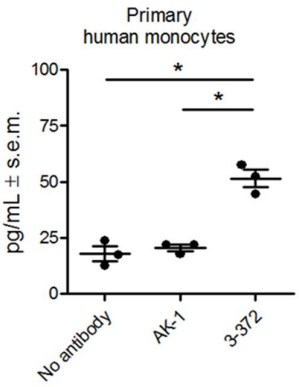

Figure 8. The amount of TNF-α secreted by primary human monocytes in response to the antibody-mediated interference of Clever-1. Monocytes were isolated from the blood of healthy volunteers and treated as indicated in the figure. The amounts of secreted TNF-α are shown. Data are presented as mean ± s.e.m., $n = 3$ for all. Statistical significance was calculated with paired Student's two-tailed *t*-test (*, $p < 0.05$).

5.5 The antibody-mediated interference of Clever-1 increases the secretion of TNF-α from primary human monocytes

In addition to investigating the effects of the mStab1 antibody in the mouse model, I also wanted to know whether the antibody against human Clever-1 (the clone Fu HI-3-372/2, referred to here as 3-372) has an effect similar to the siRNA-mediated knockdown of Clever-1 in the primary monocytes of humans. First, peripheral blood mononuclear cells were isolated by Ficoll-Paque® density gradient centrifugation from blood donated by healthy volunteers. The cells were left to attach to cell culture dishes overnight in complete IMDM, after which the unattached cells were washed away with PBS and the attached cells visually identified as monocytes. Then, the primary monocytes were incubated in complete IMDM without antibody or with 20 µg/mL of either the AK-1 isotype control or the 3-372 anti-Clever-1 antibodies for three days, after which the culture media were collected and analysed for the presence of TNF-α by ELISA. During the three-day incubation, the monocytes had secreted a detectable amount of TNF-α even in the absence of proinflammatory stimuli or antibody (17.8 ± 4.6 pg/mL, $n = 3$) (see Figure 8). Treatment with the AK-1 isotype control antibody had not affected the amount of secreted TNF-α when compared to the no-antibody control (20.4 ± 1.9 pg/mL, $n = 3$; $p > 0.05$). However, the amount of TNF-α secreted by the 3-372-treated monocytes was more than twofold higher when compared to either the no-antibody or the AK-1-treated control samples (51.4 ± 5.3 pg/mL, $n = 3$). This increase in the secretion of TNF-α was statistically significant when compared to either the no-antibody or the AK-1 isotype control samples ($p < 0.05$ for both). Therefore, the antibody-mediated interference of Clever-1 in primary human monocytes increases the secretion of TNF-α.

5.6 Clever-1 in expressed by myeloid cells in the tumour microenvironment of the E0771 and 4T1 mouse models of breast cancer

The M2 TAMs in various mouse models of cancers have been reported to express *Stab1* as determined by quantitative PCR (Movahedi & al., 2010). However, it is well known that expressed genes are not always translated into proteins. In order to validate the expression of the Clever-1 protein in the E0771 and 4T1 mouse models of breast cancer, tumours were induced by injecting 0.1 × 10^6 cancer cells in 50 µL of PBS into the mammary fat pads of syngeneic, female C57/BL6N or BALB/c mice, respectively. Tumours were induced in a total of 20 mice in both strains. The mice

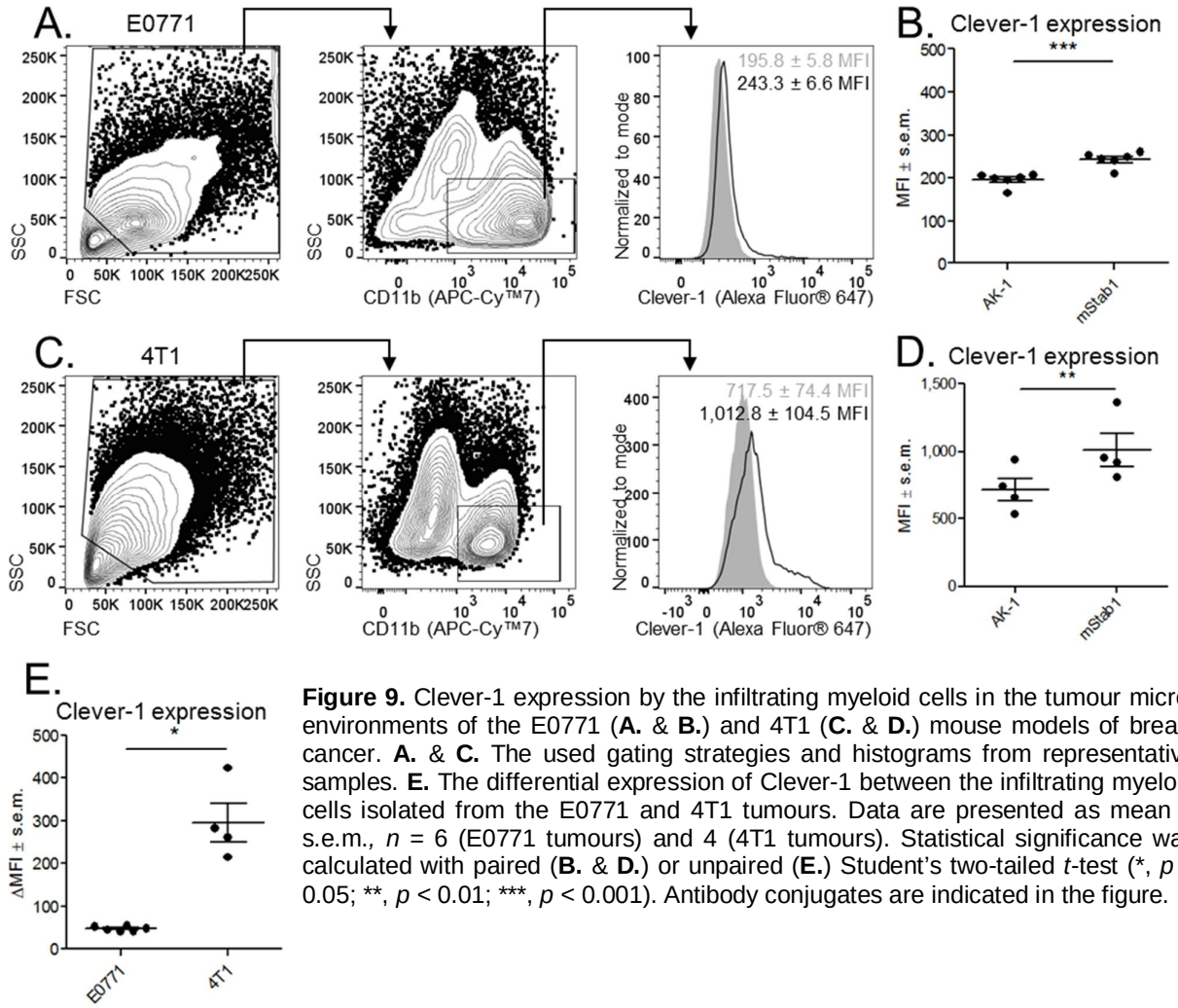

Figure 9. Clever-1 expression by the infiltrating myeloid cells in the tumour micro-environments of the E0771 (**A.** & **B.**) and 4T1 (**C.** & **D.**) mouse models of breast cancer. **A.** & **C.** The used gating strategies and histograms from representative samples. **E.** The differential expression of Clever-1 between the infiltrating myeloid cells isolated from the E0771 and 4T1 tumours. Data are presented as mean ± s.e.m., n = 6 (E0771 tumours) and 4 (4T1 tumours). Statistical significance was calculated with paired (**B.** & **D.**) or unpaired (**E.**) Student's two-tailed t-test (*, $p < 0.05$; **, $p < 0.01$; ***, $p < 0.001$). Antibody conjugates are indicated in the figure.

were split into two groups of ten, and each mouse was treated with 100 µg of either the AK-1 isotype control or the mStab1 antibody by intraperitoneal injection starting on day 3 or 4 after cancer cell inoculation and repeated every 2–3 days until the end of the experiment. The E0771 tumour mice received four doses over 14 days and the 4T1 tumour mice received seven doses over 22 days. Tumour growth was monitored with digital callipers, and the vertical and horizontal diameters were used to calculate the tumour areas ($d_{vertical} \times d_{horizontal}$).

Following the experiment, the tumours were excised and samples for flow cytometry were prepared. The tumours were mechanically minced, incubated with collagenase IV and DNase I at 37 °C for 30 min, and filtered through a 70 µm strainer. The liberated cells were surface stained with antibody against the cell surface marker CD11b, fixed with 4 % formaldehyde, permeabilized with 0.2 % saponin, and intracellularly stained with either the directly-conjugated AK-1 isotype control or mStab1 antibody. The cells were analysed by flow cytometry as described above. The expression of Clever-1 was analysed from the total population of CD11b$^+$ infiltrating myeloid cells. This population contains cells such a neutrophils that are known to be negative for Clever-1, but at the times of execution, the supply of other antibodies was limited.

When compared to the AK-1-stained controls, Clever-1 was clearly expressed by the infiltrating $CD11b^+$ myeloid cells in the tumour microenvironments of both the E0771 and 4T1 cancer models when compared to the samples stained with the mStab1 antibody, as determined by their MFI values (195.8 ± 5.8 vs 243.3 ± 6.6, n = 6 for both, and 717.5 ± 74.4 vs 1,012.8 ± 104.5, n = 6 and 4, respectively) (see Figure 9, A., B., C., & D.). These differences were also highly statistically significant ($p < 0.001$) and very statistically significant ($p < 0.01$), respectively. Interestingly, it was observed that Clever-1 was less expressed by the infiltrating $CD11b^+$ myeloid cells within the E0771 tumour microenvironment than by the same population of cells within the 4T1 tumour microenvironment, as determined by their ΔMFI values (47.5 ± 2.2 vs 295.3 ± 38.9, n = 6 and 4, respectively) (see Figure 9, E.). This difference was also statistically significant ($p < 0.05$).

5.7 Clever-1 antibody treatment may inhibit tumour growth in the 4T1 mouse model of triple-negative breast cancer

Of the ten mice in each group, eight mice in the AK-1 isotype control and ten mice in the mStab1 antibody treatment group in the E0771 cancer model and ten mice in the AK-1 isotype control and eight mice in the mStab1 antibody treatment group in the 4T1 cancer model survived to the end of the experiment. The number of E0771 cancer cells injected per mouse was too large, as the tumours grew faster than expected and the mice were administered only four out of seven planned doses before they begun to reach the humane endpoint. Therefore, the possible immunotherapeutic effect of Clever-1 antibody treatment may not have become apparent in the actualized timeframe of this experiment.

No statistically significant differences in tumour areas in response to antibody treatment were observed over the treatment periods when comparing the AK-1 isotype control and the mStab1 antibody treatment groups with each other in either the E0771 or the 4T1 cancer model when analysed by two-way ANOVA (see Figure 10, A. & C.; Appendices 1 & 3). For the E0771 cancer model, no statistically significant differences in tumour areas between the control and treatment groups were revealed after normalization of the tumour area to the first measurements taken on day 4, either (see Figure 10, C.; Appendix 2).

In the 4T1 cancer model, following normalization of the tumour size to the first measurements taken on day 3, a statistically significant decrease in the tumour area between the control and treatment groups was observed on days 7, 10, 14, 17, 20, and 22 by unpaired t-tests ($p < 0.001$ for day 7 and $p < 0.05$ for the others), although two-way ANOVA did not reveal statistical significance between these two groups overall even after normalization (see Figure 10, D.; Appendix 4). Still, in the 4T1 tumour experiment, the normalized tumour areas of the mStab1 antibody treatment group were on average 1.3 times smaller than that of the AK-1 isotype control group on day 22 (1,084.0 ± 180.7 vs 815.8 ± 252.2 % of day 3, n = 10 and 8, respectively) (see Appendix 4). Therefore, the Clever-1 antibody treatment may inhibit tumour growth in the 4T1 mouse model of triple-negative breast cancer, although this experiment should be repeated to determine its validity.

5.8 Combinatorial Clever-1 and PD-1 antibody treatment may inhibit tumour growth in the 4T1 mouse model of triple-negative breast cancer

Because of the putatively positive results obtained in the experiment above, the immunotherapeutic potential of Clever-1 antibody treatment both alone and in combination with inhibitors of the immune checkpoint proteins PD-1 and PD-L1 was investigated in the 4T1 mouse model of triple-negative breast cancer. For tumour induction, 0.1×10^6 cancer cells in 50 µL of PBS were inoculated into the mammary fat pads of 49 syngeneic, female BALB/c mice. The mice were randomized into the following groups of seven: single isotype control, combination isotype control, mStab1 treatment, anti-PD-1 treatment, anti-PD-L1 treatment, mStab1 + anti-PD-1 treatment, and mStab1 + anti-PD-L1 treatment groups. The mice were administered 100 µg of each indicated antibody by intraperitoneal injection every 2–3 days for a total five doses over 17 days. Tumour growth was monitored on treatment days with digital callipers. The humane endpoint for tumour size according to the animal experimentation licence was 1 cm in diameter. The vertical and horizontal diameters were used to calculate the tumour areas ($d_{vertical} \times d_{horizontal}$). No mice reached the humane endpoint during the experiment but a total of seven mice died spontaneously before the end of the experiment (one in the single isotype control, two in the combination isotype control, none in the mStab1 treatment, one in the anti-PD-1 treatment, one in the anti-PD-L1 treatment, two in the mStab1 + anti-PD-1 treatment, and none in the mStab1 + anti-PD-L1 treatment groups).

Following the experiment, one tumour in the single isotype control, two in the combination isotype control, one in the mStab1 treatment, one in the anti-PD-1 treatment, two in the anti-PD-L1 treatment, none in the mStab1 + anti-PD-1 treatment, and two in the mStab1 + anti-PD-L1 treatment groups were observed to have grown intraperitoneally and were excluded from the analysis of tumour size. Tumour sizes from all five measurements were obtained for five mice in the single isotype control, five in the combination isotype control, six in the mStab1 treatment, four in the anti-PD-1 treatment, four in the anti-PD-L1 treatment, seven in the mStab1 + anti-PD-1 treatment, and five in the mStab1 + anti-PD-L1 treatment groups.

Based on measurements done on day 3 after cancer cell injection, no statistically significant differences in tumour areas were observed between mice in the single isotype control group and the mStab1 treatment, anti-PD-1 treatment, or anti-PD-L1 treatment groups (8.1 ± 0.6 vs 9.2 ± 2.1, 7.7 ± 1.9, and 6.5 ± 1.4 mm², n = 5, 6, 4, and 4, respectively; $p > 0.05$ for all) or the combination isotype control group and the mStab1 + anti-PD-1 treatment or mStab1 + anti-PD-L1 treatment groups (8.1 ± 0.9 vs 6.9 ± 1.9 and 6.7 ± 2.2 mm², n = 5, 7, and 5, respectively; $p > 0.05$ for both) before antibody treatments (see Figure 11, A. & C.). On day 17, no statistically significant differences in the tumour areas were observed between the single isotype control group and the mStab1, anti-PD-1, or anti-PD-L1 treatment groups (58.2 ± 13.2 vs 50.2 ± 6.3, 45.4 ± 16.2, and 43.0 ± 6.9 mm², n = 5, 6, 4, and 4, respectively; $p > 0.05$ for all) either before or after normalization of the tumour areas to the first measurements taken on day 3 (see Figure 11, A. & B.; Appendices 5 & 6), even though mStab1 antibody treatment had shown some inhibitory effect on tumour growth in the previous experiment (see Figure 10, D.). However, the decrease in tumour area between the combination isotype control group and the mStab1 + anti-PD-1 treatment group was statistically significant (54.1 ± 10.8 vs 34.6 ±

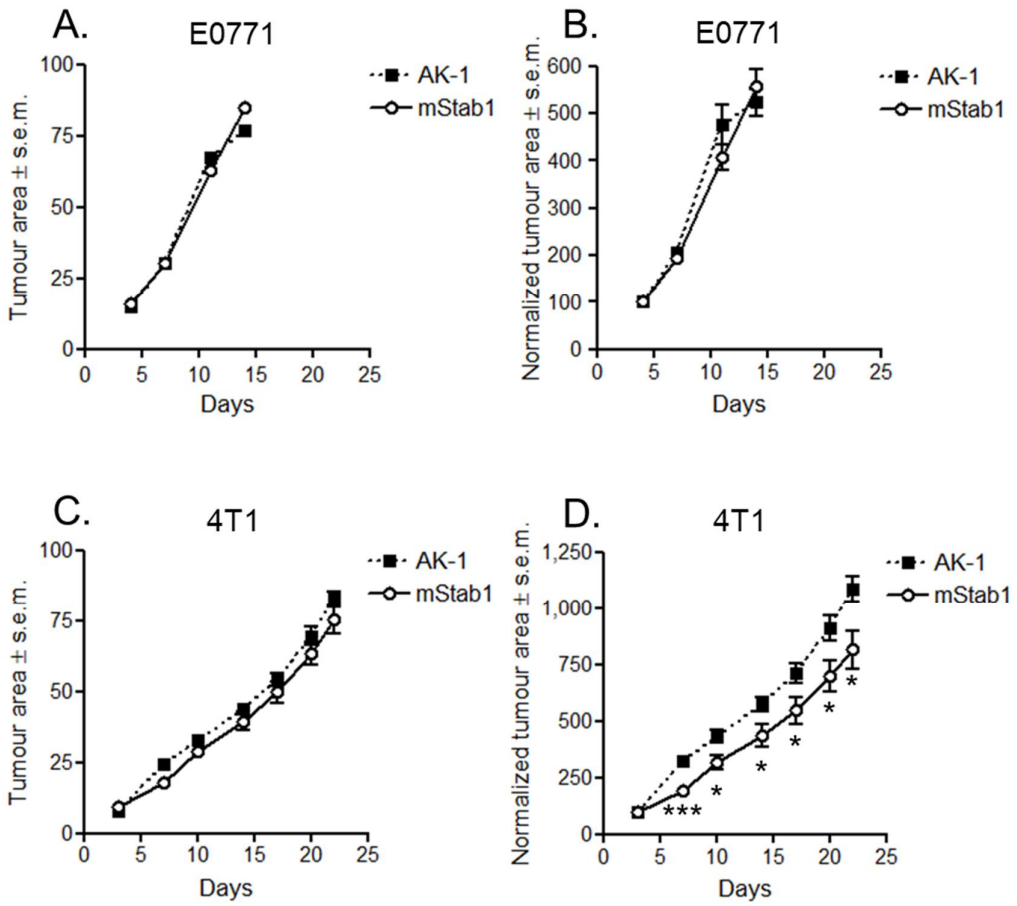

Figure 10. Growth curves for the calculated and normalized tumour areas from the E0771 (**A.** & **B.**) and 4T1 (**C.** & **D.**) tumour experiments, respectively. ■, the AK-1 isotype control group; ○, the mStab1 treatment group. In **B.** & **D.**, the tumour areas have been normalized to the first measurements, which have been set to 100 %. Data are presented as mean ± s.e.m. In **A.** & **B.**, $n = 8$ (AK-1 isotype control group) and 10 (mStab1 treatment group); in **C.** & **D.**, $n = 10$ (AK-1 isotype control group) and 8 (mStab1 treatment group). Statistical significance was calculated with unpaired Student's two-tailed *t*-test (*, $p < 0.05$; ***, $p < 0.001$).

10.0 mm², n = 5 and 7, respectively; $p < 0.05$), while the decrease in tumour area between the com-combination isotype control group and the mStab1 + anti-PD-L1 treatment group was not (54.1 ± 10.8 vs 51.4 ± 11.6 mm², n = 5 and 5, respectively; $p > 0.05$) (see Figure 11, C.). The statistical significance was observed only when comparing the non-normalized tumour areas of the combination isotype control group and mStab1 + anti-PD-1 treatment group taken at day 21 with each other (see Figure 11, D.), and two-way ANOVA between these two groups did not reveal a statistically significant difference between them overall ($p > 0.05$). Still, the mean tumour area of the group treated with mStab1 in combination with anti-PD-1 was on average 1.6 ± 0.2 times smaller than the mean tumour area of the combination isotype control group on day 17, and therefore, based on this experiment, the combinatorial Clever-1 and PD-1 antibody treatment appears to inhibit tumour growth in the 4T1 mouse model of triple-negative breast cancer. However, further experiments are required to verify the validity of this result because of the relatively small group sizes and to consolidate the incongruous results between different experiments.

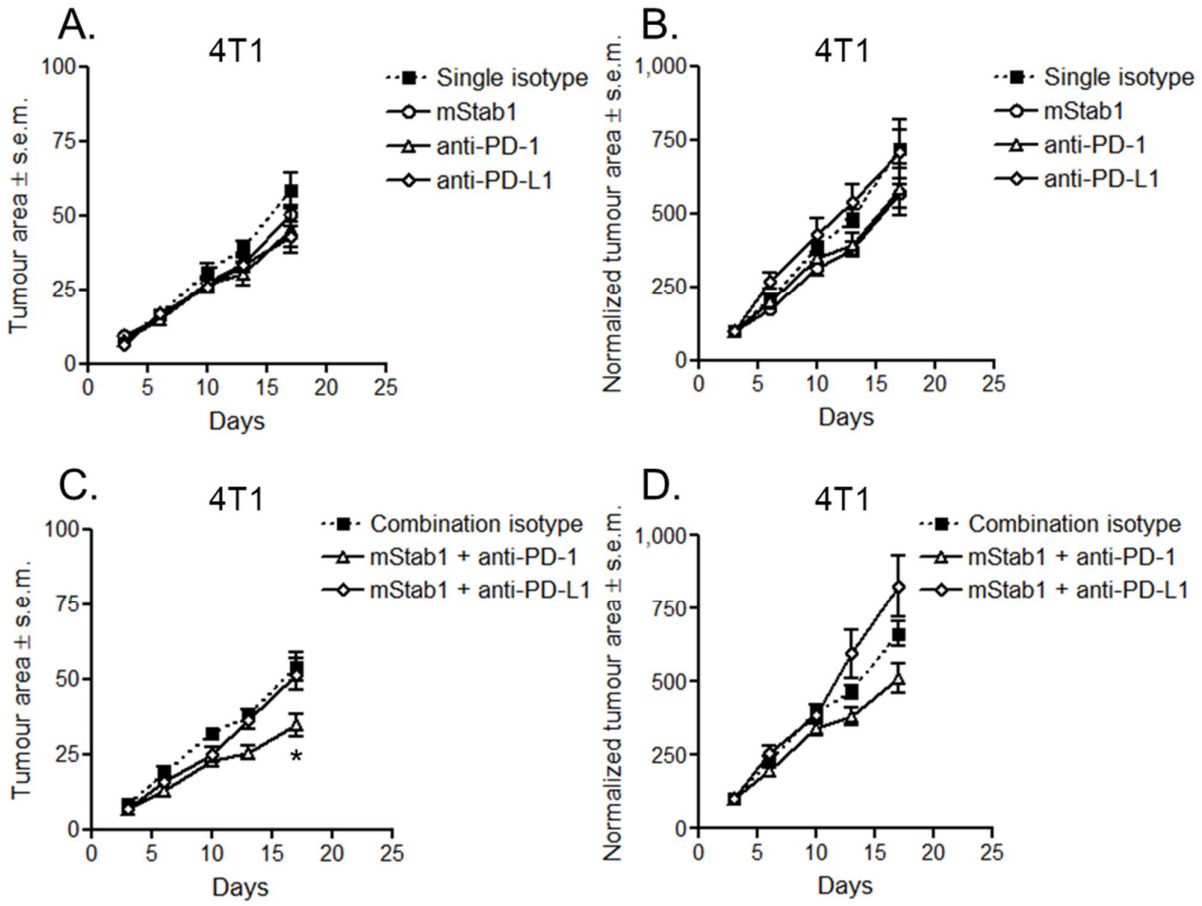

Figure 11. Growth curves drawn from the calculated and normalized tumour areas from the second 4T1 tumour experiment for the single isotype control and treatment groups (**A.** & **B.**) and the combinatorial isotype control and treatment groups (**C.** & **D.**). **A.** & **B.** ■, single isotype control group (n = 5); ○, mStab1 treatment group (n = 6); △, anti-PD-1 treatment group (n = 4); ◊, anti-PD-L1 treatment group (n = 4). **C.** & **D.** ■, combination isotype control group (n = 5); △, mStab1 + anti-PD-1 treatment group (n = 7); ◊, mStab1 + anti-PD-L1 treatment group (n = 5). In **B.** & **D.**, the tumour areas have been normalized to the first measurements, which have been set to 100 %. Data are presented as mean ± s.e.m. Statistical significance was calculated with unpaired Student's two-tailed t-test (*, $p < 0.05$).

5.9 Combinatorial Clever-1 and PD-1 antibody treatment limits the incidence of metastasis in the lymph nodes in the 4T1 mouse model of triple-negative breast cancer

The 4T1 cancer cell line used in the *in vivo* experiments has been genetically modified to express luciferase, which makes the detection of metastases possible by luminescence photometry. The mice were administered luciferin by intraperitoneal injection, ten minutes after which they were CO_2-asphyxiated. Metastasis to the draining inguinal lymph nodes and lungs was analysed by *ex vivo* imaging with the IVIS system. Positive metastasis was determined as bioluminescence signal above background and noted as yes or no, from which the incidence of metastasis was calculated (number metastasized ÷ total number of mice in group × 100 %).

Most probably due to the small sample sizes, no statistically significant differences in the incidence of metastasis to either the draining inguinal lymph nodes or the lungs were observed between the control and treatment groups with Fisher's exact test. Compared to the single isotype control group, the incidence of metastasis in the draining inguinal lymph nodes was smaller in the mStab1 treatment, anti-PD-1 treatment, and anti-PD-L1 treatment groups (67 vs 43, 33, and 50 %, respectively) (see Figure 12, A.). Compared to the combination isotype control group, no metastases were observed in the draining inguinal lymph nodes in the mStab1 + anti-PD-1 treatment group, but in the mStab1 + anti-PD-L1 treatment group, the incidence of metastases was higher (40 vs 0 and 50 %, respectively) (see Figure 12, B.). Compared to the single isotype control group, the incidence of metastasis in the lungs was smaller in the mStab1 treatment, anti-PD-1 treatment, and anti-PD-L1 treatment groups (83 vs 71, 67, and 33 %, respectively) (see Figure 12, C.). Compared to the combination isotype control group, the incidence of metastasis in the lungs was smaller also in both the mStab1 + anti-PD-1 treatment and mStab1 + anti-PD-L1 treatment groups (80 vs 33 and 33 %, respectively) (see Figure 12, D.). Taken together, while both Clever-1 and PD-1 antibody treatment reduced the incidence of metastasis on their own, the combinatorial Clever-1 and PD-1 antibody treatment appears to have had a synergistic effect in limiting both lymph node and lung metastasis in the 4T1 mouse model of triple-negative breast cancer. Similar synergy was not observed when the Clever-1 antibody treatment was combined with the PD-L1 antibody treatment. Therefore, based on this experiment, combinatorial Clever-1 and PD-1 antibody treatment limits the incidence of metastasis in the lymph nodes in the 4T1 mouse model of triple-negative breast cancer. However, further experiments are required in order to determine the statistical significance of these findings.

5.10 Combinatorial Clever-1 and PD-1 antibody treatment decreases the anti-inflammatory phenotype of TAMs in the tumour microenvironment

In order to analyse the phenotypic changes in TAMs in the tumour microenvironment in response to each treatment, samples for flow cytometry were obtained from six tumours in the single isotype control, five in the combination isotype control, six in the mStab1 treatment, six in the anti-PD-1 treatment, six in the anti-PD-L1 treatment, six in the mStab1 + anti-PD-1 treatment, and five in the mStab1 + anti-PD-L1 treatment groups. The samples were prepared for flow cytometry as described above. The liberated cells were surface stained with antibodies against the cell surface markers CD11b, CD45, CD115, class II MHC, Ly-6C, Ly-6G, F4/80, and PD-L1, fixed with 4 % formaldehyde, permeabilized with 0.2 % saponin, and intracellularly stained with antibodies against CD206 and Clever-1 (mStab1). Isotype controls were included for CD115, CD206, Clever-1, F4/80, and PD-L1 to enable the calculation of ΔMFI values for these parameters. The $CD11b^{+}$ $CD45^{+}$ $Ly\text{-}6G^{-}$ cell population was considered to consist of TAMs. The cell surface expression of Ly-6C and class II MHC was used to divide the total population of TAMs into $Ly\text{-}6C^{high}$ class II MHC^{low} inflammatory monocytes, $Ly\text{-}6C^{high}$ class II MHC^{high} immature macrophages, $Ly\text{-}6C^{low}$ class II MHC^{high} M1 TAMs, and $Ly\text{-}6C^{low}$ class II MHC^{low} M2 TAMs, as described by Movahedi & al. (2010) (see Figure 13, A.). Changes in the relative amounts of TAMs in different subpopulations as well as changes in the expression of CD115, CD206, Clever-1, F4/80, and PD-L1 within these subpopulations in response to different treatments were analysed.

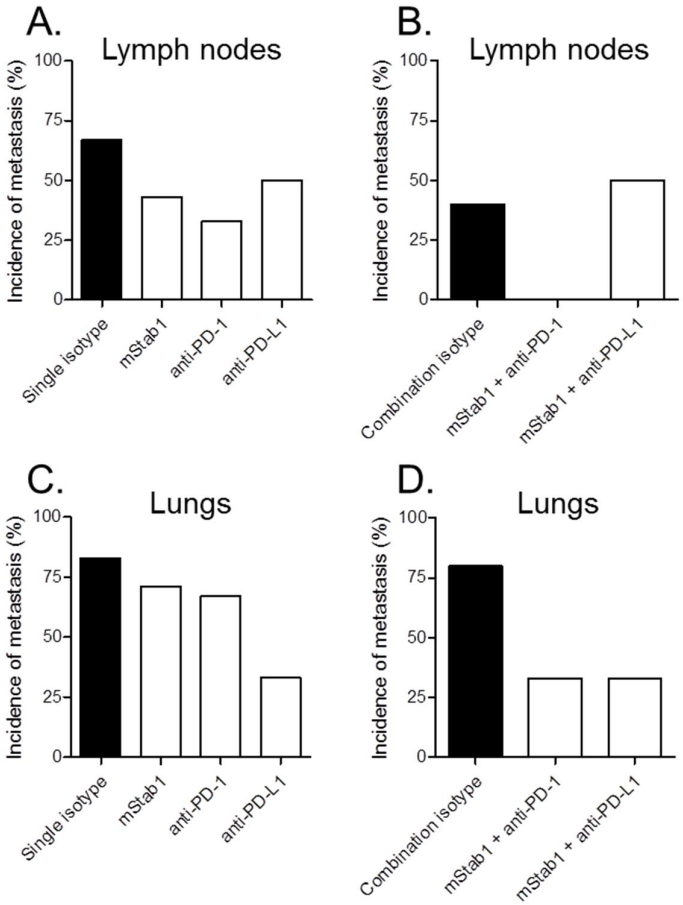

Figure 12. The incidence of metastasis in response to the indicated antibody treatments. **A.** & **B.** The incidence of metastasis in the draining inguinal lymph nodes in response to the indicated single or combinatorial antibody treatments, respectively. **C.** & **D.** The incidence of metastasis in the lungs in response to the indicated single or combinatorial antibody treatments, respectively. The incidence of metastasis was calculated as per cent of positive metastases in the indicated organ in response to each indicated treatment.

One-way ANOVA did not reveal any statistically significant differences in the compositions of TAMs between the control and treatment groups overall ($p > 0.05$ for all). No statistically significant differences were observed in the relative amounts of inflammatory monocytes, immature macrophages, M1 TAMs, or M2 TAMs between the single isotype control and the mStab1 treatment, anti-PD-1 treatment, or anti-PD-L1 treatment groups (see Figure 13, B.). However, when compared to the combination isotype control group, in the mStab1 + anti-PD-1 treatment and mStab1 + anti-PD-L1 treatment groups, the relative amount of M2 TAMs had decreased by an average of 17.0 and 13.3 %, respectively (57.1 ± 4.4 vs 47.4 ± 5.1 and 49.5 ± 3.8 %) (see Figure 13, C.). These differences were both also statistically significant ($p < 0.05$). Based on these results, the combinatorial Clever-1 and PD-1 antibody treatment decreased the anti-inflammatory phenotype of TAMs in the tumour microenvironment in the 4T1 mouse model of triple-negative breast cancer, as does the combinatorial Clever-1 and PD-L1 antibody treatment, although to a lesser extent.

Moreover, a statistically significant decrease in the expression of Clever-1 in M2 TAMs was observed between the single isotype control and the mStab1 treatment and anti-PD-1 treatment groups (842.0 ± 72.4 vs 501.8 ± 88.5 and 517.2 ± 64.9, respectively; $p < 0.05$ for both), but not between the single isotype control and the anti-PD-L1 treatment group (842.0 ± 72.4 vs 659.8 ± 109.3; $p > 0.05$) or the combination isotype control and the mStab1 + anti-PD-1 treatment or mStab1 + anti-PD-L1 treatment groups (829.2 ± 116.5 vs 648.7 ± 82.7 and 636.0 ± 137.4, respectively; $p > 0.05$ for both), as

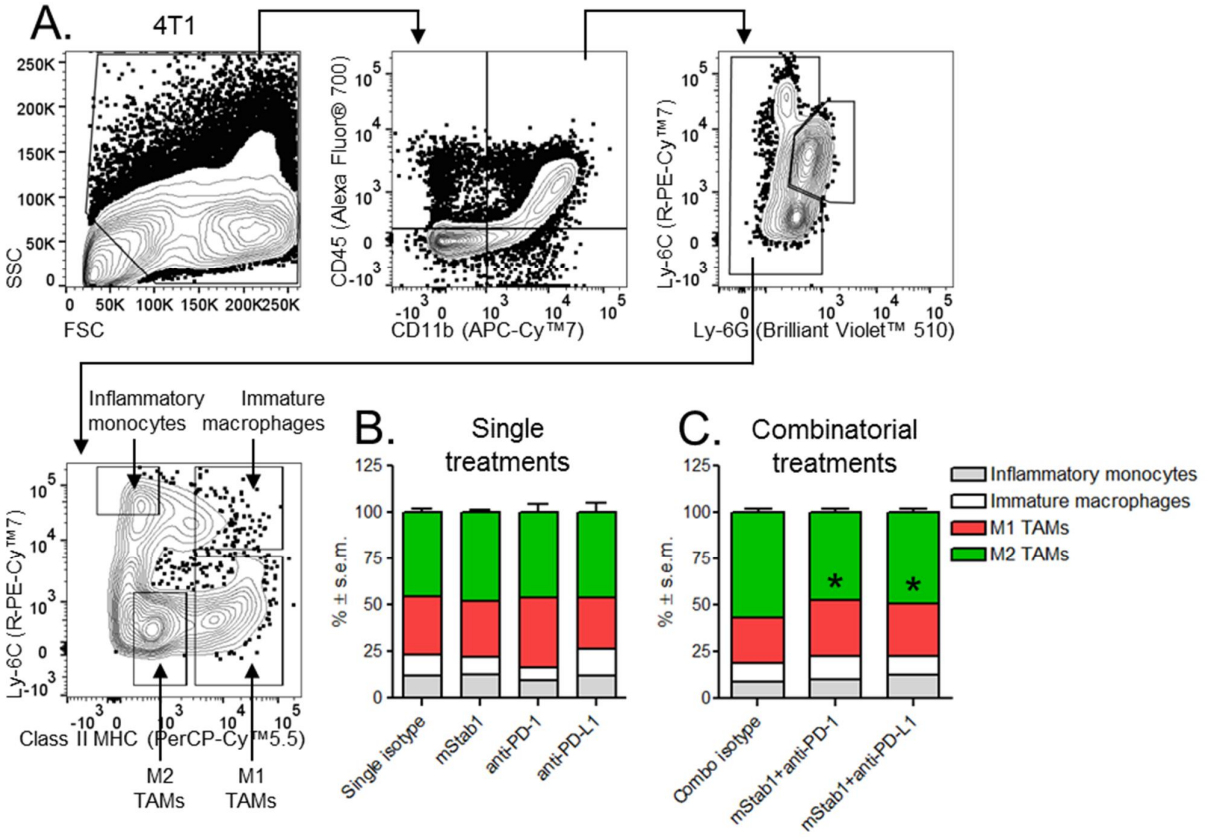

Figure 13. Changes in the relative amounts of different subpopulations of TAMs in response to single and combinatorial antibody treatments. **A.** The used gating strategy from a representative sample. **B.** & **C.** The relative amounts of TAMs in different subpopulations in response to single and combinatorial antibody treatments, respectively, as gated in **A.** Data are shown as mean ± s.e.m. For *n*, see the legend for **Figure 11**. Statistical significance was calculated with unpaired Student's two-tailed *t*-test comparing the relative amount of each TAM subpopulation in the treatment groups to the same TAM subpopulation in the respective isotype control group (*, $p < 0.05$).

determined by their ΔMFI values (see Figure 14, A. & B.). The Clever-1 antibody used for intracellular staining was the same clone as the one administered for treatments, and therefore, the decreased expression of Clever-1 in the mStab1 treatment group was probably due to the epitope being occupied by the unconjugated mStab1 antibody. This may be regarded as evidence that the mStab1 antibody reaches its target on M2 TAMs within the tumour microenvironment when administered by intraperitoneal injection. In the anti-PD-1 treatment group this would not be the case, which suggests that PD-1 antibody treatment alone decreases the expression of Clever-1 in M2 TAMs. However, the combinatorial effect of mStab1 and PD-1 antibody treatment was not synergistic in this regard, since in the mStab1 + anti-PD-1 treatment group, the expression of Clever-1 had decreased only slightly and not statistically significantly when compared to the combination isotype control group. As would be expected, the expression of Clever-1 increased as TAMs matured from inflammatory monocytes, immature macrophages, and M1 TAMs into M2 TAMs, which supports the gating used for flow cytometric analysis.

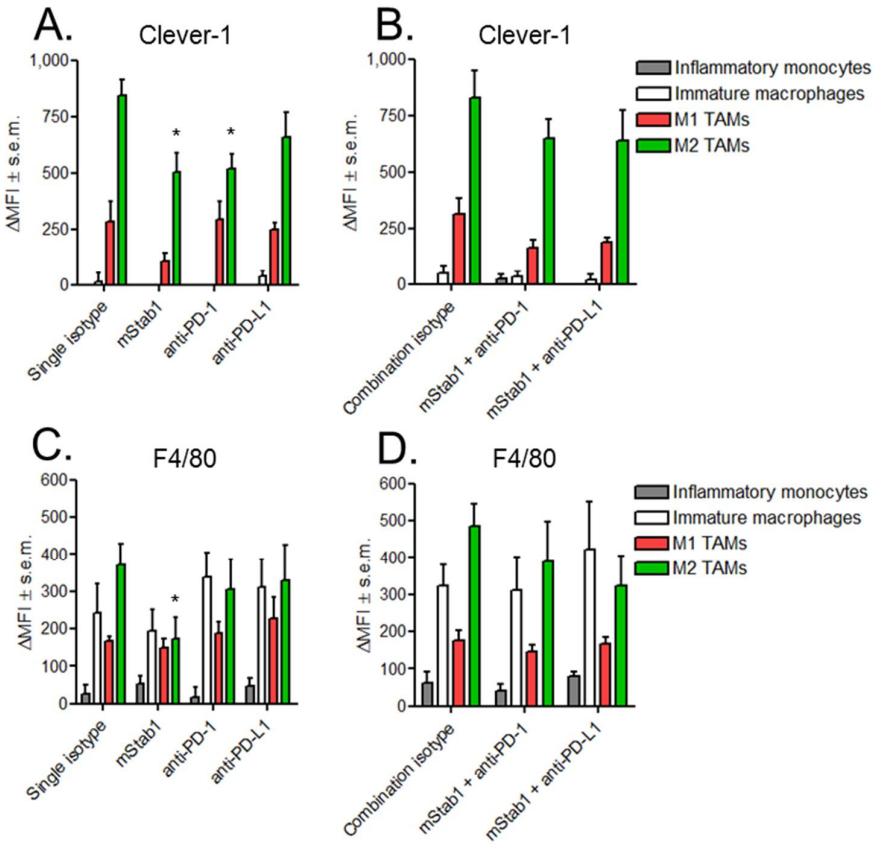

Figure 14. Phenotypic changes in different subpopulations of TAMs in response to single and combinatorial antibody treatments as gated in **Figure 13**. **A.** & **B.** The expression of Clever-1 in different TAM subpopulations in response to single and combinatorial antibody treatments, respectively. **C.** & **D.** The expression of F4/80 in response to single and combinatorial antibody treatments, respectively. Data are presented as mean ± s.e.m. For *n*, see the legend for **Figure 11**. Statistical significance was calculated with unpaired Student's two-tailed *t*-test (*, $p < 0.05$).

From the other analysed markers, when compared to the single isotype control group, the expression of F4/80 in M2 TAMs had decreased significantly in response to Clever-1 antibody treatment, as determined by their ΔMFI values (370.2 ± 56.8 vs 171.5 ± 57.2, respectively; $p < 0.05$), but not in response to PD-1 or PD-L1 antibody treatment (370.2 ± 56.8 vs 303.7 ± 81.4 and 329.7 ± 96.0, respectively; $p > 0.05$ for both) (see Figure 14, C.). A similar effect in response to the antibody-mediated interference of Clever-1 was observed by Karikoski & al. (2014), who compared the numbers of F4/80$^+$ TAMs between the single isotype control and mStab1 treatment groups. No statistically significant differences were observed between the combination isotype control and the mStab1 + anti-PD-1 treatment or the mStab1 + anti-PD-L1 treatment groups either, although the expression of F4/80 had slightly decreased between them as well, as determined by their ΔMFI values (484.2 ± 61.6 vs 389.2 ± 109.1 and 321.5 ± 82.3; $p > 0.05$ for both) (see Figure 14, D.). Although F4/80 is routinely used as a pan-macrophage marker, it is more highly expressed by M2 macrophages and has anti-inflammatory functions (Lin & al., 2005). Therefore, the decreased expression of F4/80 by Clever-1 antibody treatment supports the hypothesis that interfering with the function of Clever-1 in M2 TAMs suppresses their anti-inflammatory phenotype.

Unfortunately, no detectable signals above those from the isotype controls were acquired for CD115, CD206, or PD-L1. Since it is unlikely that these markers were not expressed by TAMs, it is possible that treating the tumour samples with collagenase IV and DNase I or fixation with formaldehyde may have rendered the epitopes unrecognizable for these particular antibody clones. As a result, these parameters could not be analysed.

Changes in the relative amounts of other infiltrating leukocytes in response to single and combinatorial antibody treatments were also analysed (see Figure 15, A.). No statistically significant differences were observed between the control and treatment groups in the relative amounts of total lymphocytes ($CD45^+$ $CD11b^-$), myeloid cells ($CD45^+$ $CD11b^+$), or neutrophils ($CD45^+$ $CD11b^+$ $Ly\text{-}6G^+$) (see Figure 15, B., C., & D.), which suggests that Clever-1 antibody treatment does not have an effect on the overall leukocyte trafficking into the tumour microenvironment.

6 Discussion

The data presented in this master's thesis support the function of Clever-1 as a regulator of the anti-inflammatory phenotype of M2 macrophages. Interestingly, it was discovered that in the mouse, as in

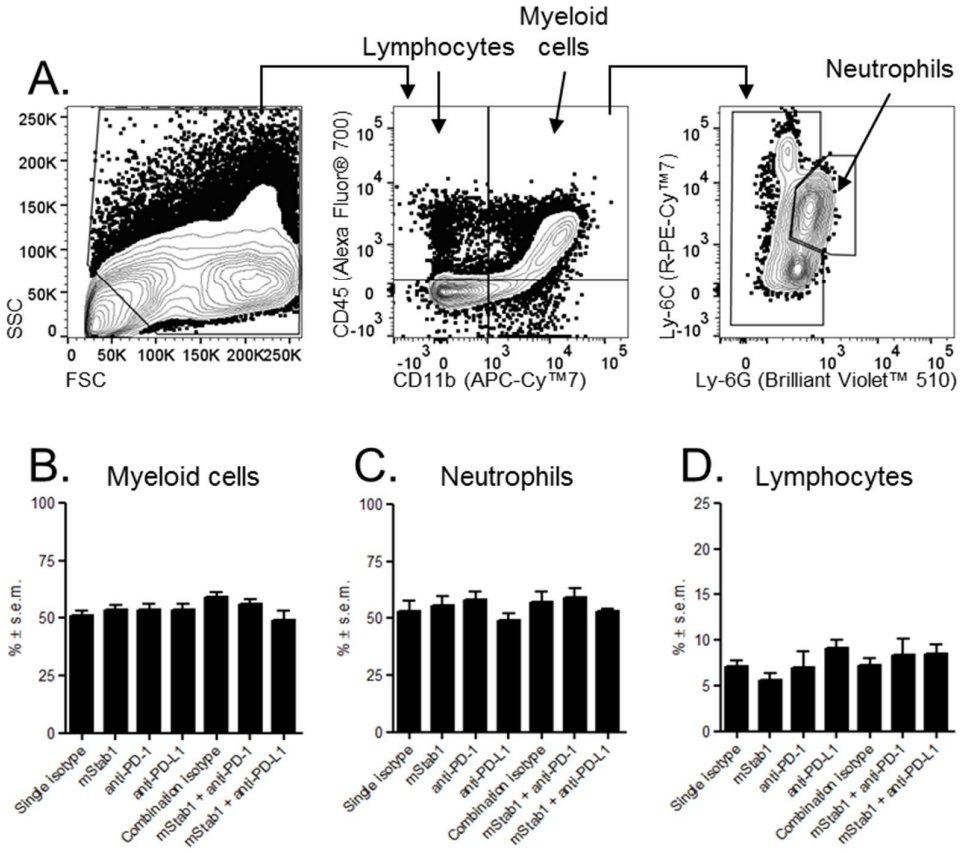

Figure 15. The relative amounts of other infiltrating leukocytes in the 4T1 tumour microenvironment in response to single and combinatorial antibody treatments. **A.** The gating strategy used to separate the different infiltrating leukocyte subpopulations shown from a representative sample. **B.** The relative amounts of $CD11b^+$ infiltrating myeloid cells as per cent of all cells in response to the indicated treatments. **C.** The relative amounts of neutrophils as per cent of myeloid cells in response to the indicated treatments. **D.** The relative amounts of lymphocytes as per cent of all cells in response to the indicated treatments. Data are presented as mean ± s.e.m. For *n*, see the legend for **Figure 11**.

humans, Clever-1 is expressed already under homoeostatic conditions by monocytes in the bone marrow and blood and that the expression of Clever-1 appears to be upregulated as monocytes depart from the bone marrow and enter circulation. Similarly to humans, in which Clever-1 is expressed by the proinflammatory classical $CD14^+$ $CD16^-$ and intermediate $CD14^+$ $CD16^+$ monocytes, in mice, Clever-1 expression was detected in the proinflammatory Ly-$6C^{high}$ monocytes, whereas the patrolling Ly-$6C^{low}$ monocytes expressed significantly less Clever-1 (Palani & al., 2016). Additionally, it was demonstrated that the antibody-mediated interference of Clever-1 led to a notable increase in the secretion of TNF-α, a central proinflammatory cytokine, by primary human macrophages, murine TAMs, and M2 BMDMs, a response observed also when Clever-1 was silenced by RNA interference (Palani & al., 2014; Palani & al., 2016). An attractive hypothesis is that Clever-1 functions as an immune checkpoint protein in proinflammatory monocytes, where it represses their M1 polarization in response to inflammatory stimuli and, thereby, prevents the excessive secretion of proinflammatory cytokines. Additionally, it was shown that Clever-1 antibody treatment results in a similar response as silencing Clever-1 with RNA interference, which suggests that these two antibodies – the Fu HI-3-372/2 clone in humans and the mStab1-1.26 clone in mice – do in fact interfere with the function of Clever-1 and can therefore be used in functional experiments.

The molecular mechanisms by which Clever-1 regulates the phenotype of M2 macrophages are poorly characterized. Here, it was shown that the activity of the mTORC1 signalling pathway is downregulated in Clever-$1^{-/-}$ M2 BMDMs. Relevantly, activation of the mTORC1 signalling pathway in myeloid cells has been shown to inhibit the activity of NF-κB and enhance the activity of STAT3, leading to the decreased secretion of proinflammatory cytokines, including TNF-α, and reduced inflammation (Weichhart & al., 2008). Accordingly, the antibody-mediated interference of Clever-1 increased the amount of secreted TNF-α. Hypothetically, Clever-1 could mediate signal transduction through or downstream of the mTORC1 complex, for example as a scaffold protein. To examine this hypothesis, the effects of disrupting Clever-1 on the phosphorylation of NF-κB and STAT3 as well as on the secretion of other cytokines should be investigated. Immunoprecipitation could be utilized to determine whether Clever-1 interacts with members of the mTORC1 signalling pathway. Conflictingly, Karikoski & al. (2009) have shown that Clever-1 antibody treatment actually has an anti-inflammatory effect *in vivo* by preventing leukocyte trafficking into the site of inflammation. However, these anti-inflammatory effects are in all likelihood produced by the antibody-mediated interference of endothelial Clever-1. It could be of interest to investigate how macrophage-specific Clever-$1^{-/-}$ mice react to similar models of inflammation.

The immunotherapeutic potential of Clever-1 as a drug target in cancer has been studied in two recent publications (Karikoski & al., 2014; Riabov & al., 2016). Encouraged by the positive findings in these publications, the immunotherapeutic potential of Clever-1 antibody treatment in two other mouse models of breast cancer, E0771 and 4T1, was investigated. Both of these models are orthotopic and immunocompetent, which makes it possible to study how Clever-1 antibody treatment modulates the immune response in addition to studying its effects on tumour growth and metastasis. Interestingly, it was observed that the tumour-infiltrating myeloid cells – which comprise of both granulocytes and TAMs, of which only TAMs express Clever-1 – in the E0771 tumours expressed much less Clever-1 than those in the 4T1 tumours. No effect on tumour growth in response to

Clever-1 antibody treatment was observed in the E0771 tumours, whereas in the 4T1 tumours, Clev-Clever-1 antibody treatment significantly limited tumour growth, although in only one of two experiments. However, it must be pointed out that the initial number of cancer cells used to induce the E0771 tumours was ten times larger than what was used to induce the 4T1 tumours, and that the former experiment had to be prematurely discontinued. Therefore, the immunotherapeutic effect of Clever-1 antibody treatment simply may not have become apparent in the actualized timeframe of the E0771 tumour experiment.

Of the two 4T1 tumour experiments, Clever-1 antibody treatment reduced tumour growth by itself in the first but not in the second experiment. However, combinatorial Clever-1 and PD-1 antibody treatment did limit both tumour growth and metastasis in the second 4T1 experiment. These results require repetition in order to determine their validity and significance because of the variability observed between experiments and even between mice in the same group within an experiment. While it seems clear that the mStab1 antibody does indeed reach its target within the tumour microenvironment, its dose may need to be increased in order to elicit a stronger response. Furthermore, data from the second 4T1 tumour experiment suggest that Clever-1 antibody treatment may inhibit metastasis also in this cancer model and that the combinatorial Clever-1 and PD-1 antibody treatment has a synergistic effect in limiting metastasis as well as tumour growth, which was probably caused by obstructing endothelial Clever-1 and, supposedly, the increased activation of T_C cells, which was not analysed here. Interestingly, such synergy was not observed when Clever-1 antibody treatment was combined to PD-L1 antibody treatment. Unfortunately, the expression of PD-L1 by TAMs or the tumour could not be assessed. Hypothetically, PD-1 antagonism could be more effective because it inhibits the activation of PD-1 by both of its ligands, PD-L1 and PD-L2.

Additionally, combinatorial Clever-1 and PD-1 or PD-L1 antibody treatment decreased the relative amount of M2 TAMs, where combination with PD-1 yielded a more potent effect, which suggests that the observed reduction in tumour growth and metastasis may have been mediated at least partly by the immunomodulation of the tumour microenvironment. Interestingly, no effect was observed in the relative amounts of total infiltrating lymphocytes, myeloid cells, or neutrophils between controls and treatments in any experiment. This suggests that Clever-1 antibody treatment does not affect leukocyte trafficking into the tumour microenvironment. While Karikoski & al. (2014) observed that the number of total TAMs and M2 TAMs, as determined by immunofluorescence microscopy and defined by the expression of F4/80 and CD206, respectively, had been reduced in response to Clever-1 antibody treatment, such an effect was not observed here in response to Clever-1 antibody treatment alone. However, while the expression of CD206 unfortunately could not be analysed, the expression of F4/80, which also has anti-inflammatory properties, had been downregulated in M2 TAMs in response to Clever-1 antibody treatment in the second 4T1 tumour experiment. Taken together, it may be that rather than controlling leukocyte trafficking into the tumour microenvironment, Clever-1 antibody treatment actually modulates the phenotype of M2 TAMs, in addition to inhibiting the migration of malignant cells through the lymphatics. Encouragingly, combining Clever-1 antibody treatment to PD-1 antagonism appeared to have a consistent, synergistic immunotherapeutic effect in the 4T1 mouse model of breast cancer in all aspects analysed. The decreases in M2 TAMs and the incidence of metastasis in response to combinatorial

Clever-1 and PD-1 antibody treatment could be explained by reduced migration of malignant cells through the lymphatics and their more efficient killing by the activated anticancer immune response. As with the other *in vivo* experiments, these results need to be replicated before making more definite conclusions.

With regard to the results from the antibody-mediated interference of Clever-1 *in vitro*, it would be interesting to examine whether Clever-1 antibody treatment increases the amount of TNF-α within the tumour microenvironment. This effect could be a double-edged sword, since, as discussed above, TNF-α can in some cases support the smouldering, chronic tumour-promoting inflammation and function as a growth factor for malignant cells. However, in combination with other immunotherapies, the increased secretion of TNF-α could hypothetically intensify the proinflammatory milieu within the tumour microenvironment. Additionally, the effects of Clever-1 antibody treatment on other tumour-infiltrating leukocytes should be analysed in later experiments. If Clever-1 antibody treatment does downregulate F4/80 in TAMs, with or without an increase in the secretion of TNF-α, it should cause a reduction in the number of T_{reg} cells within the tumour microenvironment (Lin & al., 2005). This in combination with, for example, PD-1 antagonisms, would hypothetically lead to the increased activation of T_C cells and a potent anticancer immune response. However, the possible changes in other M2 markers in response to Clever-1 antibody treatment need to be analysed as well, since in humans, the analogue of F4/80 is actually specific to eosinophils and, therefore, the translatability of this effect is questionable (Hamann & al., 2007). In later experiments, fluorescence-activated cell sorting of the different subpopulations of TAMs could be useful in order to determine the effects of Clever-1 antibody treatment more comprehensively by quantitative PCR, microarrays, RNA sequencing, or mass spectrometry.

In conclusion, the data presented in this master's thesis provide evidence that Clever-1 regulates the anti-inflammatory phenotype of M2 macrophages by activating the mTORC1 signalling pathway, leading to reduced amounts of secreted proinflammatory cytokines. In the 4T1 mouse model of triple-negative breast cancer, Clever-1 antibody treatment may have an immunotherapeutic effect on tumour growth and metastasis. However, these findings must be replicated before more definite conclusions are drawn. Hypothetically, the immunotherapeutic effect of Clever-1 antibody treatment is a result of the immunomodulation of the tumour microenvironment, where the antibody-mediated interference of Clever-1 is thought to suppress M2 TAMs and, thus, to activate the anticancer immune response.

References

Adachi, H. & Tsujimoto, M. 2002. FEEL-1, a novel scavenger receptor with *in vitro* bacteria-binding and angiogenesis-modulating activities. *J. Biol. Chem.* 277, 34264–34270.

Adachi, H. & Tsujimoto, M. 2010. Adaptor protein sorting nexin 17 interacts with the scavenger receptor FEEL-1/stabilin-1 and modulates its expression on the cell surface. *Biochim. Biophys. Acta* 1803, 553–563.

Agata, Y.; Kawasaki, A.; Nishimura, H.; Ishida, Y.; Tsubata, T.; Yagita, H.; & Honjo, T. 1996. Expression of the PD-1 antigen on the surface of stimulated mouse T and B lymphocytes. *Int. Immunol.* 8, 765–772.

Aharinejad, S.; Paulus, P.; Sioud, M.; Hofmann, M.; Zins, K.; Schäfer, R.; Stanley, E.; & Abraham. D. 2004. CSF-1 blockade by antisense oligonucleotides and small interfering RNAs suppress growth of human mammary tumor xenografts in mice. *Cancer Res.* 64, 5378–5384.

Akira, S.; Nishio, Y.; Inoue, M.; Wang, X.; Wei, S.; Matsusaka, T.; Yoshida, K.; Sudo, T.; Naruto, M.; & Kishimoto, T. 1994. Molecular cloning of APRF, a novel IFN-stimulated gene factor 3 p91-related transcription factor involved in the gp130-mediated signalling pathway. *Cell* 77, 63–71.

Alleva, D.; Burger, C.; & Elgert, K. 1994. Tumour-induced regulation of suppressor macrophage nitric oxide and TNF-α production. Role of tumour-derived IL-10, TGFβ, and prostaglandin E2. *J. Immunol.* 153, 1674–1686.

Antonios, J.; Yao, Z.; Li, C.; Rao, A.; & Goodman, S. 2013. Macrophage polarization in response to wear particles *in vitro*. *Cell. Mol. Immunol.* 10, 471–482.

Aslakson, C. & Miller, F. 1992. Selective events in the metastatic process defined by analysis of the sequential dissemination of subpopulations of a mouse mammary tumour. *Cancer Res.* 52, 1399–1405.

Balkwill, F.; Charles, K.; & Mantovani, A. 2005, Smouldering and polarized inflammation in the initiation and promotion of malignant disease. *Cancer Cell* 7, 211–217.

Bayne, L.; Beatty, G.; Jhala, N.; Clark, C.; Rhim, A.; Stanger, B.; & Vonderheide, R. 2012. Tumour-derived granulocyte-macrophage colony-stimulating factor regulates myeloid inflammation and T cell immunity in pancreatic cancer. *Cancer Cell* 21, 822–835.

Biswas, S.; Gangi, L.; Paul, S. Schioppa, T.; Saccani, A.; Sironi, M.; Bottazzi, B.; Doni, A.; Vincenzo, B.; Pasqualini, F.; Vago, L.; Nebuloni, M.; Mantovani, A.; & Sica, A. 2006. A distinct and unique transcriptional programme expressed by TAMs (defective NF-κB and enhanced IRF-3/STAT1 activation). *Blood* 107, 2112–2122.

Biswas, S. & Mantovani, A. 2010. Macrophage plasticity and interaction with lymphocyte subsets: cancer as a paradigm. *Nat. Immunol.* 11, 889–896.

Braun, D.; Fribourg, M.; & Sealfon, S. 2012. Cytokine response is determined by duration of receptor and STAT3 activation. *J. Biol. Chem.* 288, 2986–2993.

Brown, M. & Goldstein, J. 1979. Receptor-mediated endocytosis: insights from the lipoprotein receptor system. *Proc. Natl Acad. Sci. USA* 76, 3330–3337.

Brown, M.; Goldstein, J.; Krieger, M.; Ho, Y.; & Anderson, R. 1979. Reversible accumulation of cholesteryl esters in macrophages incubated with acetylated lipoproteins. *J. Cell. Biol.* 82, 567–613.

Burke, R.; Madden, K.; Perry, S.; Zettel, M.; & Brown, E. 2013. TAMs and stromal TNF-α regulate collagen structure in a breast tumour model as visualized by second harmonic generation. *J. Biomed. Opt.* 18, 086003.

Byles, V.; Covarrubias, A.; Ben-Sahra, I.; Lamming, D.; Sabatini, D.; Manning, B.; & Horng, T. 2013. The TSC-mTOR pathway upregulates macrophage polarization. *Nat Commun.* 4, 2834.

Byrne, A. & Reen, D. 2002. LPS induces rapid production of IL-10 by monocytes in the presence of apoptotic neutrophils. *J. Immunol.* 168, 1968–1977.

Canton, J.; Neculai, D.; & Grinstein, S. 2013. Scavenger receptors in homeostasis and immunity. *Nat. Rev. Immunol.* 13, 621–634.

Carswell, E.; Old, L.; Kassel, R.; Green, S.; Fiore, N.; & Williamson, B. 1975. An endotoxin-induced serum factor that causes necrosis of tumours. *Proc. Natl Acad. Sci. USA* 72, 3666–3670.

Chaudhry, A.; Samstein, R.; Treuting, P.; Liang, Y.; Pils, M.; Heinrich, J.-M.; Sack, R.; Wunderlich, F.; Brüning, J.; Müller, W.; & Rudensky, A. 2011. IL-10 signalling in T_{reg} cells is required for suppression of T_H17-cell-mediated inflammation. *Immunity* 34, 566–578.

Conze, D.; Weiss, L.; Regen, P.; Bhushan, A.; Weaver, D.; Johnson, P.; & Rincón, M. 2001. Autocrine production of IL-6 causes multidrug resistance in breast cancer cells. *Cancer Res.* 61, 8851–8858.

Courtois, G. & Gilmore, T. 2006. Mutations in the NF-κB signalling pathway: implications for human disease. *Oncogene* 25, 6831–6843.

Coussens, L.; Zitvogel, L.; & Palucka, A. 2013. Neutralizing tumour-promoting chronic inflammation: a magic bullet? *Science* 339, 286–291.

Crotty, S. 2011. Follicular helper CD4 T cells (T_{FH}). *Annu. Rev. Immunol.* 29, 621–663.

Dauer, D.; Ferraro, B.; Song, L.; Yu, B.; Mora, L.; Buettner, R.; Enkemann, S.; Jove, R.; & Haura, E. 2005. STAT3 regulated genes common to both wound healing and cancer. *Oncogene* 24, 3397–3408.

David, C.; Nance, J.; Hubbard, J.; Hsu, M.; Binder, D.; & Wilson, E. 2012. Stabilin-1 expression in tumour-associated macrophages. *Brain Res.* 1481, 71–78.

De Visser, K.; Eichten, A.; & Coussens, L. 2006. Paradoxical roles of the immune system during cancer development. *Nat. Rev. Cancer* 6, 24–37.

De Waal Malefyt, R.; Haanen, J.; Spits, H.; Roncarolo, M.-G.; te Velde, A.; Figdor, C.; Johnson, K.; Kastelein, R.; Yssel, H.; & de Vries, J. 1991. IL-10 and viral IL-10 strongly reduce antigen-specific human T cell proliferation by diminishing the antigen-presenting capacity of monocytes via downregulation of class II MHC expression. *J. Exp. Med.* 174, 915–924.

DeNardo, D.; Barreto, J.; Andreu, P.; Vasquez, L.; Tawfik, D.; Kolhatkar, N.; & Coussens, L. 2009. $CD4^+$ T cells regulate pulmonary metastasis of mammary carcinomas by enhancing protumor properties of macrophages. *Cancer Cell* 16, 91–102.

DeNardo, D.; Brennan, D.; Rexhepaj, E.; Ruffell, B.; Shiao, S.; Madden, S.; Gallagher, W.; Wadhwani, N.; Keil, S.; Junaid, S.; Rugo, H.; Hwang, E.; Jirström, K.; West, B.; & Coussens, L. 2011. Leukocyte complexity predicts breast cancer survival and functionally regulates response to chemotherapy. *Cancer Disc.* 1, 54–67.

Ding, L. & Shevach, E. 1992. IL-10 inhibits mitogen-induced T cell proliferation by selectively inhibiting macrophage costimulatory function. *J. Immunol.* 148, 3133–3139.

Ding, L.; Linsley, P.; Huang, L.; Germain, R.; & Shevach, E. 1993. IL-10 inhibits macrophage costimulatory activity by selectively inhibiting the upregulation of B7 expression. *J. Exp. Med.* 151, 1224–1234.

Dong, H.; Strome, S.; Salomao, D.; Tamura, H.; Hirano, F.; Flies, D.; Roche, P.; Lu, J.; Zhu, G.; Tamada, K.; Lennon, V.; Celis, E.; & Chen, L. 2002. Tumour-associated B7-H1 promotes T cell apoptosis: a potential mechanism of immune evasion. *Nat. Med.* 8, 793–800.

Duluc, D.; Delneste, Y.; Tan, F.; Moles, M.-P.; Grimaud, L.; Lenoir, J.; Preisser, L.; Anegon, I.; Catala, L.; Ifrah, N.; Descamps, P.; Gamelin, E.; Gascan, H.; Hebbar, M.; & Jeannin, P. 2007. Tumour-associated LIF and IL-6 skew monocyte differentiation into TAM-like cells. *Blood* 110, 4319–4330.

Dunn, G.; Bruce, A.; Ikeda, H.; Old, L.; & Schreiber, R. 2002. Cancer immunoediting: from immunosurveillance to tumour escape. *Nat. Immunol.* 3, 991–998.

Dunn, G.; Old, L.; & Schreiber, R. 2004. The three Es of cancer immunoediting. *Annu. Rev. Immunol.* 22, 329–360.

Dvorak, H. 1986. Tumours: wounds that do not heal. Similarities between tumour stroma generation and wound healing. *N. Eng. J. Med.* 315, 1650–1659.

Fadok, V.; Bratton, D.; Konowal, A.; Freed, P.; Westcott, J.; & Henson, P. 1998. Macrophages that have ingested apoptotic cells *in vitro* inhibit proinflammatory cytokine production through autocrine/paracrine mechanisms involving TGFβ, PGE-2, and PAF. *J. Clin. Invest.* 101, 890–898.

Falkowski, M.; Schledzewski, K.; Hansen, B.; & Goerdt, S. 2003. Expression of Stabilin-2, a novel fasciclin-like hyaluronan receptor protein, in murine sinusoidal endothelia, vascular tissues, and at solid/liquid interfaces. *Histochem. Cell Biol.* 120, 361–369.

Feng, X-.H.; & Derycnk, R. 2005. Specificity and versatility in TGFβ signalling through Smads. *Ann. Rev. Cell Dev. Immunol.* 21, 659–693.

Fiorentino, D.; Zlotnik, A.; Vieira, P.; Mosmann, T.; Howard, M.; Moore, K.; & O'Garra, A. 1991. IL-10 acts on the APC to inhibit cytokine production by T_H1 cells. *J. Immunol.* 146, 3444–3451.

Foucher, E.; Blanchard, S.; Preisser, L.; Garo, L.; Garo, E.; Ifrah, N.; Guardiola, P.; Delneste, Y.; & Jeannin, P. 2013. IL-34 induces the differentiation of human monocytes into immunosuppressive macrophages. Antagonistic effects of GM-CSF and IFN-γ. *PLOS ONE* 9, 10.

Freeman, G.; Long, A.; Iwai, Y.; Bourque, K.; Chernova, T.; Nishimura, H.; Fitz, L.; Malenkovich, N.; Okazaki, T.; Byrne, M.; Horton, H.; Fouser, L.; Carter, L.; Ling, V.; Bowman, M.; Carreno, B.; Collins, M.; Wood, C.; & Honjo, T. 2000. Engagement of the PD-1 immunoinhibitory receptor by a novel B7 family member leads to negative regulation of lymphocyte activation. *J. Exp. Med.* 192, 1027–1034.

Fukada, T.; Hibi, M.; Yamanaka, Y.; Takahashi-Tezuka, M.; Fujitani, Y.; Yamaguchi, T.; Nakajima, K.; & Hirano, T. 1996. Two signals are necessary for cell proliferation induced by a cytokine receptor gp130: involvement of STAT3 in antiapoptosis. *Immunity* 5, 449–460.

Gillette, J. & Mitchell, J. 1991. Ornithine decarboxylase: a biochemical marker of repair in damaged tissue. *Life Sci.* 48, 1501–1510.

Gocheva, V.; Wang, H.; Gadea, B.; Shree, T.; Hunter, K.; Garfall, A.; Berman, T.; & Joyce, J. 2010. IL-4 induces cathepsin protease activity in TAMs to promote cancer growth and invasion. *Genes Dev.* 24, 241–255.

Goerdt, S.; Walsh, L.; Murphy, G.; & Pober, J. 1991. Identification of a novel high molecular weight protein preferentially expressed by sinusoidal endothelial cells in normal human tissues. *J. Cell Biol.* 113, 1425–1437.

Goerdt, S.; Bhardwaj, R.; & Sorg, C. 1993. Inducible expression of MS-1 high-molecular-weight protein by endothelial cells of continuous origin and by dendritic cells/macrophages *in vivo* and *in vitro*. *Am. J. Pathol.* 142, 1409–1422.

Grivennikov, S. & Karin, M. 2008. Autocrine IL-6 signalling: a key event in tumorigenesis? *Cancer Cell* 13, 7–9.

Hagemann, T.; Robinson, S.; Schulz, M.; Trümper, L.; Balkwill, F.; & Binder, C. 2004. Enhanced invasiveness of breast cancer cell lines upon co-cultivation with macrophages is due to TNF-α-dependent upregulation of matrix metalloproteases. *Carcinogenesis* 25, 1543–1549.

Hagemann, T.; Wilson, J.; Burke, F.; Kulbe, H.; Li, N.; Plüddemann, A.; Charles, K.; Gordon, S.; & Balkwill, F. 2006. Ovarian cancer cells polarize macrophages towards a tumour-associated phenotype. *J. Immunol.* 176, 5023–5032.

Hamann, J.; Koning, N.; Pouwels, W.; Ulfman, L.; van Eijk, M.; Stacey, M.; Lin, H.; Gordon, S.; Kwakkenbos, M. 2007. EMR1, the human homologue of F4/80, is an eosinophil-specific receptor. *Eur. J. Immunol.* 37, 2797–2802.

Hanahan, D. & Weinberg, R. 2000. The hallmarks of cancer. *Cell* 100, 57–70.

Hanahan, D. & Weinberg, R. 2011. The hallmarks of cancer: the next generation. *Cell* 144, 646–674.

Hanahan, D. & Coussens, L. 2012. Accessories to the crime: functions of cells recruited to the tumour microenvironment. *Cancer Cell* 21, 309–322.

Hansen, B.; Longati, P.; Elvevold, K.; Nedredal, G.; Schledzewski, K.; Olsen, R.; Falkowski, M.; Kzhyshkowska, J.; Carlsson, F.; Johansson, S.; Smedsrod, B.; Goerdt, S.; Johansson, S.; & McCourt, P. 2005. Stabilin-1 and Stabilin-2 are both directed into the early endocytic pathway in hepatic sinusoidal endothelium via interactions with clathrin/AP-2, independent of ligand binding.

Harris, E.; Weigel, J.; & Weigel, P. 2004. Endocytic function, glycosaminoglycan specificity, and antibody sensitivity of the recombinant human 190-kDa hyaluronan receptor for endocytosis (HARE). *J. Biol. Chem.* 279, 36201–36209.

Hefetz-Sela, S.; Stein, I.; Klieger, Y.; Porat, R.; Sade-Feldman, M.; Zreik, F.; Nagler, A.; Pappo, O.; Quagliata, L.; Dazert, E.; Eferl, R.; Terracciano, L.; Wagner, E.; Ben-Neriah, Y.; Baniyash, M.; & Pikarsky, E. 2014. Acquisition of an immunosuppressive protumorigenic macrophage phenotype depending on c-Jun phosphorylation. *Proc. Natl Acad. Sci. USA* 111, 17582–17587.

Hofseth, L.; Saito, S.; Hussain, S.; Espey, M.; Miranda, K.; Araki, Y.; Jhappan, C.; Higashimoto, Y.; He, P.; Linke, S.; Quezado, M.; Zurer, I.; Rotter, V.; Wink, D.; Appella, E.; & Harris, C. 2003. Nitric oxide-induced cellular stress and p53 activation in chronic inflammation. *Proc. Natl Acad. Sci. USA* 100, 143–148.

Hollmén, M.; Roudnicky, F.; Karaman, S.; & Detmar, M. 2015a. Characterization of macrophage–cancer cell crosstalk in oestrogen receptor positive and triple-negative breast cancer. *Sci. Rep.* 17, 9188.

Hollmén, M.; Karaman, S.; Schwager, S.; Lisibach, A.; Christiansen, A.; Maksimow, M.; Varga, Z.; Jalkanen, S.; & Detmar, M. 2015b. G-CSF regulates macrophage phenotype and associates with poor overall survival in human triple-negative breast cancer. *Oncoimmunology* 5, e1115177.

Irjala, H.; Elima, K.; Johansson, E.-L.; Merinen, M.; Kontula, K.; Alanen, K.; Grenman, R.; Salmi, M.; & Jalkanen, S. 2003a. The same endothelial receptor controls lymphocyte traffic both in vascular and lymphatic vessels. *Eur. J. Immunol.* 33, 815–824.

Irjala, H.; Alanen, K.; Grénman, R.; Heikkilä, P.; Joensuu, H.; & Jalkanen, S. 2003b. MR and Clever-1 direct the binding of cancer cells to the lymph vessel endothelium. *Cancer Res.* 63, 4671–4676.

Jäger, E.; Ringhoffer, M.; Karbach, J.; Arand, M.; Oesch, F.; & Knuth, A. 1998. Inverse relationship of melanocyte differentiation antigen in melanoma tissues and $CD8^+$ T_C cell responses: evidence for immunoselection of antigen-loss variants *in vivo*. *Intl J. Cancer* 66, 470–476.

Kano, A. 2015. Tumour cell secretion of soluble factor(s) for specific immunosuppression. *Sci. Rep.* 5, 8913.

Kantoff, P.; Higano, C.; Shore, N.; Berger, R.; Small, E., Penson, D.; Redfern, C.; Ferrari, A.; Dreicer, R.; Sims, R.; Xu, Y.; Frohlich, M.; & Schellhammer, P. for the IMPACT Study Investigators. 2010. Sipuleucel-T immunotherapy for castration-resistant prostate cancer. *New Eng. J. Med.* 363, 411–422.

Karikoski, M.; Irjala, H.; Maksimow, M.; Miiluniemi, M.; Granfors, K.; Hernesniemi, S.; Elima, K.; Moldenhauer, G.; Schledzewski, K.; Kzhyshkowska, J.; Goerdt, S.; Salmi, M.; & Jalkanen, S. 2009. Clever-1/Stabilin-1 regulates lymphocyte migration within lymphatics and leukocyte entrance to sites of inflammation. *Eur. J. Immunol.* 39, 3477-3487.

Karikoski, M.; Marttila-Ichihara, F.; Elima, K.; Rantakari, P.; Hollmén, M.; Kelkka, T.; Gerke, H.; Huovinen, V.; Irjala, H.; Holmdahl, R.; Salmi, M.; & Jalkanen, S. 2014. Clever-1/Stabilin-1 controls cancer growth and metastasis. *Clin. Cancer Res.* 20, 6452–6464.

Karin, M. 2006. NF-κB in cancer development and progression. *Nature* 441, 431–436.

Khong, H. & Restifo, N. 2002. Natural selection of tumour variants in the generation "tumour escape" phenotypes. *Nat. Immunol.* 3, 999–1005.

Kitamura, T.; Qian, B.; & Pollard, J. 2015. Immune cell promotion of metastasis. *Nat. Rev. Immunol.* 15, 73–86.

Kondo, A.; Yamashita, T.; Tamura, H.; Zhao, W.; Tsuji, T.; Shimizu, M.; Shinya, E.; Takahashi, H.; Tamada, K.; Chen, L.; Dan, K.; & Ogata, K. IFN-γ and TNF-α induce an immunoinhibitory molecule, B7-H1, via NF-κB activation in myelodysplastic syndromes. *Blood* 116, 1124–1131.

Korn, T.; Oukka, M.; Kuchroo, V.; & Bettelli, E. 2007. T_H17 cells: effector T cells with inflammatory properties. *Semin. Immunol.* 19, 362–371.

Kuang, D.; Zhao, Q.; Peng, C.; Xu, J.; Zhang, J.; Wu, C.; & Zheng, L. 2009. Activated monocytes in peritumoral stroma of hepatocellular carcinoma foster immune privilege and disease progression through PD-L1. *J. Exp. Med.* 206, 1327–1337.

Kulbe, H.; Thompson, R.; Wilson, J.; Robinson, S.; Hagemann, T.; Fatah, R.; Gould, D.; Ayhan, A.; & Balkwill, F. 2007. The inflammatory cytokine TNF-α generates an autocrine tumour-promoting network in epithelial ovarian cancer cells. *Cancer Res.* 67, 585–592.

Kzhyshkowska, J.; Gratchev, A.; Martens, J.-H.; Pervushina, O.; Mamidi, S.; Johansson, S.; Schledzewski, K.; Hansen, B.; He, X.; Tang, J.; Nakayama, K.; & Goerdt, S. 2004. Stabilin-1 localizes to endosomes and the *trans*-Golgi network in human macrophages and interacts with GGA adaptors. *J. Leukoc. Biol.* 76, 1151–1161.

Kzhyshkowska, J.; Gratchev, A.; Brundiers, H.; Mamidi, S.; Krusell, L.; & Goerdt, S. 2005. PI3K activity is required for Stabilin-1-mediated endosomal transport of acLDL. *Immunobiol.* 210, 161–173.

Kzhyshkowska, J.; Workman, G.; Cardó-Vila, M.; Arap, W.; Pasqualini, R.; Gratchev, A.; Krusell, L.; Goerdt, S.; & Sage, H. 2006a. Novel function of alternatively activated macrophages: Stabilin-1-mediated clearance of SPARC. *J. Immunol.* 176, 5825–5832.

Kzhyshkowska, J.; Gratchev, A.; & Goerdt, S. 2006b. Stabilin-1, a homoeostatic scavenger receptor with multiple functions. *J. Cell. Mol. Med.* 10, 635–649.

Kzhyshkowska, J.; Mamidi, S.; Gratchev, A.; Kremmer, E.; Schmuttermaier, C.; Krusell, L.; Haus, G.; Utikal, J.; Schledzewski, K.; Scholtze, J.; & Goerdt, S. 2006c. Novel Stabilin-1 interacting chitinase-like protein (SI-CLP) is upregulated in alternatively activated macrophages and secreted via lysosomal pathway. *Blood* 107, 3221–3228.

Lai, C.-F.; Ripperger, J.; Morella, K.; Jurlander, J.; Hawley, T.; Carson, W.; Kordula, T.; Caligiuri, M.; Hawley, R.; Fey, G.; & Baumann, H. 1996. Receptors for IL-10 and IL-6-type cytokines use similar signalling mechanisms for inducing transcription through IL-6 response elements. *J. Biol. Chem.* 271, 13968–13975.

Laoui, D.; van Overmeire, E.; di Conza, G.; Aldeni, C.; Keirsse, J.; Morias, Y.; Movahedi, K.; Houbracken, I.; Schouppe, E.; Elkrim, Y.; Karroum, O.; Jordan, B.; Carmeliet, P.; Gysemans, C.; de Baetselier, P.; Mazzone, M.; & van Ginderachter, J. 2014. Tumour hypoxia does not drive differentiation of tumour-associated macrophages but rather fine-tunes the M2-like macrophage population. *Cancer Res.* 74, 24–30.

Le, D.; Lutz, E.; Uram, J.; Sugar, E.; Onners, B.; Solt, S.; Zheng, L.; Diaz, L., Jr.; Donehower, R.; Jaffee, E.; & Laheru, D. 2013. Evaluation of ipilimumab in combination with allogeneic pancreatic tumor cells transfected with a GM-CSF gene in previously treated pancreatic cancer. *J. Immunother.* 36, 382–389.

Li, M.; Wan, Y.; Sanjabi, S.; Robertson, A.-K.; & Flavell, R. 2005. TGFβ regulation of immune responses. *Ann. Rev. Immunol.* 24, 99–146.

Liang, C.; Latchman, Y.; Buhlmann, J.; Tomczak, M.; Horwitz, B.; Freeman, G.; & Sharpe, A. 2003. Regulation of PD-1, PD-L1, and PD-L2 expression during normal and autoimmune responses. *Eur. J. Immunol.* 33, 2706–2716.

Lin, H.; Chen, C.; & Chen, B. 2001. Resistance of BMDMs to apoptosis is associated with the expression of X-linked inhibitor of apoptosis protein in primary cultures of bone marrow cells. *Biochem. J.* 353, 299–306.

Lin, E.; Nguyen, A.; Russell, R.; & Pollard, J. 2001. CSF-1 promotes progression of mammary tumours to malignancy. *J. Exp. Med.* 193, 727–740.

Lin, H.-H.; Faunce, D.; Stacey, M.; Terajewicz, A.; Nakamura, T.; Zhang-Hoover, J.; Kerley, M.; Mucenski, M.; Gordon, S.; & Stein-Streilein, J. 2005. The macrophages F4/80 receptor is required for the induction of antigen-specific efferent T_{reg} cells in peripheral tolerance. *J. Exp. Med.* 201, 1615–1625.

Lin, E.; Li; J.; Gnatovskiy, L.; Deng, Y.; Zhu, L.; Grzesik, D.; Qian, H.; Xue, X.; & Pollard, J. 2006. Macrophages regulate the angiogenic shift in a mouse model of breast cancer. *Cancer Res.* 66, 11238–11246.

Lombardo, E.; Alvarez-Barrientos, A.; Maroto, B.; Boscá, L.; & Knaus, U. 2007. TLR4-mediated survival of macrophages is MyD88-dependent and requires TNF-α autocrine signalling. *J. Immunol.* 15, 3731–3739.

Lu, T.; Ramakrishnan, R.; Altiok, S.; Youn, J.-I.; Cheng, P.; Celis, E.; Pisarev, V.; Sherman, S.; Sporn, M.; & Gabrilovich, D. 2011. Tumour-infiltrating myeloid cells induce tumour cell resistance to T_C cells in mice. *J. Clin. Invest.* 121, 4015–4029.

Mantovani, A.; Sozzani, S.; Locati, M.; Allavena, P.; & Sica, A. 2002. Macrophage polarization: TAMs as a paradigm for polarized M2 mononuclear phagocytes. *Trends Immunol.* 23, 549–555.

Mantovani, A.; Allavena, P.; & Balkwill, F. 2008. Cancer-related inflammation. *Nature* 454, 436–444.

Martens, J.; Kzhyshkowska, J.; Falkowski-Hansen, M.; Schledzewski, K.; Gratchev, A.; Mansmann, U.; Schmuttermaier, C.; Dippel, E.; Koenen, W.; Riedel, F.; Sankala, M.; Tryggvason, K.; Kobzik, L.; Moldenhauer, G.; Arnold, B.; & Goerdt, S. 2006. Differential expression of a gene signature for scavenger/lectin receptors by endothelial cells and macrophages in human lymph node sinuses, the primary sites of regional metastasis. *J. Pathol.* 208, 574–589.

Martinez, F.; Gordon, S; Locati, M.; & Mantovani, A. 2006. Transcriptional profiling of the human monocyte-to-macrophage differentiation and polarization: new molecules and patterns of gene expression. *J. Immunol.* 177, 7303–7311.

Massagué, J. 2008. TGFβ in cancer. *Cell* 134, 215–230.

Maude, S.; Frey, N.; Shaw, P.; Aplenc, R.; Barrett, D.; Bunin, N.; Chew, A.; Gonzalez, V.; Zheng, Z.; Lacey, S.; Mahnke, Y.; Melenhorst, J.; Rheingold, S.; Shen, A.; Teachey, D.; Levine, B.; June, C.; Porter, D.; & Grupp, S. 2014. Chimeric antigen receptor T cells for sustained remissions in leukaemia. *New Eng. J. Med.* 371, 1507–1517.

McAllister, S.; & Weinberg, R. 2014. The tumour-induced systemic environment as a critical regulator of cancer progression and metastasis. *Nat. Cell. Biol.* 16, 717–727.

Mezrich, J.; Fechner, J.; Zhang, X.; Johnson, B.; Burlingham, W.; & Bradfield, C. 2010. An interaction between kynurenine and the aryl hydrocarbon receptor can generate T_{reg} cells. *J. Immunol.* 15, 3190–3198.

Mills, C.; Kincaid, K.; Alt, J.; Heilman, M.; & Hill, A. 2000. M1/M2 macrophages and the T_H1/T_H2 paradigm. *J. Immunol.* 164, 6166–6173.

Mitchem, J.; Brennan, D.; Knolhoff, B.; Belt, B.; Zhu, Y.; Sanford, D.; Belaygorod, L.; Carpenter, D.; Collins, L.; Piwnica-Worms, D.; Hewitt, S.; Mallya Udupi, G.; Gallagher, W.; Wegner, C.; West, B.; Wang-Gillam, A.; Goedegebuure, P.; Linehan, D.; & DeNardo, D. 2013. Targeting TAMs decreases tumour-initiating cells, relieves immunosuppression, and improves chemotherapeutic responses. *Cancer Res.* 73, 1128–1141.

Mitchison, N. 1955. Studies on the immunological response to foreign tumour transplants in the mouse. *J. Exp. Med.* 102, 157–177.

Mok, S.; Koya, R.; Tsui, C.; Xu, J.; Robert, L.; Wu, L.; Graeber, T.; West, B.; Bollag, G.; & Ribas, A. 2014. Inhibition of CSF-1R improves the antitumor efficacy of adoptive cell transfer immunotherapy. *Cancer Res.* 74, 153–161.

Molon, B.; Ugel, S.; del Pozzo, F.; Soldani, C.; Zilio, S.; Avella, D.; de Palma, A.; Mauri, P.; Monegal, A.; Rescigno, M.; Savino, B.; Colombo, P. Jonjic, N.; Pecanic, S.; Lazzarato, L.; Fruttero, R.; Gasco, A.; Bronte, V.; & Viola, A. 2011. Chemokine nitration prevents intratumoral infiltration of antigen-specific T cells. *J. Exp. Med.* 208, 1949–1962.

Mosmann, T. & Coffman, R. 1989. T_H1 and T_H2 cells: different patterns of lymphokine secretion lead to different functional properties. *Annu. Rev. Immunol.* 7, 145–173.

Mosser, D.; & Edwards, J. 2008. Exploring the full spectrum of macrophage activation. *Nat. Rev. Immunol.* 8, 958–969.

Movahedi, K.; Laoui, D.; Gysemans, C. ; Baeten, M. ; Stangé, G. ; van den Bossche, J.; Mack, M.; Pipeleers, D.; in 't Veld, P.; de Baetselier, P.; & van Ginderachter, J. 2010. Different tumour microenvironments contain functionally distinct subsets of macrophages derived from Ly-6C^{high} monocytes. *Cancer Res.* 70, 5728–5739.

Murphy, J.; Tedbury, P.; Homer-Vanniasinkam, S.; Walker, J.; & Ponnambalam, S. 2005. Biochemistry and cell biology of mammalian scavenger receptors. *Atherosclerosis* 182, 1–15.

Nagaraj, S.; Gupta, K.; Pisarev, V.; Kinarsky, L.; Sherman, S.; Kang, L.; Herber, D.; Schneck, J.; & Gabrilovich, D. 2007. Altered recognition of antigen is a mechanism of CD8$^+$ T cell tolerance in cancer. *Nat. Med.* 13, 828–835.

Nakamura, T.; Matsumoto, K.; Kiritoshi, A.; Tano, Y.; & Nakamura, T. 1997. Induction of hepatocyte growth factor in fibroblasts by tumour-derived factors affects invasive growth of tumour cells: *in vitro* analysis of tumour–stromal interactions. *Cancer Res.* 57, 3305–3313.

Naylor, M.; Stamp, G.; Foulkes, W.; Eccles, D.; & Balkwill, F. 1993. TNF and its receptors in human ovarian cancer. Potential role in disease progression. *J. Clin. Invest.* 91, 2194–2206.

Niemand, C.; Nimmergern, A.; Haan, S.; Fischer, P.; Schaper, F.; Rossaint, R.; Heinrich, P.; & Müller-Newen, G. 2003. Activation of STAT3 by IL-6 and IL-10 in primary human macrophages is differentially modulated by SOCS3. *J. Immunol.* 170, 3263–3272.

Noy, R. & Pollard, J. 2014. TAMs: from mechanisms to therapy. *Immunity* 41, 49–61.

Ojalvo, L.; King, W.; Cox, D.; & Pollard, J. 2009. High-density gene expression analysis of TAMs from mouse mammary tumours. *Am. J. Pathol.* 174, 1048–1064.

Ostuni, R.; Kratochvill, F.; Murray, P.; & Natoli, G. 2015. Macrophages and cancer: from mechanisms to therapeutic implications. *Trends Immunol.* 36, 229–239.

Pagano, J.; Blaser, M.; Buendia, M.-A.; Damania, B.; Khalili, K.; Raab-Traub, N.; & Roizman, B. 2004. Infectious agents and cancer: criteria for a causal relation. *Sem. Cancer Biol.* 14, 453–471.

Pagliari, L.; Perlman, H.; Liu, H.; Pope, R. 2000. Macrophages require constitutive NF-κB activation to maintain A1 expression and mitochondrial homeostasis. *Mol. Cell. Biol.* 20, 8855–8865.

Palani, S.; Maksimow, M.; Miiluniemi, M.; Auvinen, K.; Jalkanen, S.; & Salmi, M. 2011. Stabilin-1/Clever-1, a type 2 macrophage marker, is an adhesion and scavenging molecule on human placental macrophages. *Eur. J. Immunol.* 41, 2052–2063.

Palani, S.; Elima, K.; Ekholm, E.; Jalkanen, S.; & Salmi, M. 2016. Monocyte Stabilin-1 suppresses the activation of T_H1 lymphocytes. *J. Immunol.* 196, 115–123.

Park, S.-Y.; Jung, M.-Y.; Lee, S.-J.; Kang, K.-B.; Gratchev, A.; Riabov, V.; Kzhyshkowska, J.; & Kim, I.-S. 2009. Stabilin-1 mediates phosphatidylserine-dependent clearance of cell corpses in alternatively activated macrophages. *J. Cell Sci.* 122, 3365–3373.

Parker, B.; Rautela, J.; & Hertzog, P. 2016. Antitumor actions of interferons: implications for cancer therapy. *Nat. Rev. Cancer* 16, 131–144.

Paulus, P.; Stanley, E.; Schäfer, R.; Abraham, D.; & Aharinejad, S. 2006. CSF-1 antibody reverses chemoresistance in human MCF-7 breast cancer xenografts. *Cancer Res.* 66, 4349–4356.

Pettersen, J.; Fuentes-Duculan, J.; Suárez-Fariñas, M.; Pierson, K.; Pitts-Kiefer, A.; Fan, L.; Belkin, D.; Wang, C.; Bhuvanendran, S.; Johnson-Huang, L.; Bluth, M.; Krueger, J.; Lowes, M.; & Carucci, J. 2011. TAMs in the cutaneous SCC microenvironment are heterogeneously activated. *J. Invest. Dermatol.* 131, 1322–1330.

Piali, L.; Fichtel, A.; Terpe, H.-J.; Imhof, B.; & Gisler, R. 1995. Endothelial vascular cell adhesion molecule-1 expression is suppressed by melanoma and carcinoma. *J. Exp. Med.* 181, 811–816.

Politz, O.; Gratchev, A.; McCourt, P.; Schledzewski, K.; Guillot, P.; Johansson, S.; Svineng, G.; Franke, P.; Kannicht, C.; Kzhyshkowska, J.; Longati, P.; Velten, F.; Johansson, S.; & Goerdt, S. 2002. Stabilin-1 and -2 constitute a novel family of fasciclin-like hyaluronan receptor homologues. *Biochem. J.* 362, 155–164.

Prevo, R.; Banerji, S.; Ni, J.; & Jackson, D. 2004. Rapid plasma membrane–endosomal trafficking of the lymph node sinus and high endothelial venule scavenger receptor/homing receptor Stabilin-1 (Feel-1/Clever-1). *J. Biol. Chem.* 279, 52580–52592.

Pucci, F.; Venner, M.; Biziato, D.; Nonis, A.; Moi, D.; Sica, A.; di Serio, C.; Naldini, L.; & de Palma, M. 2009. A distinguishing gene signature shared by tumour-infiltrating Tie2-expressing monocytes, blood "resident" monocytes, and embryonic macrophages suggests common functions and developmental relationships. *Blood* 114, 901–914.

Pyonteck, S.; Akkari, L.; Schuchmacher, A.; Bowman, R.; Sevenich, L.; Quail, D.; Olson, O.; Quick, M.; Huse, J.; Teijeiro, V.; Setty, M.; Leslie, C.; Oei, Y.; Pedraza, A.; Zhang, J.; Brennan, C.; Sutton, J.; Holland, E.; Daniel, D.; & Joyce, J. 2013. CSF-1R inhibition alters macrophage polarization and blocks glioma progression. *Nat. Med.* 19, 1264–1272.

Qian, H.; Johansson, S.; McCourt, P.; Smedsrod, B.; Ekblom, M.; & Johansson, S. 2009. Stabilins are expressed in bone marrow sinusoidal endothelial cells and mediate scavenging and cell adhesive functions. *Biochem. Biophys. Res. Commun.* 390, 883–886.

Qian, B.; & Pollard, J. 2010. Macrophage diversity enhances tumour progression and metastasis. *Cell* 141, 39–51.

Raffaghello, L.; Prigione, I.; Airoldi, I.; Camoriano, M.; Levreri, I.; Gambini, C.; Pende, D.; Steinle, A.; Ferrone, S.; & Pistoia, V. 2004. Downregulation and/or release of NKG2D ligands as immune evasion strategy of human neuroblastoma. *Neoplasia* 6, 558–568.

Reese, D. & Slamon, D. 1997. HER-2/neu signal transduction in human breast and ovarian cancer. *Stem Cells* 15, 1–8.

Restifo, N.; Marincola, F.; Kawakami, Y.; Taubenberger, J.; Yannelli, J.; & Rosenberg, S. 1996. Loss of functional β_2-microglobulin in metastatic melanomas from five patients receiving immunotherapy. *J. Natl Cancer Inst.* 88, 100–108.

Riabov, V.; Yin, S.; Song, B.; Avdic, A.; Schledzewski, K.; Ovsiy, I.; Gratchev, A.; Verdiell, M.; Sticht, C.; Schmuttermaier, C.; Schönhaber, H.; Weiss, C.; Fields, A.; Simon-Keller, K.; Pfister, F.; Berlit, S.; Marx, A.; Arnold, B.; Goerdt, S.; & Kzhyshkowska, J. 2016. Stabilin-1 is expressed in human breast cancer and supports tumour growth in mammary adenocarcinoma mouse model. *Oncotarget* 7, 31097–31110.

Ries, C.; Cannarile, M.; Benz, J.; Wartha, K.; Runza, V.; Rey-Giraud, F.; Pradel, L.; Feuerhake, F.; Klaman, I.; Jones, T.; Jucknischke, U.; Scheiblich, S.; Kaluza, K.; Gorr, I.; Walz, A.; Abiraj, K.; Cassier, P.; Sica, A.; Gomez-Roca, C.; de Visser, K.; Italiano, A.; Le Tourneau, C.; Delord, J.; Levitsky, H.; Blay, J.; & Rüttinger, D. 2014. Targeting TAMs with anti-CSF-1R antibody reveals a strategy for cancer therapy. *Cancer Cell* 25, 846–859.

Rodriguez, P.; Zea, A.; DeSalvo, J.; Culotta, K.; Zabaleta, J.; Quiceno, D.; Ochoa, J.; & Ochoa, A. 2003. L-arginine consumption by macrophages modulates the expression of CD3 ζ chain in T lymphocytes. *J. Immunol.* 171, 1232–1239.

Rodriguez, P.; Quiceno, D.; Zabaleta, J.; Ortiz, B.; Zea, A.; Piazuelo, M.; Delgado, A.; Correa, P.; Brayer, J.; Sotomayor, E.; Antonia, S.; Ochoa, J.; & Ochoa, A. 2004. ARG-1 production in the tumour microenvironment by mature myeloid cells inhibits T cell receptor expression and antigen-specific T cell responses. *Cancer Res.* 64, 5839–5849.

Rosenberg, A. 2014. IL-2: The first effective immunotherapy for human cancer. *J. Immunol.* 192, 5451–5428.

Royal, R.; Levy, C.; Turner, K.; Mathur, A.; Hughes, M.; Kammula, U.; Sherry, R.; Topalian, S.; Yang, J.; Lowy, I.; & Rosenberg, S. 2010. Phase 2 trial of single agent ipilimumab (anti-CTLA-4) for locally advanced or metastatic pancreatic adenocarcinoma. *J. Immunother.* 33, 828–833.

Ruffell, B.; Au, A.; Rugo, H.; Esserman, L.; Hwang, E.; & Coussens, L. 2012. Leukocyte composition of human breast cancer. *Proc. Natl Acad. Sci. USA* 109, 2796–2801.

Ruffell, B.; Chang-Strachan, D.; Chan, V.; Rosenbusch, A.; Ho, C.; Pryer, N.; Daniel, D.; Hwang, E.; Rugo, H.; & Coussens, L. 2014. Macrophage IL-10 blocks $CD8^+$ T-cell-dependent responses to chemotherapy by suppressing IL-12 expression in intratumoral dendritic cells. *Cancer Cell* 26, 623–637.

Ruffell, B. & Coussens, L. 2015. Macrophages and therapeutic resistance in cancer. *Cancer Cell* 27, 462–472.

Ryder, M.; Gild, M.; Hohl, T.; Pamer, E.; Knauf, J.; Ghossein, R.; Joyce, J.; & Fagin, J. 2013. Genetic and pharmacological targeting of CSF-1/CSF-1R TAMs and impairs BRAF-induced thyroid cancer progression. *PLoS ONE* 8, e54302.

Salmi, M.; Koskinen, K.; Henttinen, T.; Elima, K.; & Jalkanen, S. 2004. Clever-1 mediates lymphocyte transmigration through vascular and lymphatic endothelium. *Blood* 104, 3849–3857.

Salmon, H.; Franciszkiewicz, K.; Damotte, D.; Dieu-Nosjean, M.-C.; Validire, P.; Trautmann, A.; Mami-Chouaib, F.; & Donnadieu, E. 2012. Matrix architecture defines the preferential localization and migration of T cells into the stroma of human lung tumours. *J. Clin. Invest.* 122, 899–910.

Ségaliny, A.; Mohamadi, A.; Dizier, B.; Lokajczyk, A. ; Brion, R.; Lanel, R.; Amiaud, J.; Charrier, C.; Boisson-Vidal, C.; & Heymann, D. 2015. IL-34 promotes tumour progression and metastatic process

in osteosarcoma through induction of angiogenesis and macrophage recruitment. *Int. J. Cancer* 137, 73–85.

Shetty, S.; Weston, C.; Oo, Y.; Westerlund, N.; Stamataki, Z.; Youster, J.; Hubscher, S.; Salmi, M.; Jalkanen, S.; Lalor, P.; & Adams, D. 2015. Clever-1 mediates the transmigration of T_{reg} cells across human hepatic sinusoidal endothelium. *J. Immunol.* 186, 4147–4155.

Slamon, D.; Godolphin, W.; Jones, L.; Holt, J.; Wong, S.; Keith, D.; Levin, W.; Stuart, S.; Udove, J.; Ullrich, A.; & Press, M. 1989. Studies of the HER-2/neu proto-oncogene in human breast and ovarian cancer. *Science* 244, 707–712.

Solinas, G.; Schiarea, S.; Liguori, M.; Fabbri, M.; Pesce, S.; Zammataro, L.; Pasqualini, F.; Nebuloni, M.; Chiabrando, C.; Mantovani, A.; & Allavena, P. 2010. Tumour-conditioned macrophages secrete migration-stimulating factor: a new marker for M2 polarization, influencing tumour cell motility. *J. Immunol.* 185, 642–652.

Stackpole, C.; Cremona, P.; Leonard, C.; & Stremmel, P. 1980. Antigenic modulation as a mechanism for tumour escape from immune destruction: identification of modulation-positive and modulation-negative mouse lymphomas with xenoantisera to murine leukaemia virus gp70. *J. Immunol.* 125, 1715–1723.

Stout, R.; Jiang, C.; Matta, B.; Tietzel, I.; Watkins, S.; & Suttles, J. 2005. Macrophages sequentially change their functional phenotype in response to changes in microenvironmental influences. *J. Immunol.* 175, 342–349.

Stratchan, D.; Ruffell, B.; Oei, Y.; Bissell, M.; Coussens, L.; Pryer, L.; & Daniel, D. 2013. CSF-1R inhibition delays cervical and mammary tumour growth in murine models by attenuating the turnover of TAMs and enhancing infiltration by $CD8^+$ T cells. *Oncoimmunology* 2, e26968.

Sugiura, K.; & Stock, C. 1952. Studies in a tumour spectrum. I. Comparison of the action of methylbis (2-chloroethyl)amine and 3-bis(2-chloroethyl)aminomethyl-4-methoxymethyl -5-hydroxy-6-methylpyridine on the growth of a variety of mouse and rat tumours. *Cancer* 5, 382–402.

Swierczak, A.; Cook, A.; Lenzo, J.; Restall, C.; Doherty, J.; Anderson, R.; & Hamilton, J. 2014. The promotion of breast cancer metastasis caused by inhibition of CSF-1R/CSF-1 signalling is blocked by targeting the G-CSF receptor. *Cancer Immunol. Res.* 2, 765–776.

Szanto, A.; Balint, B.; Nagy, Z.; Barta, E.; Dezso, B.; Pap, A.; Szeles, L.; Poliska, S.; Oros, M.; Evans, R.; Barak, Y.; Schwabe, J.; & Nagy, L. 2010. STAT6 transcription factor is a facilitator of the nuclear receptor PPARγ-regulated gene expression in macrophages and dendritic cells. *Immunity* 33, 699–712.

Takeda, K.; Kaisho, T.; Yoshida, N.; Takeda, J.; Kishimoto, T.; & Akira, S. 1998. STAT3 activation is responsible for IL-6-dependent T cell proliferation through preventing apoptosis: Generation and characterization of T-cell-specific STAT3-deficient mice. *J. Immunol.* 161, 4652–4660.

Tamura, Y.; Adachi, H.; Osuga, J.; Ohashi, K.; Yahagi, N.; Sekiya, M.; Okazaki, H.; Tomita, S.; Iizuka, Y.; Shimano, H.; Nagai, R.; Kimura, S.; Tsujimoto, M.; & Ishibashi, S. 2003. Feel-1 and Feel-2 are endocytic receptors for advanced glycation end products. *J. Biol. Chem.* 278, 12613–12617.

Tang, Q. & Bluestone, J. 2008. The Foxp3$^+$ T_{reg} cell: a jack of all trades, master of regulation. *Nat. Immunol.* 9, 239–244.

Uyttenhove, C.; Pilotte, L.; Théate, I.; Stroobant, V.; Colau, D.; Parmentier, N.; Boon, T.; & van den Eynde, B. 2003. Evidence for a tumoral immune resistance mechanism based on tryptophan degradation by IDO. *Nat. Med.* 9, 1269–1274.

Voll, R.; Herrmann, M.; Roth, E.; Stach, J.; Kalden, J.; & Girkontaite, I. 1997. Immunosuppressive effects of apoptotic cells. *Nature* 390, 350–351.

Vu, T. & Claret, F. 2012. Trastuzumab: updated mechanisms of action and resistance in breast cancer. *Front. Oncol.* 2, 62.

Wajant, H.; Pfizenmaier, K.; & Scheurich, P. 2003. TNF signalling. *Cell Death Differ.* 10, 45–65.

Wallach, D. 1984. Preparations of lymphotoxin induce resistance to their own cytotoxic effect. *J. Immunol.* 132, 2464–2469.

Walsh, L.; Goerdt, S.; Pober, J.; Sueki, H.; & Murphy, G. 1991. MS-1 sinusoidal endothelial antigen is expressed by factor XIIIa$^+$, HLA-DR$^+$ dermal perivascular dendritic cells. *Lab. Invest.* 65, 732–741.

Wang, B.; Li, Q.; Zhao, S.; Wang, J.; & Chen, X. 2011. Transition of TAMs from MHC class II^{hi} to MHC class II^{low} mediated tumour progression in mice. *BMC Immunol.* 12.

Weichhart, T.; Constantino, G.; Poglitsch, M.; Rosner, M.; Zeyda, M.; Stuhlmeier, K.; Kolbe, T.; Stulnig, T.; Hörl, W.; Hengstschläger, M.; Müller, M.; & Säemann, M. 2008. The TSC-mTOR signalling pathway regulates the innate inflammatory response. *Immunity* 29, 565–577.

Witsell, A. & Schook, L. 1992. TNF-α is an autocrine growth regulator during macrophage differentiation. *Proc. Natl Acad. Sci. USA* 89, 4754–4758.

Xu, J.; Lamouille, S.; & Derynck, R. 2009. TGFβ-induced epithelial-to-mesenchymal transition. *Cell Res.* 19, 156–172.

Yu, H.; Kortylewski, M.; & Pardoll, D. 2007. Crosstalk between cancer and immune cells: role of STAT3 in the tumour microenvironment. *Nat. Rev. Immunol.* 7, 41–51.

Zhao, Q.; Kuan, D.-M.; Wu, Y.; Xiao, X.; Li, X.-F.; Li, T.-J.; & Zheng, L. 2012. Activated CD69$^+$ T cells foster immune privilege by regulating IDO expression in tumour-associated macrophages. *J. Immunol.* 188, 1117–1124.

Zhang, X.; Goncalves, R.; & Mosser, D. 2008. The isolation and characterization of murine macrophages. *Curr. Protoc. Immunol.* 83, 14.1.1–14.1.14.

Zheng, X.-F.; Hong, Y.-X.; Feng, G.-J.; Zhang, G.-F.; Rogers, H.; Lewis, M.; Williams, D.; Xia, Z.-F.; Song, B.; & Wei, X.-Q. 2013. LPS-induced M2-to-M1 macrophage transformation for IL-12p70 production is blocked by *Candida albicans*-mediated upregulation of EBI3 expression. *PLoS ONE* 8, e63967.

Zhong, Z.; Weng, Z.; & Darnell, J., Jr. 1994. STAT3: a STAT family member activated by tyrosine phosphorylation in response to EGF and IL-6. *Science* 264, 95–98.

Zins, K.; Abraham, D.; Sioud, M.; & Aharinejad, S. 2007. Colon cancer cell-derived TNF-α mediates the tumour growth-promoting response in macrophages by up-regulating the CSF-1 pathway. *Cancer Res.* 67, 1038–1045.

Appendices

Appendix 1. Calculated tumour areas from the E0771 tumour experiment

Treatment	Cage	Mouse	Day							Notes
			4	7	11	14	18	21	25	
AK-1	Cage 1	1	13.8	35.7	61.7	70.0				i.p.
		2	11.3	23.6	82.1					endpoint
		3	12.3	20.6	45.3	61.2				i.p.
		4	15.0	36.3	82.2					endpoint
		5	14.8	38.4	83.6	94.1				
	Cage 3	1	12.5	25.2	77.9	76.7				
		2	20.3	43.3	55.9	71.3				i.p.
		3	14.6	23.3	62.0	77.1				
		4	14.3	23.7	52.3	75.9				
		5	16.9	31.1	70.6	89.2				
Statistics		**mean**	**14.6**	**30.1**	**67.3**	**76.9**				
		s.e.m.	**0.8**	**2.4**	**4.2**	**3.5**				
		n	**10**	**10**	**10**	**8**				
mStab1	Cage 2	1	17.9	42.8	81.4	101.2				
		2	15.7	29.2	59.7	79.9				
		3	18.9	28.9	65.7	82.2				
		4	12.5	27.9	48.9	68.5				i.p.
		5	12.6	27.9	59.9	84.4				
	Cage 4	2	15.0	23.9	53.6	89.0				i.p.
		3	11.3	26.0	66.9	91.0				
		4	20.0	38.7	70.2	81.5				
		5	18.6	27.3	58.5	87.8				
Statistics		**mean**	**15.8**	**30.3**	**62.8**	**85.0**				
		s.e.m.	**1.0**	**2.0**	**3.0**	**2.8**				
		n	**9**	**9**	**9**	**9**				

Abbreviations: i.p., tumour grew intraperitoneally; endpoint, tumour reached the humane endpoint

Appendix 2. Normalized tumour areas from the E0771 tumour experiment

Treatment	Cage	Mouse	Days							Notes
			4	7	11	14	18	21	25	
AK-1	Cage 1	1	100 %	258 %	446 %	506 %				i.p.
		2	100 %	210 %	728 %					endpoint
		3	100 %	167 %	369 %	498 %				i.p.
		4	100 %	241 %	546 %					endpoint
		5	100 %	259 %	564 %	635 %				
	Cage 3	1	100 %	201 %	621 %	611 %				
		2	100 %	213 %	275 %	351 %				i.p.
		3	100 %	159 %	424 %	527 %				
		4	100 %	166 %	366 %	531 %				
		5	100 %	184 %	417 %	527 %				
Statistics		**mean**	**100 %**	**206 %**	**476 %**	**523 %**				
		s.e.m.	**0 %**	**35 %**	**130 %**	**80 %**				
		n	**10**	**10**	**10**	**8**				
mStab1	Cage 2	1	100 %	239 %	454 %	564 %				
		2	100 %	187 %	381 %	510 %				i.p.
		3	100 %	153 %	348 %	435 %				
		4	100 %	223 %	390 %	547 %				i.p.
		5	100 %	222 %	476 %	671 %				
	Cage 4	1								i.p.
		2	100 %	159 %	357 %	593 %				
		3	100 %	231 %	594 %	808 %				
		4	100 %	194 %	352 %	408 %				
		5	100 %	147 %	315 %	473 %				
Statistics		**mean**	**100 %**	**195 %**	**407 %**	**557 %**				
		s.e.m.	**0 %**	**34 %**	**82 %**	**117 %**				
		n	**9**	**9**	**9**	**9**				

Abbreviations: i.p., tumour grew intraperitoneally; endpoint, tumour reached the humane endpoint

Normalized tumour areas are presented as % of day 4, which has been set as 100 %.

Appendix 3. Calculated tumour areas from the first 4T1 tumour experiment

Treatment	Cage	Mouse	Days							Notes
			3	7	10	14	17	20	22	
AK-1	Cage 1	1	5.5	25.9	33.6	42.1	52.4	59.6	79.3	
		2	10.3	27.5	35.5	55.9	65.8	79.6	98.5	
	Cage 2	1	7.5	24.7	30.9	37.0	45.1	59.3	70.3	
		2	7.9	25.5	34.1	46.5	55.3	70.0	80.4	
	Cage 3	1	6.3	22.1	35.5	46.0	54.7	81.1	80.6	
		2	9.0	20.7	33.0	44.6	51.1	80.6	89.7	
	Cage 4	1	8.4	26.4	30.3	38.6	41.1	52.5	71.5	
		2	7.4	22.4	31.4	45.7	63.8	75.9	94.6	
	Cage 5	1	7.6	28.9	31.8	42.1	52.6	65.2	82.0	
		2	8.1	21.1	30.5	39.7	59.5	72.0	79.8	
Statistics		**mean**	**7.8**	**24.5**	**32.7**	**43.8**	**54.1**	**69.6**	**82.7**	
		s.e.m.	**1.3**	**2.7**	**1.9**	**5.1**	**7.3**	**9.6**	**8.7**	
		n	**10**	**10**	**10**	**10**	**10**	**10**	**10**	
mStab1	Cage 1	3	9.3	11.8	17.8	31.0	35.9	46.4	63.8	
		4	13.1	17.4	27.3	34.0	43.1	59.4	61.9	
	Cage 2	3	7.9	23.8	37.5	55.6	66.3	79.7	92.4	
		4	9.6	15.4	24.4	32.6	38.4	52.5	71.0	
	Cage 3	3	8.2	17.5	32.1	48.4	62.3	76.5	88.2	
		4	9.7	21.1	26.7	54.8	64.3	76.0	99.1	
	Cage 4	3	8.1	19.6	32.1	34.4	52.5	67.2		tumour gone
		4								i.p.
	Cage 5	3	11.4	19.0	28.6	29.2	41.9	49.6	52.8	
		4	8.1	13.9	32.0	35.1	41.6	62.9	72.5	
Statistics		**mean**	**9.5**	**17.7**	**28.7**	**39.5**	**49.6**	**63.3**	**75.2**	
		s.e.m.	**1.7**	**3.5**	**5.3**	**9.9**	**11.3**	**11.7**	**15.3**	
		n	**9**	**9**	**9**	**9**	**9**	**9**	**8**	

Abbreviations: i.p., tumour grew intraperitoneally

Appendix 4. Normalized tumour areas from the first 4T1 tumour experiment

Treatment	Cage	Mouse	Days							Notes
			3	7	10	14	17	20	22	
AK-1	Cage 1	1	100 %	474 %	615 %	770 %	959 %	1090 %	1450 %	
		2	100 %	268 %	346 %	545 %	642 %	776 %	961 %	
	Cage 2	1	100 %	330 %	412 %	494 %	601 %	791 %	938 %	
		2	100 %	324 %	433 %	591 %	703 %	889 %	1022 %	
	Cage 3	1	100 %	352 %	566 %	733 %	872 %	1294 %	1286 %	
		2	100 %	230 %	367 %	496 %	569 %	897 %	998 %	
	Cage 4	1	100 %	312 %	360 %	457 %	487 %	622 %	847 %	
		2	100 %	302 %	424 %	617 %	862 %	1026 %	1278 %	
	Cage 5	1	100 %	378 %	417 %	552 %	689 %	854 %	1074 %	
		2	100 %	261 %	376 %	490 %	735 %	888 %	985 %	
Statistics		**mean**	**100 %**	**323 %**	**432 %**	**575 %**	**712 %**	**913 %**	**1084 %**	
		s.e.m.	**0 %**	**14 %**	**20 %**	**25 %**	**38 %**	**56 %**	**44 %**	
		n	**10**	**10**	**10**	**10**	**10**	**10**	**10**	
mStab1	Cage 1	3	100 %	127 %	191 %	332 %	385 %	498 %	684 %	
		4	100 %	133 %	209 %	260 %	330 %	454 %	473 %	
	Cage 2	3	100 %	303 %	477 %	707 %	842 %	1012 %	1175 %	
		4	100 %	161 %	255 %	340 %	401 %	548 %	741 %	
	Cage 3	3	100 %	214 %	392 %	592 %	762 %	935 %	1079 %	
		4	100 %	217 %	275 %	563 %	661 %	781 %	1019 %	
	Cage 4	3	100 %	242 %	397 %	426 %	650 %	831 %		tumour gone
		4								i.p.
	Cage 5	3	100 %	167 %	252 %	257 %	368 %	436 %	464 %	
		4	100 %	171 %	393 %	432 %	512 %	773 %	892 %	
Statistics		**mean**	**100 %**	**193 %**	**316 %**	**434 %**	**546 %**	**697 %**	**816 %**	
		s.e.m.	**0 %**	**18 %**	**32 %**	**49 %**	**59 %**	**68 %**	**89 %**	
		n	**9**	**9**	**9**	**9**	**9**	**9**	**8**	
		t-test	–	0.00034	0.016	0.034	0.047	0.032	0.025	
		summary	–	***	*	*	*	*	*	

Abbreviations: i.p., tumour grew intraperitoneally

Normalized tumour areas are presented as % of day 3, which has been set as 100 %.

Appendix 5. Calculated tumour areas from the second 4T1 tumour experiment

Treatment	Mouse	Days				
		3	6	10	13	17
Single isotype control	2	8.2	18.1	30.4	39.6	57.4
	4	7.8	12.1	25.2	30.5	35.3
	1	8.3	14.4	30.3	35.8	72.8
	3	9.0	21.2	42.5	46.1	69.6
	4	7.0	16.7	26.6	41.8	55.9
Statistics	**mean**	**8.1**	**16.5**	**31.0**	**38.8**	**58.2**
	s.e.m.	**0.6**	**3.1**	**6.1**	**5.3**	**13.2**
	n	**5**	**5**	**5**	**5**	**5**
Combination isotype control	5	9.4	21.9	36.8	43.0	70.2
	2	8.1	22.2	33.1	37.6	41.9
	4	8.6	22.7	30.7	41.1	62.9
	1	6.9	14.4	34.5	37.5	50.5
	3	7.7	11.4	25.3	29.4	44.7
Statistics	**mean**	**8.1**	**18.5**	**32.1**	**37.7**	**54.1**
	s.e.m.	**0.9**	**4.7**	**3.9**	**4.7**	**10.8**
	n	**5**	**5**	**5**	**5**	**5**
mStab1	1	8.8	18.9	27.8	33.9	51.7
	3	13.5	15.4	30.3	39.8	55.7
	5	7.1	13.6	25.7	33.3	39.4
	2	7.2	13.7	27.2	30.6	58.8
	4	8.8	14.1	30.0	32.5	46.2
	1	9.8	14.9	24.4	32.0	49.5
Statistics	**mean**	**9.2**	**15.1**	**27.6**	**33.7**	**50.2**
	s.e.m.	**2.1**	**1.8**	**2.1**	**2.9**	**6.3**
	n	**6**	**6**	**6**	**6**	**6**
anti-PD-1	2	10.8	18.9	33.4	36.8	57.8
	4	7.3	9.7	27.1	32.8	44.0
	1	7.1	16.0	27.5	34.6	60.1
	2	5.6	15.2	18.5	17.2	19.6
Statistics	**mean**	**7.7**	**14.9**	**26.6**	**30.3**	**45.4**
	s.e.m.	**1.9**	**3.3**	**5.3**	**7.7**	**16.1**
	n	**4**	**4**	**4**	**4**	**4**
anti-PD-L1	5	8.4	18.1	27.4	37.3	40.4
	4	5.6	16.6	26.9	39.4	53.7
	1	7.0	15.2	21.4	27.8	34.8
	3	4.8	16.9	28.5	29.2	42.9
Statistics	**mean**	**6.5**	**16.7**	**26.0**	**33.4**	**43.0**
	s.e.m.	**1.4**	**1.0**	**2.7**	**5.0**	**6.9**
	n	**4**	**4**	**4**	**4**	**4**

Treatment	Mouse	Days				
		3	6	10	13	17
Appendix 5, continued						
mStab1 + anti-PD1	2	5.3	11.1	16.4	20.4	30.7
	4	8.3	11.0	21.0	24.7	49.0
	1	4.4	12.4	21.1	23.7	32.9
	3	6.4	14.2	22.6	22.9	25.1
	5	7.9	16.4	30.4	34.9	40.6
	2	10.3	13.5	27.9	32.8	44.8
	4	5.7	11.3	19.1	19.3	19.1
Statistics	**mean**	**6.9**	**12.8**	**22.7**	**25.5**	**34.6**
	s.e.m.	**1.9**	**1.9**	**4.5**	**5.6**	**10.0**
	n	**7**	**7**	**7**	**7**	**7**
	***t*-test**					**0.015**
	summary					*****
mStab1 + anti-PD-L1	3	3.5	11.0	17.4	26.1	35.9
	2	10.1	16.2	32.7	39.8	64.5
	1	7.4	16.7	29.8	34.8	50.7
	3	7.0	17.2	20.5	33.5	41.6
	5	5.5	17.9	23.3	48.3	64.5
Statistics	**mean**	**6.7**	**15.8**	**24.7**	**36.5**	**51.4**
	s.e.m.	**2.2**	**2.5**	**5.7**	**7.4**	**11.6**
	n	**5**	**5**	**5**	**5**	**5**

Tumours that grew intraperitoneally or did not have day 3 measurements were removed from the calculations of tumour areas.

Appendix 6. Normalized tumour areas from the second 4T1 tumour experiment

Treatment	Mouse	Days				
		3	6	10	13	17
Single isotype control	2	100 %	221 %	371 %	483 %	699 %
	4	100 %	154 %	322 %	391 %	452 %
	1	100 %	174 %	367 %	433 %	881 %
	3	100 %	235 %	471 %	511 %	771 %
	4	100 %	238 %	378 %	593 %	793 %
Statistics	**mean**	**100 %**	**205 %**	**382 %**	**482 %**	**719 %**
	s.e.m.	**0 %**	**15 %**	**22 %**	**31 %**	**65 %**
	n	**5**	**5**	**5**	**5**	**5**
Combination isotype control	5	100 %	232 %	390 %	456 %	745 %
	2	100 %	275 %	411 %	467 %	520 %
	4	100 %	265 %	359 %	481 %	735 %
	1	100 %	210 %	502 %	547 %	736 %
	3	100 %	148 %	327 %	380 %	578 %
Statistics	**mean**	**100 %**	**226 %**	**398 %**	**466 %**	**663 %**
	s.e.m.	**0 %**	**20 %**	**27 %**	**24 %**	**42 %**
	n	**5**	**5**	**5**	**5**	**5**
mStab1	1	100 %	216 %	317 %	387 %	591 %
	3	100 %	115 %	225 %	296 %	414 %
	5	100 %	191 %	359 %	466 %	552 %
	2	100 %	191 %	381 %	428 %	821 %
	4	100 %	161 %	342 %	370 %	526 %
	1	100 %	152 %	250 %	327 %	507 %
Statistics	**mean**	**100 %**	**171 %**	**312 %**	**379 %**	**568 %**
	s.e.m.	**0 %**	**13 %**	**23 %**	**23 %**	**51 %**
	n	**6**	**6**	**6**	**6**	**6**
anti-PD-1	2	100 %	175 %	309 %	341 %	536 %
	4	100 %	133 %	372 %	451 %	606 %
	1	100 %	225 %	384 %	484 %	841 %
	2	100 %	269 %	328 %	305 %	347 %
Statistics	**mean**	**100 %**	**200 %**	**349 %**	**395 %**	**582 %**
	s.e.m.	**0 %**	**25 %**	**15 %**	**37 %**	**88 %**
	n	**4**	**4**	**4**	**4**	**4**
anti-PD-L1	5	100 %	214 %	325 %	442 %	479 %
	4	100 %	294 %	476 %	699 %	952 %
	1	100 %	218 %	307 %	398 %	498 %
	3	100 %	355 %	596 %	612 %	900 %
Statistics	**mean**	**100 %**	**270 %**	**426 %**	**538 %**	**707 %**
	s.e.m.	**0 %**	**29 %**	**59 %**	**61 %**	**110 %**
	n	**4**	**4**	**4**	**4**	**4**

Treatment	Mouse	Days				
		3	6	10	13	17
Appendix 6, continued						
mStab1 + anti-PD1	2	100 %	210 %	311 %	386 %	581 %
	4	100 %	132 %	253 %	297 %	590 %
	1	100 %	282 %	480 %	539 %	748 %
	3	100 %	223 %	354 %	358 %	393 %
	5	100 %	209 %	387 %	444 %	517 %
	2	100 %	130 %	270 %	318 %	433 %
	4	100 %	199 %	336 %	339 %	337 %
Statistics	**mean**	**100 %**	**198 %**	**342 %**	**383 %**	**514 %**
	s.e.m.	**0 %**	**18 %**	**27 %**	**29 %**	**49 %**
	n	**7**	**7**	**7**	**7**	**7**
mStab1 + anti-PD-L1	3	100 %	319 %	504 %	755 %	1041 %
	2	100 %	160 %	324 %	393 %	638 %
	1	100 %	225 %	401 %	468 %	682 %
	3	100 %	245 %	292 %	478 %	594 %
	5	100 %	326 %	423 %	879 %	1174 %
Statistics	**mean**	**100 %**	**255 %**	**389 %**	**595 %**	**826 %**
	s.e.m.	**0 %**	**28 %**	**34 %**	**84 %**	**105 %**
	n	**5**	**5**	**5**	**5**	**5**

Tumours that grew intraperitoneally or did not have day 3 measurements were removed from the calculations of tumour areas.

Normalized tumour areas are presented as % of day 3, which has been set to 100 %.